

SUBMICRON POLYMER EMULSION INSIDE
TWIN SCREW EXTRUDER

**SUBMICRON POLYMER EMULSION INSIDE
TWIN SCREW EXTRUDER**

BY AHMAD AREFI, B.SC, M.SC

A Thesis Submitted to the School of Graduate Studies in Partial
Fulfillment of the Requirements for the Degree Doctor of Philosophy

McMaster University © Copyright by Ahmad Arefi, Feb 2023

McMaster University DOCTOR OF PHILOSOPHY (2023) Hamilton, Ontario
(Chemical Engineering)

TITLE: Submicron Polymer Emulsion Inside Twin Screw Extruder

AUTHER: Ahmad Arefi, B.Sc., M.Sc.

SUPERVISOR: Professor Michael Thompson

NUMBER OF PAGES: xii, 109

Abstract

Solvent-free extrusion emulsification (SFEE) is a recently developed process for producing submicron particles with high viscosity polymers inside a twin-screw extruder without the use of hazardous solvents. Its dependency on a catastrophic phase inversion makes the process knowingly sensitive to a variety of formulation and operational variables, causing a narrow window of production. The purpose of this thesis was to investigate and improve process stability as well as widening operational window. Transient effects of the start-up procedure was investigated by considering the process stability and particle size distribution. The transient sensitivity corresponded to the residency of material in the dispersion zone. When a sub-optimal water/surfactant fraction was allowed to produce an undesired polymer-water (thick lamella) morphology, this morphology continued to persist until the critical first half of the dispersion zone was purged of existing mass. Lot to lot variability of polyester resin was used to investigate the sensitivities of the SFEE process more deeply to better understand the mechanism involved. In this case, acid number was shown to have a significant effect on the initial amount of water needed in the dispersion zone for phase inversion, resulting in an emulsification boundary dependent on the resin acid number. In fact, a significant correlation was found between the acidic end groups of the resin and the maximum amount of water content that could be used in the dispersion zone. The effect of feed rate, screw speed, dispersion length, and surfactant concentration were studied for their individual influence on widening the emulsification boundary. The most significant improvement was observed by applying a longer dispersion length or lower feed rate because both significantly increase the residence time. The effect of residence time on the emulsification boundary was attributed to the total strain imposed on the polymer/water mixture which was related to interfacial growth in the dispersion zone.

Acknowledgement

First and foremost, I would like to sincerely thank my supervisor Dr. Michael Thompson for his continuous support during the last four years. His advice, knowledge and plentiful experience have encouraged me in all the time of my academic research and daily life. I would like to thank Dr. Prashant Mhaskar and Dr. Hassan Teimoori for their technical advice, support, and helpful suggestion on my project. I would like to thank Dr. John Pawlak, Dr. Chieh-Min Cheng, and David Lawton at Xerox Corporation for all their help, useful discussion, and various technical support during my study. I also would like to thank my friend Heera Marway at McMaster Manufacturing Research Institute (MMRI) Lab for his assistance in all stages of my experimental work.

Table of Content

Abstract	iv
Acknowledgement.....	v
List of Figures.....	vii
List of Tables.....	x
List of Abbreviations & Symbols.....	xi
Chapter 1- Introduction and Literature Review.....	1
1.1. Overview	2
1.2. Emulsions	4
1.3. Classical droplet breakup theory.....	6
1.4. Phase inversion emulsification	9
1.5. Similar works and recent developments.....	13
1.6. Solvent free extrusion emulsification (SFEE).....	15
1.7. Objective of the current project.....	16
1.8. Thesis outline.....	18
1.9. References.....	19
Chapter 2- Transient dynamics of polymer emulsification inside a twin screw extruder: Effect on process stability and particle size distribution.....	26
Chapter 3- Relationship of polyester properties with water content requirements for solvent-free extrusion emulsification.....	51
Chapter 4- Understanding the influence of mixing on a high viscous polymer emulsification process using a twin-screw extruder.....	81
Chapter 5- Conclusion.....	104
5.1. Key findings and contributions.....	105
5.2. Recommendations and future work.....	107

List of Figures

Chapter 1

Figure 1. Schematic of solvent-free extrusion emulsification setup.....	3
Figure 2. Ca_{cri} for drop breakup vs viscosity ratio (μ) in simple shear and elongation flow [7]...	5
Figure 3. Breakup of a droplet of 1mm diameter in simple shear flow of Newtonian fluids at viscosity ratio of 0.14 (a little bit above its critical capillary number) [7].....	6
Figure 4. Emulsions can be water in oil (W/O), oil in water (O/W), or bicontinuous system [14].....	8
Figure 5. various instability and processes in emulsions [20].....	9
Figure 6. Catastrophic Phase inversion Pathway [15].....	10
Figure 7. formulation composition map illustrating emulsion types in phase inversion emulsification [15].....	11
Figure 8. Emulsion Dynamic Inversion in the formulation-composition map [25]	12
Figure 9. SFEE Setup used for the current project.....	16
Figure 10. Main parameters affecting the SFEE process.....	17

Chapter 2

Figure 11. Schematic layout of twin-screw extruder used for the emulsification.....	31
Figure 12. Flowrate charts for the three different starting procedures used for the study are shown using an example transient time of $TT=3min$	34
Figure 13. Particle size distributions corresponding to Procedure 1 comparing two transient times at start-up of SFEE ($TT=0$ min vs $TT=6$ min).....	37
Figure 14. Particle distribution moments of D10, D50 and D90 plotted versus three transient times for the start up procedures, a) Procedure 1, b) Procedure 2, c) Procedure 3.....	38
Figure 15. Average D90 versus transient time for Procedures 1 and 2 (at $TT=0$ min, Procedure 2 is equal to Procedure 1). Uncertainty based on three repeated samples was 8.91% RSD (Procedure 1) and 4.86% RSD (Procedure 2). Horizontal line included to highlight a threshold above which the process was considered to be operating in an unacceptable manner.....	39
Figure 16. SEM micrographs of a co-continuous lamella morphology developed in the dispersion zone of the twin screw extruder at three resolutions (From right to left: $3\mu m$, $1\mu m$, $0.5\mu m$) [17].....	41

Figure 17. Examples of the output from the extruder indicative of an unstable and stable process. A) Unemulsified resin separated from water from unsuccessful emulsification collected on a 1 mm Mesh screen. B) Milky white emulsion from stable operations (will not accumulate on a screen).....	43
Figure 18. Average D90 for samples collected before purging (Procedure 1, TT= 6 min) and after purging (Procedure 1, TT= 0 min).....	46
Chapter 3	
Figure 19. Schematic of dynamic emulsion inversion point in phase inversion emulsification systems.....	55
Figure 20. Conceptual progression of emulsification for the twin-screw extruder setup.....	57
Figure 21. Flowchart for varying R/W1 in the experiments to identify the emulsification boundary (i.e. lowest R/W above which the process was stable).....	58
Figure 22. Complex shear viscosity curves at 100 °C for the different batch lots of the same grade of polyester (relative standard error of Resin 1: 9.2%, Resin 2: 8.5%, Resin 3: 8.6%, Resin 4: 3.5%, Resin 5: 7.6%, Resin 6: 8.1%, Resin 7: 7.8%).....	62
Figure 23. AN and viscosity (at a shear rate of 50 s ⁻¹) for all resins.....	63
Figure 24. Emulsification boundary for R/W1 for different batch lots of the polyester based on AN. All trials were conducted with a fixed NaOH concentration of 1% (w/w) on a resin basis.....	64
Figure 25. Extrudate neutralization ratio, NR vs AN of virgin resin for samples based on whether the extruded system emulsified or did not phase invert (non-emulsion). A) calculated NR, and B) NR corrected for hydrolysis.....	67
Figure 26. Particle size distribution of emulsion extrudates (NR-T and NR-A stand for the theoretical and actual NR respectively).....	71
Figure 27. Formulation-Composition map for phase inversion mechanism in the SFEE vs Batch systems.....	74
Figure 28. Illustration of dynamic PIA for low and high AN resin in formulation-composition map (at constant location that results in varied water content) and TSE machine (at constant water content that results in varied PIA location).....	75

Chapter 4

Figure 29. Twin Screw Extruder Setup used in the SFEE process- 1) Hopper for feeding resin in the TSE, 2) Melting zone, 3) Dispersion zone, 4) Dilution zone, 5) first liquid injection port 6) Second liquid injection port, 7) Thermocouple 1, 8) Thermocouple 2, 9) Submicron polymer dispersion extrudate.....	86
Figure 30. Possible outcomes of the SFEE process. A: Ideal perfect emulsion, B: Common emulsion, C: Not completely emulsified, D: Not emulsified at all/Wet plastic. (A & B classified as “Inside Emulsification” window and C&D classified as “Outside Emulsification” window).....	89
Figure 31. Effect of dispersion length and surfactant concentration on emulsification boundary (feed rate 8 kg/hr and screw speed 300 rpm	91
Figure 32. Effect of feed rate on the emulsification boundary at screw speed of 300 rpm for the short dispersion zone length and 4% (w/w) surfactant. Included balloons show the feed rate and D50 value of each sample. No error bars shown for purposes of clarity.....	91
Figure 33. Effect of screw speed on the emulsification boundary at a feed rate of 8 kg/hr, 4% surfactant using the short dispersion zone length.....	92
Figure 34. Residence time distributions at different screw speeds for a fixed feed rate of 8 kg/hr (short dispersion length, 4% (w/w) surfactant).....	95
Figure 35. Residence time distribution at different feed rates for a constant screw speed of 300 rpm (short dispersion length, 4% (w/w) surfactant).....	95
Figure 36. Stain Distribution Function for different flowrate and screw speeds inside the twin-screw extruder.....	98
Figure 37. Effect of feed rate on different screw speed to find out minimum screw speed required for emulsification at R/W1=5 and different feed rates (4% Surfactant and short dispersion length)..	100
Figure 38. Effect of feed rate on the minimum surfactant concentration required for emulsification at R/W1=5.0 (screw speed of 300 rpm). Lines included for purpose of clarity.....	100
Chapter 5	
Figure 39. Gear Mixer used generally for liquid/polymer mixing [2].....	109

List of Tables

Chapter 2

Table 1. Number of successful and unsuccessful operations in various transient times (all procedures).....	44
--	----

Chapter 3

Table 1. Total surface energy and acid number of polyester resins.....	61
Table 2. Correlation between maximum water content in dispersion and resin properties.....	65
Table 3. Effect of varying NR on the process for different resins (R/W1=3.5).....	70

Chapter 4

Table 1. Experimental conditions used as the base case.....	87
Table 2. Variables of interest studied to widen the emulsification boundary.....	87

List of Abbreviations and Symbols

AN: Acid Number	O/W: Oil-in-Water
Ca: Capillary Number	PIA: Phase Inversion Area
CPI: Catastrophic Phase Inversion	PIT: Phase Inversion Temperature
D: Diameter	R/W ₁ : Resin-to-Water in dispersion zone of SFEE
DR: Degradation Ratio	R/W _T : Resin-to-Water in dilution zone of SFEE
f _w : water fraction	SFEE: Solvent-Free Extrusion Emulsification
f _{w,inv} : Water fraction at phase inversion point	SDF: Strain Distribution Function
HIPE: High internal phase emulsion	TPI: Transitional Phase Inversion
HLB: Hydrophilic Lipophilic Balance	TSE: Twin Screw Extruder
HLD: Hydrophilic Lipophilic Difference	TT: Transient Time
L/D: Length to Diameter Ratio	WOR: Water to Oil Ratio
MEK: Methyl Ethyl Ketone	W/O: Water-in-Oil
M _n : Number average molecular weight	σ: Interfacial Tension
M _w : Weight average molecular weight	γ: Strain
MRT: Mean Residence Time	γ̇= Shear Rate
NaOH: Sodium Hydroxide	
nm: Nano Meter	
NR: Neutralization Ratio	

Chapter 1. Introduction and Literature Review

1.1 Overview

Solid-Liquid dispersion refers to a type of mixture where immiscible solid particles are suspended in a liquid. These types of materials are thermodynamically unstable but kinetically stable suspensions, having many applications that include adhesives, coatings, printing inks, pharmaceuticals, etc. Following a top-down approach to emulsification, micron-sized dispersions can be obtained using high mechanical shear forces, whereas submicron emulsions are usually produced by chemically-driven techniques dependent upon phase inversion [1]. Both methods are directly suited to low and medium viscosity systems (~ 1 Pa.s) and have received extensive study in the literature. Highly viscous polymers are more appropriate for a broader range of industrial applications, but a good solvent is classically required to lower the system viscosity to a comparable level with these other material systems. However, increasing environmental and health concerns make the use of organic solvents contrary to the desire for more sustainable methods as well as eco-friendly materials, which makes the use of water more attractive despite the difficulties involved without depression of the system's viscosity. The present thesis examines many aspect of the challenges with emulsifying a highly viscous polymer in water, which is a topic of industrial interest but has received minimal attention in the literature because of the equipment required. On the other hand, this thesis does not examine emulsion polymerization technique, which consider the polymerization of a monomer in an emulsion because the approach does not apply to various polymers such as polyesters or polyolefins [2].

A relatively new technology has arisen for producing submicron polymer dispersion (100-500 nm) in an aqueous phase without the use of organic solvents in a twin-screw extruder (TSE) machine [3]. The method is specifically targeted to emulsification of highly viscous polymers, reliant on the capacity of a TSE to apply heat and varying deformational forces in this case to

control the state of interactions between the oil-like polymer phase and water. A schematic of the continuous process called solvent-free extrusion emulsification (SFEE) is depicted in Figure 1. First, an oleophilic resin is introduced to the extruder and is heated until fully melted, in the region called the melting zone. Then, a mixture of water and emulsifiers (surfactant and NaOH) is added to the melted polymer in the so-called dispersion zone where an initial concentrate of water in oil (W/O) emulsion is generated. At the end, a larger amount of water will be injected into the extruder to initiate phase inversion where the water in oil (W/O) emulsion is inverted to an oil in water (O/W) emulsion. This final region is named the dilution or inversion zone. The complexity associated with the catastrophic phase inversion (CPI) technique applied in the current process along with the sensitivity of the process to various chemistry and machine-related variables, results in an unfortunately narrow window of stable operation. It is recognized these complexities arises from mixing a system of such high viscosity ratio ($10^6:1$) within a limited residence time and with few sites for water addition. Therefore, a comprehensive study to identify the influential variables and their impact on the process would be necessary for widening the operational window and commercial scale-up.

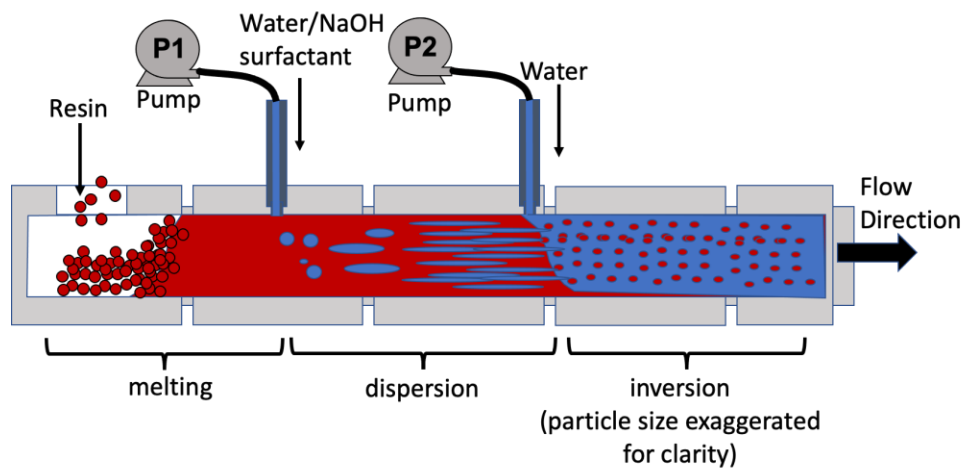


Figure 1. Schematic of solvent-free extrusion emulsification setup

In this chapter, a scientific review on the theory and the mechanisms involved in the process will be provided.

1.2. Emulsions

Emulsions or dispersions are a thermodynamically unstable but kinetically stable mixture of two immiscible liquids in which one phase is dispersed (dispersed phase) in the other phase (continuous phase) in the form of droplets. A large number of applications in food, agriculture, pharmaceutical, cosmetics, and paints are based on emulsions [4]. While one might think that the dispersed phase is the smaller portion and the continuous phase is the larger one, determining which phase disperses in the other phase is not easy and it depends on various factors such as physical properties (density, viscosity, interfacial properties), volume fraction, stirring speed, particle size and in some case, the geometry of the vessel [5]. Usually, one chemical species constitutes the organic phase (oil phase) and water forms the other phase (water phase), though in some cases, the two chemical phases merge to such an extent that it is impossible to find out which one is the dispersed phase and which one is the continuous phase, in this case being referred to as a co-continuous or bicontinuous phase. Due to the general immiscibility of water (W) with oil (O), W/O or O/W emulsions tend to be unstable thermodynamically, resulting in phase separation. One way to make a kinetically stable emulsion is to add surfactants, which are chemical compounds containing both lipophilic and hydrophilic properties; these compounds are also called amphiphilic or amphipathic. Different types of emulsion systems and the role of surfactant are shown in Figure 2. The role of surfactant in general is to lower the interfacial tension, with their effects widely studied [1,4,6–9].

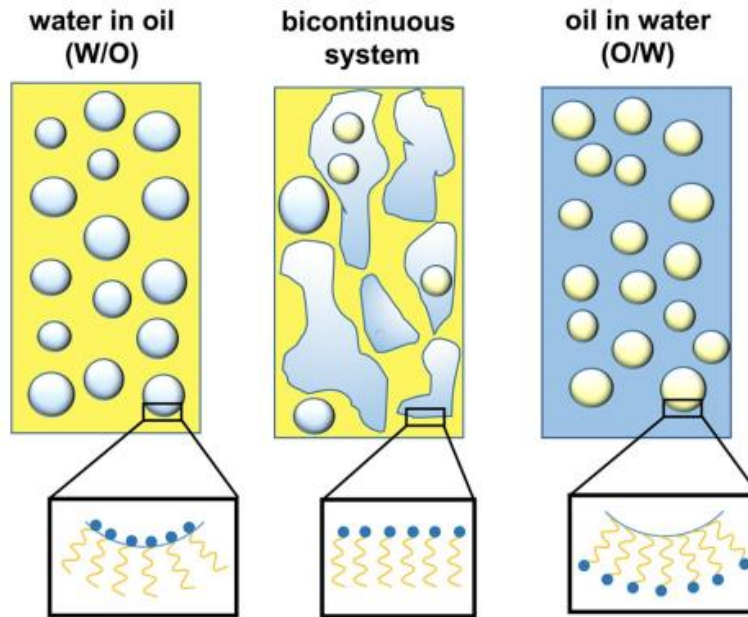


Figure 2. Emulsions can be water in oil (W/O), oil in water (O/W), or bicontinuous system [10]

Phase separation as a result of emulsion instability can make industrial applications of emulsions challenging. All types of instability as well as phase inversion (which is usually not considered instability process) are depicted in Figure 3 as phenomenon causing the emulsion to change in morphology. Creaming (or sedimentation) can occur because of the density difference between the phases. Coalescence will happen when two droplets merge into each other, where if droplets tend to agglomerate in clusters it is called flocculation. Finally, when small particles diffuse into the larger ones, Ostwald ripening is considered to be taking place [11]. To increase emulsion stability and avoid phase separation, the addition of a properly selected surfactant is appropriate but also other techniques such as minimizing the density between two phases, reducing the droplet size, and increasing the continuous phase viscosity are recommended [4,12–15].

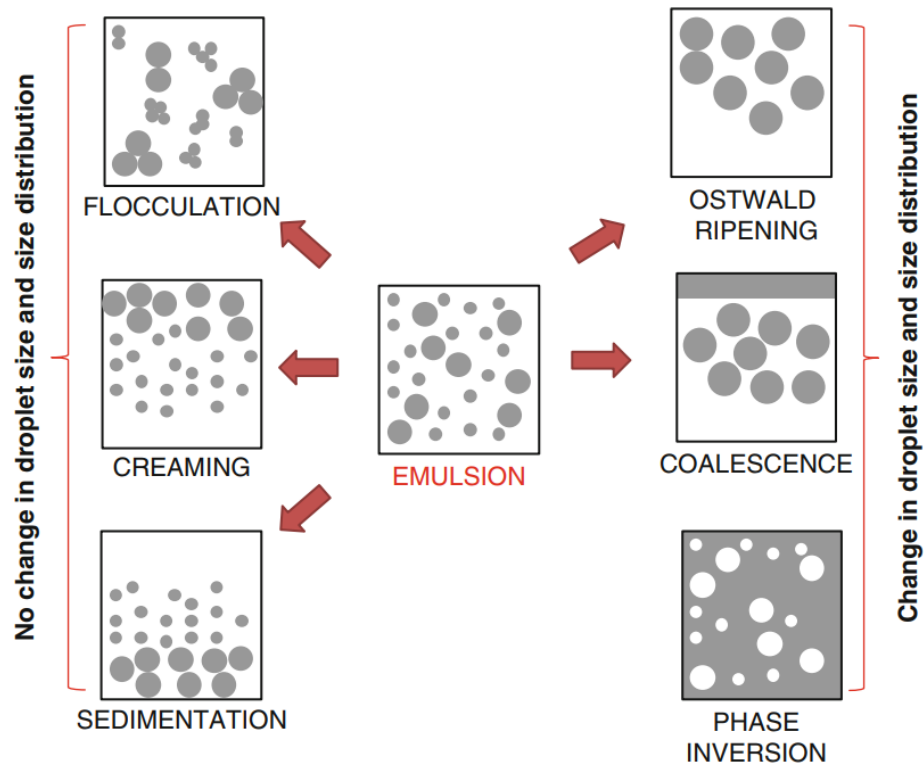


Figure 3. various instability and processes in emulsions [16]

1.3. Classical Droplet Breakup Theory

As explained earlier, dispersion or emulsion consist of two phases, an internal or dispersed phase and a matrix or continuous phase. In general, the size of particles in a dispersion depends on how the internal phase breaks down when mechanical shear forces are introduced to the mixture. Taylor [17] was the first researcher who extensively studied droplet deformation and developed breakup theories. Taylor showed that in a simple steady-state shear flow with zero droplet-droplet interactions, droplet behavior is dependent on the viscosity ratio of internal phase and continuous phase and driving forces described by the Capillary Number (Ca) as defined with equations 1 and 2 respectively:

$$\lambda = \mu_i / \mu_c \quad \text{eq.1}$$

$$Ca = \frac{\tau}{\sigma/R} = \frac{\mu_c \dot{\gamma} R}{\sigma} \quad \text{eq.2}$$

where μ_i refers to the viscosity of the internal phase and μ_c is continuous phase viscosity, τ is the shear stress created by the flow field in the mixing machine and is generally defined as $\tau = \mu_c \dot{\gamma}$ and $\dot{\gamma}$ is the shear rate, R is the droplet radius and σ is the water/oil interfacial energy. For a given water/oil mixing system with a known flow field and viscosity ratio, there should be a critical capillary number (Ca_{cri}) above which droplets are unstable and break into smaller ones. Therefore, the maximum droplet size which could exist at a given capillary number can be calculated according to eq. 3 below [2]:

$$R_{max} = \frac{\sigma}{\eta_c \dot{\gamma}} Ca_{cri} \quad \text{eq. 3}$$

According to this theory and eq. 3, while droplets with a radius of R_{max} (and above) are unstable and will break into smaller ones, smaller droplets will remain stable (though possibly deformed). Following Taylor, others have studied and experimented with droplet breakup theory, such as Rumscheidt and Mason [18] who measured droplet deformation of a large number of fluid mixtures with a wide range of viscosity ratio in hyperbolic and shear flows. They found that a droplet will breakup when the pressure drop created across the interface becomes larger than the surface tension and cohesive forces which hold the droplet together. One of the most extensive experimental studies on droplet breakup was conducted by Grace [19] in 1982. Grace mapped the importance of the viscosity ratio and more importantly, highlighted the superiority of elongational stresses versus shear stress to create droplet breakup. The author's experimental mapping is shown in Figure 4 where the critical capillary number is plotted as a function of viscosity ratio in simple shear and elongation flow of Newtonian fluids. Figure 5 shows a sequence of photographs showing

a 1mm Newtonian drop as a spheroid that deforms and finally breaks into smaller droplets at Ca above its critical value in a simple shear flow.

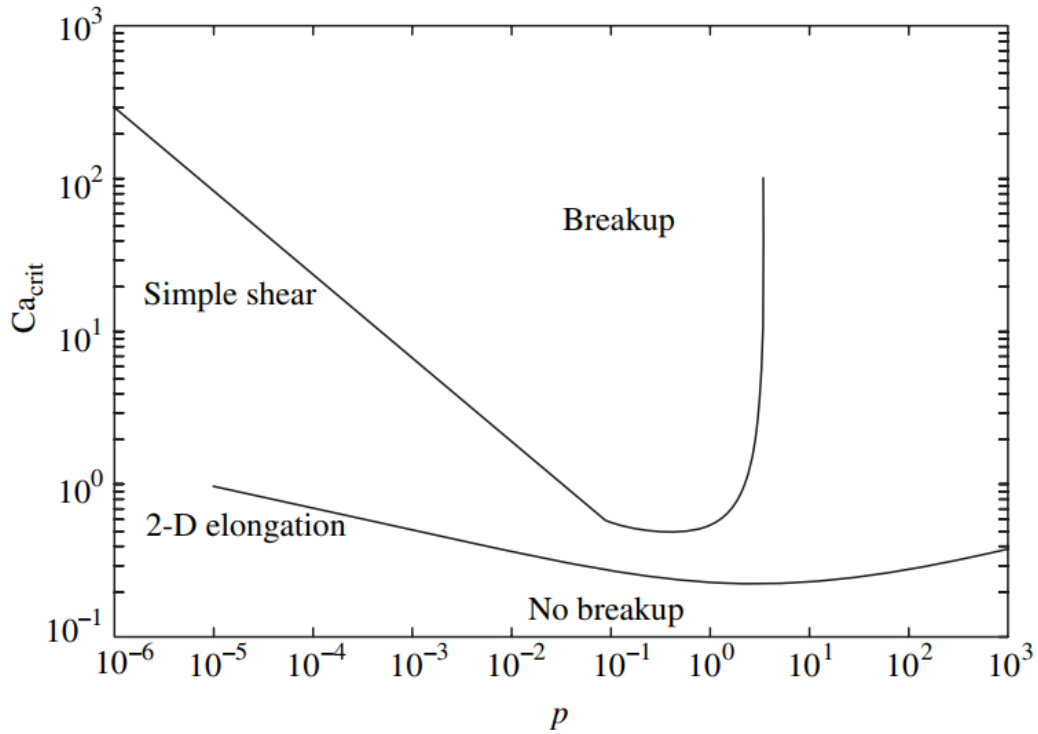


Figure 4. Ca_{crit} for drop breakup vs viscosity ratio (p) in simple shear and elongation flow [20]

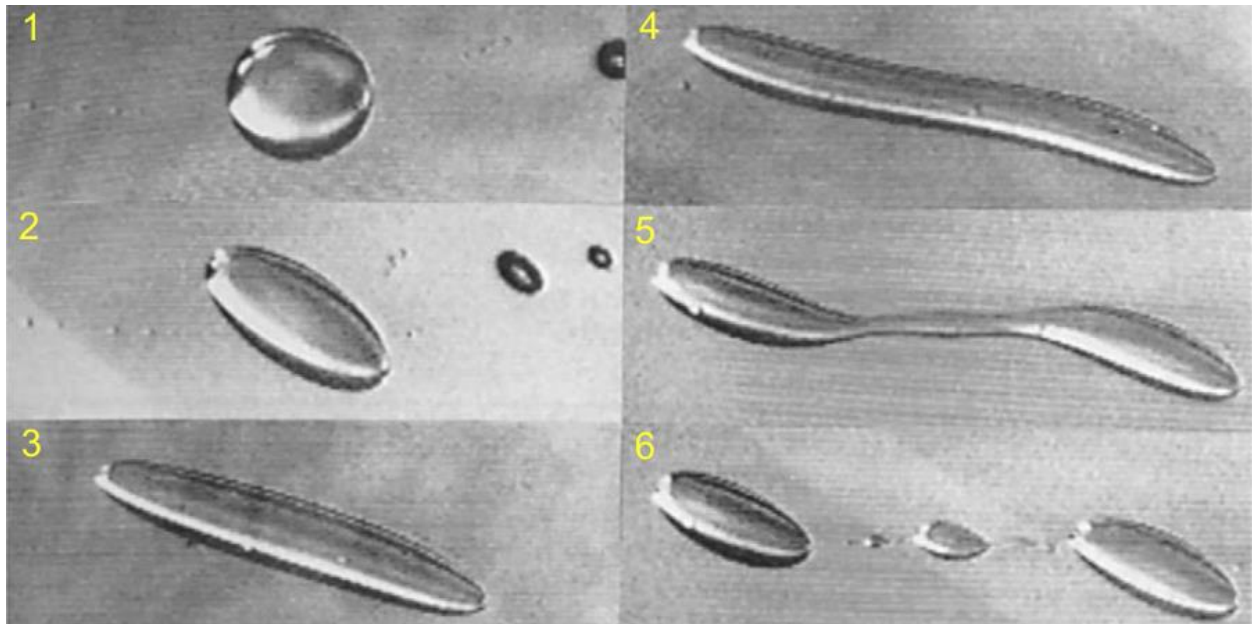


Figure 5. Breakup of a droplet of 1mm diameter in simple shear flow of Newtonian fluids at viscosity ratio of 0.14 (a little bit above its critical capillary number). Numbering corresponds to the order of the images taken over time. [20]

1.4. Phase Inversion Emulsification

For numerous applications, it is necessary to create submicron sized polymer droplets (or particles once solidified) with a diameter of less than $1 \mu\text{m}$ and narrow particle size distribution. Generating such a particle using conventional mechanical shear techniques requires a huge amount of energy because breaking small droplets into even smaller ones requires overcoming a large Laplace pressure [4]. To obtain these industrially desired emulsions with mechanical techniques requires a large amount of surfactant, which is not economically favorable. Thus, an alternative low-energy chemical technique that can be used for a variety of emulsions as well as nanoemulsions is strongly desirable.

Phase inversion emulsification (PIE) causes physiochemical properties of an emulsion to change, resulting in a water-in-oil (W/O) emulsion to invert into an oil-in-water (O/W) emulsion

(or vice versa) [1,5]. Phase inversion emulsification is broadly classified into two main categories: Transitional and Catastrophic. Transitional phase inversion (TIP) is related to a change in the extent of partitioning for a surfactant between water and oil phases with respect to the system temperature [4]. For example, the interaction between water and the hydrophilic part of a nonionic surfactant could be improved by decreasing the temperature. By TIP, at a high temperature, a W/O will more likely be formed and by a gradual decrease in temperature, it will be inverted into O/W. The temperature at which inversion takes place is called the phase inversion temperature (PIT) [21].

In contrast to TIP technique, in catastrophic phase inversion (CPI), by changing the water-to-oil ratio (WOR), a W/O emulsion can be inverted into an O/W emulsion and vice versa; the volume ratio at which inversion occurs is called the phase inversion point (PIP) or emulsion phase inversion (EIP) [22]. The pathway of catastrophic phase inversion is shown in Figure 6.

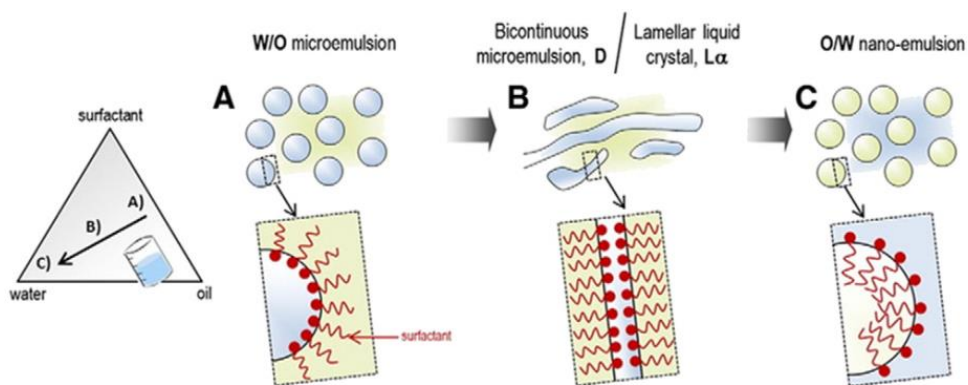


Figure 6. Catastrophic Phase inversion Pathway [11]

To have a better understanding about the mechanism, some concepts need to be understood. A concept widely used in the emulsion industry, even if somewhat erroneous, is the hydrophilic-lipophilic balance (HLB) which is an index that estimates the affinity of a surfactant towards oil

($HLB < 10$) or water ($HLB > 10$) [23]. A more general formulation concept the so-called Hydrophilic-Hydrophobic Difference (HLD) was also utilized [24]. Based on its definition, for $HLD < 0$, a surfactant has more affinity for water and is suitable for stabilizing O/W emulsion, whereas the opposite is true for the oil phase when $HLD > 0$. When $HLD = 0$ the affinity for both water and oil phases are equal and in such cases, a bicontinuous microemulsion phase can be observed. A formulation composition map similar to Figure 7 could be utilized to understand emulsification process based on phase inversion.

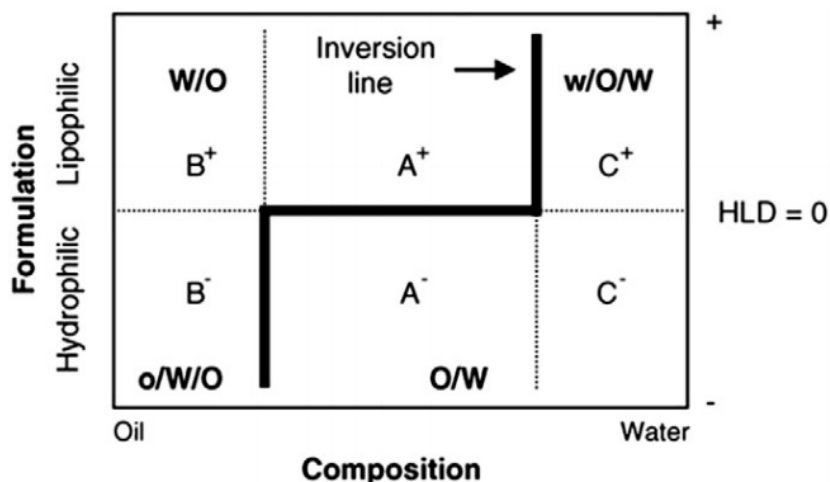


Figure 7. formulation composition map illustrating emulsion types in phase inversion emulsification [11]

A catastrophic phase inversion occurs when a transition from abnormal emulsion (B^- and C^+) to a normal emulsion (A^+ and A^-) takes place by moving horizontally in the diagram and crossing the inversion line (EIP). In this picture $o/W/O$ and $w/O/W$ refer to multiple emulsion also called complex emulsion that is oil in water in oil and water in oil in water emulsion respectively. When varying the water-to-oil ratio to move the system between B^- and A^- or between C^+ and A^+ across the inversion point, phase inversion can suffer from a delay because of the formation of multiple emulsion ($w/O/W$ or $o/w/O$) such that in both cases, inversion does not occur at their

expected WOR. In this scenario, the inversion lines are replaced by an “uncertainty area” on the formulation-composition map when it is impossible to determine the exact location of the inversion point. This zone called a hysteresis is identified by a triangular shaded area in Figure 8 (rightmost image) and the associated behaviour is known as dynamic inversion [11,25,26].

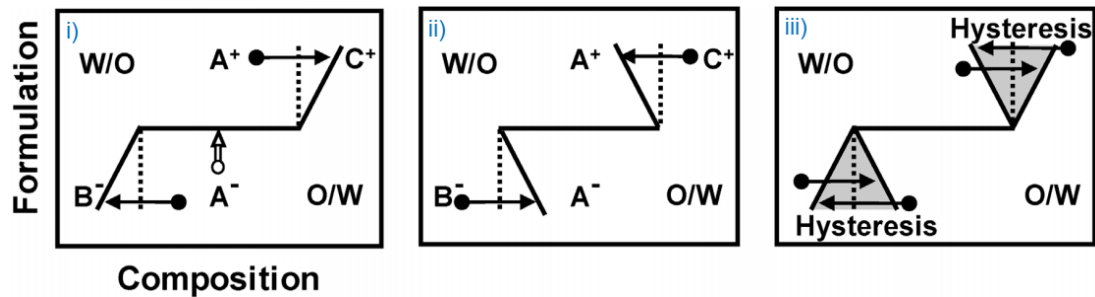


Figure 8. Emulsion Dynamic Inversion in the formulation-composition map. i & ii) Deviation from theoretical PIP in various emulsions. The tip of the arrows indicates the actual location of PIP where the emulsion invert, iii) Uncertainty area developed where emulsion type changes in reality [25]

Studies on the CIP technique show that EIP is varied for a defined system as a function of various variables such as mixing intensity, rate of dispersed phase addition, surfactant type and concentration, interfacial tension between the phases, etc. The inversion of an emulsion is a complicated process and the reaction of the process to those variables is not easily controllable; for example, while lower interfacial tension will generally favor making an emulsion, it requires a higher volume fraction of the dispersed phase for the phase inversion but the inversion of these systems becomes challenging when volume fraction of dispersed phase increases [27]. The phenomena of catastrophic phase inversion and the variables affecting the process have been studied for quite some time now and yet still it is not fully understood mechanistically [10,22,27–36].

1.4. Similar works and recent developments

In this section, a literature review will be summarized on phase inversion emulsification, challenges and progress, and recent developments, with a focus on the limited amount of information on emulsification of high viscous systems. It is stressed that all of these studies were conducted in a batch environment, unlike SFEE. In one of the earliest works on this topic, a new mechanism was introduced for spontaneous emulsification by Greiner and Evans [30]. They prepared a highly viscous W/O microemulsion of methyl ester of partially hydrogenated rosin and introduced it to a quiescently adjacent water phase without any stirring. The inversion resulted in a homogenous O/W emulsion containing droplets as small as 150 nm. In an intensive processing condition, flow-induced phase inversion of high viscous epoxide resin was investigated by Akay [32]. They argued that in systems in which phase inversion is not spontaneous, the type of flow (laminar or turbulent, shear or extensional) and their intensity significantly influenced the degree of phase inversion and final particle size. A theoretical and experimental study was carried out by Yang et al. [34,37] on phase inversion emulsification of Bisphenol A epoxy resin having an average molecular weight of 1000 g/mol in aqueous media. They found out that emulsifier concentration and emulsification temperature play an important role in controlling both the water fraction needed for inversion ($f_{w,inv}$) for PIP and droplet size. A relatively high surfactant concentration of around 10 wt% and a low temperature of around 70 °C could facilitate a complete inversion where all water presented in the system simultaneously changed to becoming the continuous phase. In another work [38], the emulsification of low-density polyethylene (LDPE) was carried out by flow-induced phase inversion using different surface-active species. It was shown that the molecular structure of the emulsifier was the most influential variable in controlling the emulsifying polymer melt. While small-molecule surfactants were unable to lower interfacial

tension, polymeric surfactants (i.e. modified water-soluble polymers) showed promising results. However, the ability of these modified water-soluble polymers to stay in the interface was reduced when the hydrophobic chain length of the emulsifier approached 18 carbons or more.

The dynamics of phase inversion were first studied by Brooks et al. [22] and they found that the location of the phase inversion point (PIP) was highly dependent on the agitation intensity and addition rate of the aqueous phase. The $f_{w,inv}$ increased along with the addition rate because less time was available for developing the microemulsion droplets required for inversion. This resulted in a delay that manifested as a higher $f_{w,inv}$. This behavior was also reported by others [26]. Brooks et al. [31] later developed a quantitative formula to show the relationships between particle size, agitation speed, and water and oil ratio. The dynamic mechanism of phase inversion was studied by Bouchama et al. [39] by applying different ways of adding water. It was shown that PIP is a strong function of both the amount of water being added and the procedure of its addition. When a small amount of water was continuously being added over a defined period of time, it was possible to develop a non-desired morphology where neither agitation intensity nor water flowrate could change the phase inversion locus. In contrast, when the same water addition rate but with a larger amount of water is added at longer time intervals, a lower $f_{w,inv}$ was observed. The effect of following different routes to emulsification on final particle size was carried by Fernandez et al. [29] where it was shown that particles smaller than 1 μm could be obtained above a critical surfactant concentration by following the phase inversion route while changing the emulsification route to direct emulsification, fine particles could not be achieved and particle size was now governed only by the mechanical energy intensity. Dynamic phase inversion was observed by another group of researchers while emulsifying different polydimethylsiloxanes (PDMS) with a viscosity range of 1 Pa-s to 12.5 Pa-s [13]. They found that the phase inversion point for a system

based on 1 Pa-s PDMS was different from 12.5 Pa-s. Increasing the water addition rate resulted in an earlier PIP for the lower viscosity system. This concept of a route to phase inversion was investigated by Pierlor et al. [25] to emulsify a viscous alkyd resin. It was observed that when the resin was not neutralized, particle size and PIP decreased as surfactant content increased; however, when the resin is completely neutralized by KOH, after a critical surfactant concentration i.e. 2 wt% the PIP is independent of surfactant concentration and droplets as small as 200 nm can be obtained. They also found out that for a non-neutralized resin, by reducing water addition rate around droplets of around 500 nm could also be obtained in a longer process.

1.5. Solvent-Free Extrusion Emulsification (SFEE)

In none of the examples reviewed so far, was a continuous system used. In a new approach, a twin screw extruder (TSE) which is conventional continuous mixing equipment in the polymer industry was utilized for the emulsification of a polyester resin which is referred to as the Solvent Free Extrusion Emulsification (SFEE) process developed by Xerox Corp. and studied for several years [3,8,9,41–44]. The physical setup used for the SFEE process to produce submicron polyester waterborne dispersion is shown in Figure 9. The process schematic was also illustrated earlier in Figure 1.



Figure 9. SFEE Setup used for the current project

In the next section, the challenges related to this process and the aim of the current project will be explained.

1.6. Objective of the current project

SFEE process has been studied for several years [3,8,9,41–44]; however, the inherent complexity associated with its reliance upon phase inversion and the high viscosities it is intended to handle, creates sensitivities in its large number of variables, as illustrated in Figure 10. These sensitivities make the process difficult to troubleshoot, control, and scaleup. Enough studies have been carried out now to indicate that focusing on what is happening in the dispersion zone is needed to address these difficulties, and so this thesis intended to study the influence of variables

of interest in this zone on the mean particle size or particle size distribution. Most of the previous studies were carried out within a stable operation window and only considered the emulsion obtained. They described the process by the mean particle size obtained as the key performance indicator (KPI) and not the whole particle size distribution. It was the central hypothesis of this thesis that the missed information on the process was needed to fully understand how variables are affecting the mechanism and process stability. To address this research question, variables showing the greatest sensitivity to the phase inversion mechanism and emulsification boundary (which will be defined in detail later in chapter 3 and 4) were examined in order to widen the operational window.

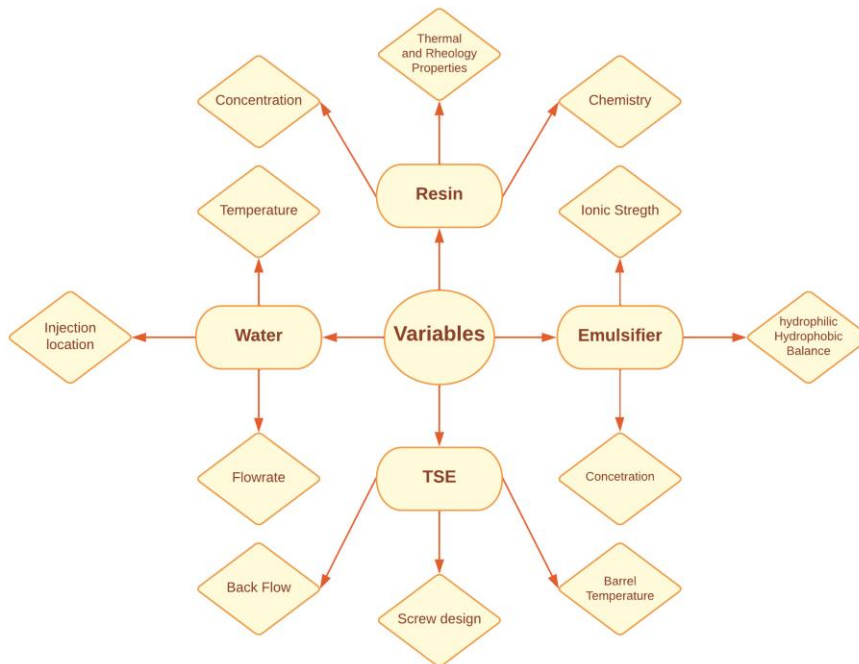


Figure 10. Main parameters considered to be affecting the SFEE process

1.7. Thesis outline

The current thesis is comprised of the following chapters:

1.7.1. Chapter 1: Introduction and Literature Review

In chapter one, an introduction is given on classical droplet breakup theory. It includes a summary on the basics of emulsions and their various preparation techniques, with a focus on catastrophic phase inversion. Finally, solvent free extrusion emulsification is defined and its associated challenges are explained before the objective of the thesis are explained.

1.7.2. Chapter 2: Transient dynamics of polymer emulsification inside a twin screw extruder: Effect on process stability and particle size distribution

The sensitivity of the process to startup dynamics was investigated in this chapter. The studies attempts to explain how the atypical response of the process to differing startup conditions can occur based on the phase inversion mechanism and mixing dynamics inside the extruder. Different scenarios to reaching pseudo steady state conditions were examined.

1.7.3. Chapter 3: Relationship of polyester properties with water content requirements for solvent-free extrusion emulsification

In this chapter, sensitivity of the SFEE process to material variables was studied by considering how minor lot-to-lot variations of the polymer affected the emulsification boundary and process stability. Various properties of the current resin differed between batches allowing for a detailed investigation and new information on the mechanism inside the dispersion zone.

1.7.4. Chapter 4: Understanding the influence of mixing on a high viscosity polymer emulsification process using a twin screw extruder

More operational variables affecting the process window (polymer feed rate, screw speed, mixing length, and surfactant concentration) were investigated for their influence on the emulsification boundary of SFEE. Mixing and residence time were key considerations as each variable was adjusted to control the process, with the goal of widening the operational window.

1.7.5. Chapter 5: Conclusion, key findings, and recommendations

In the final chapter, the contribution of the current thesis and key findings about SFEE are presented. Then, based on the results of the studies and four years of experience acquired from the current project, some useful recommendations as well as potential research for future work is presented.

1.8. References

- [1] S.L. Duraikkannu, R. Castro-Muñoz, A. Figoli, A review on phase-inversion technique-based polymer microsphere fabrication, *Colloids Interface Sci. Commun.* 40 (2021).
<https://doi.org/10.1016/j.colcom.2020.100329>.
- [2] R.D. Priestley, R.K. Prud'homme, *Polymer Colloids: Formation, Characterization and Application*, The Royal Society of Chemistry, 2020.
- [3] A. Goger, M.R. Thompson, J.L. Pawlak, M.A. Arnould, D.J.W. Lawton, Solvent-free polymer emulsification inside a twin-screw extruder, *AIChE J.* 64 (2018) 2113–2123.
<https://doi.org/10.1002/aic.16066>.
- [4] A. Kumar, S. Li, C.M. Cheng, D. Lee, *Recent Developments in Phase Inversion*

- Emulsification, *Ind. Eng. Chem. Res.* 54 (2015) 8375–8396.
<https://doi.org/10.1021/acs.iecr.5b01122>.
- [5] J.M. Maffi, G.R. Meira, D.A. Estenoz, Mechanisms and conditions that affect phase inversion processes: A review, *Can. J. Chem. Eng.* 99 (2021) 178–208.
<https://doi.org/10.1002/cjce.23853>.
- [6] M.P. Aronson, The Role of Free Surfactant in Destabilizing Oil-in-Water Emulsions, *Langmuir*. 5 (1989) 494–501. <https://doi.org/10.1021/la00086a036>.
- [7] T.J. Lin, H. Kurihara, H. Ohta, Prediction of Optimum O/W Emulsification Via Solubilization Measurements, *J. Soc. Cosmet. Chem. Japan*. 11 (1977) 32–42.
https://doi.org/10.5107/sccj1976.11.2_32.
- [8] T. Ivancic, M.R. Thompson, J.L. Pawlak, D.J.W. Lawton, Influence of anionic and non-ionic surfactants on nanoparticle synthesis by solvent-free extrusion emulsification, *Colloids Surfaces A Physicochem. Eng. Asp.* 587 (2020).
<https://doi.org/10.1016/j.colsurfa.2019.124328>.
- [9] T. Ivancic, M.R. Thompson, J.L. Pawlak, D.J.W. Lawton, Influence of anionic and non-ionic surfactants on nanoparticle synthesis by solvent-free extrusion emulsification, *Colloids Surfaces A Physicochem. Eng. Asp.* 587 (2020).
<https://doi.org/10.1016/j.colsurfa.2019.124328>.
- [10] G. Vanti, Recent strategies in nanodelivery systems for natural products: a review, *Environ. Chem. Lett.* 19 (2021) 4311–4326. <https://doi.org/10.1007/s10311-021-01276-x>.
- [11] A. Perazzo, V. Preziosi, S. Guido, Phase inversion emulsification: Current understanding

and applications, *Adv. Colloid Interface Sci.* 222 (2015) 581–599.

<https://doi.org/10.1016/j.cis.2015.01.001>.

- [12] S. Tcholakova, I. Lesov, K. Golemanov, N.D. Denkov, S. Judat, R. Engel, T. Danner, Efficient emulsification of viscous oils at high drop volume fraction, *Langmuir*. 27 (2011) 14783–14796. <https://doi.org/10.1021/la203474b>.
- [13] J. Galindo-Alvarez, V. Sadtler, L. Choplin, J.L. Salager, Viscous oil emulsification by catastrophic phase inversion: Influence of oil viscosity and process conditions, *Ind. Eng. Chem. Res.* 50 (2011) 5575–5583. <https://doi.org/10.1021/ie102224k>.
- [14] D. Song, W. Zhang, R.K. Gupta, E.G. Melby, Droplet size and viscosity of tackifier emulsions formed via phase inversion, *Can. J. Chem. Eng.* 87 (2009) 862–868. <https://doi.org/10.1002/cjce.20221>.
- [15] H. Schubert, R. Engel, Product and formulation engineering of emulsions, *Chem. Eng. Res. Des.* 82 (2004) 1137–1143. <https://doi.org/10.1205/cerd.82.9.1137.44154>.
- [16] A. Brunetti, R. Di Felice, *Encyclopedia of Membranes*, 2016. <https://doi.org/10.1007/978-3-662-44324-8>.
- [17] G.I. Taylor, The formation of emulsions in definable fields of flow, *Proc. R. Soc. London. Ser. A, Contain. Pap. a Math. Phys. Character.* 146 (1934) 501–523. <https://doi.org/10.1098/rspa.1934.0169>.
- [18] F.D. Rumscheidt, S.G. Mason, Particle motions in sheared suspensions XII. Deformation and burst of fluid drops in shear and hyperbolic flow, *J. Colloid Sci.* 16 (1961) 238–261. [https://doi.org/10.1016/0095-8522\(61\)90003-4](https://doi.org/10.1016/0095-8522(61)90003-4).

- [19] H.P. Grace, Dispersion phenomena in high viscosity immiscible fluid systems and application of static mixers as dispersion devices in such systems, *Chem. Eng. Commun.* 14 (1982) 225–277. <https://doi.org/10.1080/00986448208911047>.
- [20] Z. Tadmor, *Principles of polymer processing*, 2nd ed., 2006.
- [21] S.E. Friberg, R.W. Corkery, I.A. Blute, Phase inversion temperature (PIT) emulsification process, *J. Chem. Eng. Data.* 56 (2011) 4282–4290. <https://doi.org/10.1021/je101179s>.
- [22] B.W. Brooks, H.N. Richmond, Dynamics of liquid-liquid phase inversion using non-ionic surfactants, *Colloids and Surfaces.* 58 (1991) 131–148. [https://doi.org/10.1016/0166-6622\(91\)80203-Z](https://doi.org/10.1016/0166-6622(91)80203-Z).
- [23] J.T. Davies, Reprinted from : *Gas/Liquid and Liquid/Liquid Interfaces. Proceedings of 2nd International Congress Surface Activity, Aquantitive Kinet. Theory Emuls. Type. I Phys. Chem. Emuls. Agent.* (1957) 426–438.
http://www.firp.ula.ve/archivos/historicos/57_Chap_Davies.pdf.
- [24] F. Ostertag, J. Weiss, D.J. McClements, Low-energy formation of edible nanoemulsions: Factors influencing droplet size produced by emulsion phase inversion, *J. Colloid Interface Sci.* 388 (2012) 95–102. <https://doi.org/10.1016/j.jcis.2012.07.089>.
- [25] C. Pierlot, J.F. Ontiveros, M. Royer, M. Catté, J.L. Salager, Emulsification of viscous alkyd resin by catastrophic phase inversion with nonionic surfactant, *Colloids Surfaces A Physicochem. Eng. Asp.* 536 (2018) 113–124.
<https://doi.org/10.1016/j.colsurfa.2017.07.030>.
- [26] N. Zambrano, E. Tyrode, I. Mira, L. Márquez, M.P. Rodríguez, J.L. Salager, Emulsion

- catastrophic inversion from abnormal to normal morphology. 1. Effect of the water-to-oil ratio rate of change on the dynamic inversion frontier, *Ind. Eng. Chem. Res.* 42 (2003) 50–56. <https://doi.org/10.1021/ie0205344>.
- [27] M.A. Norato, C. Tsouris, L.L. Tavlarides, Phase inversion studies in liquid-liquid dispersions, *Can. J. Chem. Eng.* 76 (1998) 486–494. <https://doi.org/10.1002/CJCE.5450760319>.
- [28] L.K. Saw, B.W. Brooks, K.J. Carpenter, D. V. Keight, Different dispersion regions during the phase inversion of an ionomeric polymer-water system, *J. Colloid Interface Sci.* 257 (2003) 163–172. [https://doi.org/10.1016/S0021-9797\(02\)00030-9](https://doi.org/10.1016/S0021-9797(02)00030-9).
- [29] P. Fernandez, V. André, J. Rieger, A. Kühnle, Nano-emulsion formation by emulsion phase inversion, *Colloids Surfaces A Physicochem. Eng. Asp.* 251 (2004) 53–58. <https://doi.org/10.1016/j.colsurfa.2004.09.029>.
- [30] W.O. Microemulsion, R.W. Greiner, Spontaneous Formation of from Water-Continuous Emulsion a, (1990) 1793–1796.
- [31] B.W. Brooks, H.N. Richmond, Phase inversion in non-ionic surfactant-oil-water systems-II. Drop size studies in catastrophic inversion with turbulent mixing, *Chem. Eng. Sci.* 49 (1994) 1065–1075. [https://doi.org/10.1016/0009-2509\(94\)80012-X](https://doi.org/10.1016/0009-2509(94)80012-X).
- [32] G. Akay, Flow-induced phase inversion in the intensive processing of concentrated emulsions, *Chem. Eng. Sci.* 53 (1998) 203–223. [https://doi.org/10.1016/S0009-2509\(97\)00199-1](https://doi.org/10.1016/S0009-2509(97)00199-1).
- [33] Z. Yang, D. Zhao, M. Xu, Y. Xu, Mechanistic investigation on the formation of epoxy

- resin multi-hollow spheres prepared by a phase inversion emulsification technique, *Macromol. Rapid Commun.* 21 (2000) 574–578. [https://doi.org/10.1002/1521-3927\(20000601\)21:9<574::AID-MARC574>3.0.CO;2-O](https://doi.org/10.1002/1521-3927(20000601)21:9<574::AID-MARC574>3.0.CO;2-O).
- [34] Z.Z. Yang, Y.Z. Xu, D.L. Zhao, M. Xu, Preparation of waterborne dispersions of epoxy resin by the phase-inversion emulsification technique. 2. Theoretical consideration of the phase-inversion process, *Colloid Polym. Sci.* 278 (2000) 1103–1108. <https://doi.org/10.1007/s003960000376>.
- [35] C.Z. Chuaia, K. Almdal, J. Lyngaae-Jørgensen, Phase continuity and inversion in polystyrene/poly(methyl methacrylate) blends, *Polymer (Guildf)*. 44 (2002) 481–493. [https://doi.org/10.1016/S0032-3861\(02\)00632-8](https://doi.org/10.1016/S0032-3861(02)00632-8).
- [36] E. Tyrode, I. Mira, N. Zambrano, L. Márquez, M. Rondón-Gonzalez, J.L. Salager, Emulsion catastrophic inversion from abnormal to normal morphology. 3. Conditions for triggering the dynamic inversion and application to industrial processes, *Ind. Eng. Chem. Res.* 42 (2003) 4311–4318. <https://doi.org/10.1021/ie0300629>.
- [37] Z.Z. Yang, Y.Z. Xu, D.L. Zhao, M. Xu, Preparation of waterborne dispersions of epoxy resin by the phase-inversion emulsification technique. 1. Experimental study on the phase-inversion process, *Colloid Polym. Sci.* 278 (2000) 1164–1171. <https://doi.org/10.1007/s003960000375>.
- [38] G. Akay, L. Tong, Preparation of colloidal low-density polyethylene latexes by flow-induced phase inversion emulsification of polymer melt in water, *J. Colloid Interface Sci.* 239 (2001) 342–357. <https://doi.org/10.1006/jcis.2001.7615>.
- [39] F. Bouchama, G.A. Van Aken, A.J.E. Autin, G.J.M. Koper, On the mechanism of

- catastrophic phase inversion in emulsions, *Colloids Surfaces A Physicochem. Eng. Asp.* 231 (2003) 11–17. <https://doi.org/10.1016/j.colsurfa.2003.08.011>.
- [40] J.L. Salager, A. Forgiarini, L. Márquez, A. Peña, A. Pizzino, M.P. Rodriguez, M. Rondón-González, Using emulsion inversion in industrial processes, *Adv. Colloid Interface Sci.* 108–109 (2004) 259–272. <https://doi.org/10.1016/j.cis.2003.10.008>.
- [41] A. Goger, M.R. Thompson, J.L. Pawlak, D.J.W. Lawton, In situ rheological measurement of an aqueous polyester dispersion during emulsification, *Ind. Eng. Chem. Res.* 54 (2015) 5820–5829. <https://doi.org/10.1021/acs.iecr.5b00765>.
- [42] A. Goger, M.R. Thompson, J.L. Pawlak, M.A. Arnould, A. Klymachyov, D.J.W. Lawton, Effect of Viscosity on Solvent-Free Extrusion Emulsification: Molecular Structure, *Ind. Eng. Chem. Res.* 56 (2017) 12538–12546. <https://doi.org/10.1021/acs.iecr.7b03370>.
- [43] A. Goger, M.R. Thompson, J.L. Pawlak, M.A. Arnould, A. Klymachyov, R. Sheppard, D.J.W. Lawton, Inline rheological behavior of dispersed water in a polyester matrix with a twin screw extruder, *Polym. Eng. Sci.* 58 (2018) 775–783. <https://doi.org/10.1002/pen.24613>.
- [44] A. Goger, M.R. Thompson, J.L. Pawlak, M.A. Arnould, D.J.W. Lawton, Effect of Viscosity on Solvent-Free Extrusion Emulsification: Varying System Temperature, *Ind. Eng. Chem. Res.* 57 (2018) 12071–12077. <https://doi.org/10.1021/acs.iecr.8b02649>.

Chapter 2: Transient dynamics of polymer emulsification inside a twin-screw extruder: Effect on process stability and particle size distribution

The formatting of this chapter has been set up as a journal manuscript. The work has not been submitted to any journal at the time of examination but is intended for publishing in the near future

ABSTRACT

Solvent-free extrusion emulsification (SFEE) is a recently developed process for producing submicron particles with high viscosity polymers inside a twin-screw extruder without the use of hazardous solvents. Its dependency on a catastrophic phase inversion makes the process knowingly sensitive to a variety of formulation and operational variables, causing a narrow window of production. The impact of startup dynamics on steady state operations was studied in this work, considering the influence of rate-of-water addition on the output particle size distribution and process stability. The results showed the startup state was critical to achieving phase inversion; in other words, the path to reaching steady conditions was much more relevant to successful emulsification compared to the actual steady state conditions chosen. This was particularly evident by the sensitivity shown for the water fraction first introduced to the polymer melt and the reliance on appropriate interfacial area growth in the short time afforded for mixing of the two phases, prior to the dilution stage intended to initiate phase inversion. The transient sensitivity was considered to be related to thickened lamella caused by insufficient surface-active species for some of these transient startup cases. Once an undesirable phase morphology formed, it appeared to persist as a segregated regime of the flow field long after start-up, making it impossible to return to the operating window unless the critical first half of the dispersion zone was purged of existing mass. The results showed that the first half of the dispersion zone was mostly responsible for the interfacial growth and chemical processes regarding water/NaOH reaching the resin acid end-groups while the second half, which contains more vigorous dispersive mixing elements, plays a more mechanical role in thinning the developed lamellar morphology.

Keywords: phase inversion emulsification, twin-screw extruder, transient dynamics phase, particle size distribution, process stability

1. INTRODUCTION

The literature offers few studies on dynamic variables affecting catastrophic phase inversion, possibly because most examined cases are not rate-limited by mixing of the phases. For systems displaying sensitivity to transient dynamics, the issue is that formulation and operating conditions at steady state do not necessarily dictate successful emulsification. Startup and the rate of change of process variables appear to have significant relevance to the state of the final product.

In the earlier work of Brooks et al. [1], researchers found that the boundaries at which phase inversion occurred depended markedly on the dynamic conditions used, such as changing agitation speed or addition rate of the aqueous phase. They showed that when the addition rate of water decreased, the water fraction needed for phase inversion ($f_{w,inv}$) also decreased, because the dispersion (mixing) time related to addition time was high enough to suitably form the necessary state of microemulsion droplets in the water-in-oil (W/O) emulsion ahead of inversion. On the other hand, at faster water addition rates, inversion occurred after a delay and without the occurrence of the microemulsion. This sensitivity was observed by others as well [2]. Brooks et al. [3] later figured out that droplet size was dependent on the process dynamics, and gave a quantitative formula to express the relationships between particle size, agitation speed, and phase ratio. Bouchama et al. [4] also studied the dynamics of phase inversion and in their case, considered different methods of water addition. Their results revealed that the locus of phase inversion was notably dependent on both how water was being introduced and the quantity of water addition. They showed that small amounts of water added over a defined time step could trap the emulsified system in a non-preferred morphology, where neither agitation speed nor water addition rate could subsequently alter the phase inversion locus. Conversely, with the same water addition rate but

with larger amounts of water added for each time step, a lower water fraction was needed for inversion to occur.

For such mixing dependent phenomena to affect emulsification, the viscous nature of the phases would naturally be suspected as an influential factor. A previous study reported on the effect of water phase addition rate as it affected the capacity to emulsify several systems of differing oil phase viscosity, as high as 10 Pa-s [5]. For their 1 Pa-s system, increasing the addition rate was found to decrease $f_{w,inv}$, which was a contradictory finding to the previously mentioned studies above (where higher addition rates of the dispersed phase usually delayed phase inversion). However, for their more viscous oil phase (10 Pa-s), the water addition rate was now found to be insignificant as a factor affecting $f_{w,inv}$. This study is the only known case to show the tendency of $f_{w,inv}$ to decrease with the use of a more viscous oil phase, and their highest viscosity of study was at least an order of magnitude lower than the typical systems to undergo phase inversion in a new process called Solvent-Free Extrusion Emulsification (SFEE).

SFEE is a green continuous technology reliant upon catastrophic phase inversion for producing submicron waterborne dispersions (100-500 nm), developed to handle highly viscous polymers (100-1000 Pa-s) without the need for any hazardous solvents by use of a twin-screw extruder (TSE) [6]. From our studies of SFEE, we have only recently become aware of its sensitivities to dynamic variables where steady-state conditions may not govern the success of a twin-screw extruder in emulsifying a polymer. As background information, the process has three defined zones inside the extruder, as displayed in Figure 1: i) melting zone, where the polymer is melted and additives can be mixed with the melt, ii) dispersion zone, where surfactants and a small fraction of water are added to create a striated lamellae morphology in the established water-in-oil (W/O) emulsion, and iii) inversion zone, where a much larger amount of water is now added to

initiate phase inversion, changing the system from a W/O to O/W emulsion with a typical solids content of 50-70%. The dispersion zone has attracted the majority of attention in researching this process [6–12] due to the extreme viscosity ratio (nearly $10^6:1$) impeding mixing of the two main phases and the need to address an absence of understanding in the literature on phase inversions when the mixed state of the system prior to this event is rate limited.

The previously mentioned studies [6–10] showing the potential for dynamic morphological states to influence catastrophic phase inversion, were done in batch and semi-batch systems where variable changes over time, like water concentration, are more controllable. Continuous processes like SFEE can not accommodate the near infinite number of injection ports that would be required for equivalent control as a batch system. This difference makes it difficult to translate knowledge on the influential nature of transient dynamics to SFEE. To begin to understand this problem, in the current study, the effects of water addition rate related to startup conditions were evaluated and sources of the transient dynamics were analyzed with the intent of establishing a more robust process for the industry. To the best of our knowledge, the transient dynamics of catastrophic phase inversion for a continuous high viscosity emulsification process has not yet been reported in the literature. The work is divided into two parts, with the first part being a study of the effect of different initiating procedures on the final particle size distribution (if emulsification is successful) and the second part, to find the most robust start-up procedure using statistical analysis.

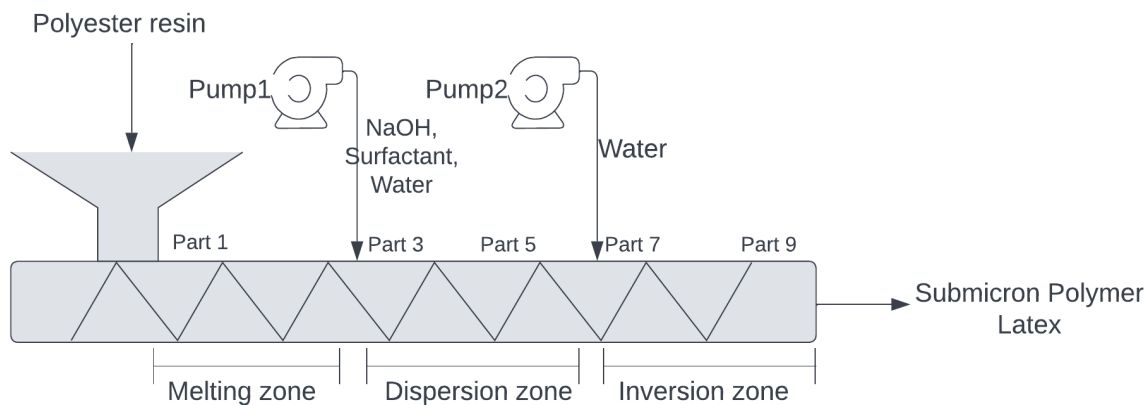


Figure 1. Schematic layout of twin-screw extruder used for the emulsification (the TSE consists of 9 heating parts)

2. EXPERIMENTAL

2.1. Material

A polyester synthesized from fumaric acid (FA) and dipropoxylated bisphenol A (pBPA) was provided by Xerox Corporation (Webster, NY). The polyester had a molecular weight of 14,215 g/mol and acid value of 14 mg KOH/g. Alkyldiphenyloxide disulfonate (Calfax DB-45; Pilot Chemical Company) was used as the surfactant and provided by Xerox Corporation (Webster, NY). It had a reported hydrophilic-lipophilic balance (HLB) of 16.7. Deionized Milli-Q water was used for the experiments, and sodium hydroxide (NaOH) was purchased from Caledon Laboratories Ltd.

2.2. Process Description and Formulation

Emulsification trials were carried out inside a Leistritz ZSE-HP 27 mm 40 L/D co-rotating twin-screw extruder with the same setup as described in previous work [6]. An intensive screw configuration was used similar to [13], though its design is proprietary to Xerox Corporation (Webster, NY). The resin was fed at 8 kg/h by a Brabender T-20 gravimetric feeder while the

screw speed was fixed at 300 RPM. The single hole die was used with a 10 mm diameter exit. A schematic of the extruder and its configuration of pumps and feeder was shown in Figure 1.

The location of Pump 1 (model 260D syringe pump; Teledyne ISCO Inc, Nebraska USA) represented the start of the dispersion zone, adding a small amount of water to generate the W/O emulsion within the extruder. This introduced volume of solution is normally at a resin-to-water (R/W) mass ratio in the range of 3.5 to 5.0 (equivalent to a water mass fraction, f_w of 0.22 to 0.17 respectively) to maintain the water/polymer system well below $f_{w,inv}$ prior to the second pump [6,7,9,11]; a R/W below 3.0 in the dispersion zone introduces too much water to mix and effectively grow the interfacial area between the phases, giving an exiting product after the subsequent inversion zone (mentioned below) that is described as only partially inverted or just wet plastic. A $f_w = 0.17$ was chosen for the present study in the dispersion zone. The liquid added by Pump 1 included 1% (w/w) NaOH and 4% (w/w) surfactant per resin basis, which have been previously shown to be highly effective for stable emulsification of the polyester [11,14].

The location of Pump 2 (Optos 3HM metering pump; Eldex Inc, California USA) denoted the end of the dispersion zone in the extruder, adding in a much larger amount of pure water to invoke phase inversion where the W/O emulsified mixture inverted into an O/W emulsion. The R/W ratio decreased to 1.3 by this final addition of water ($f_w = 0.43$). Although in theory, Pump 2 could be eliminated from the process setup by injecting all water along with the surfactant solution at the start of the dispersion zone, in reality, this approach reduces the overall shear forces applied to the mixture and only serves to extend the mixing length required for the water and polymer to generate the desired pre-inversion morphology (where $f_{w,inv}$ is met and uniform across the system at the end of the zone), which is not possible in practice with an extruder machine having limited residence time.

It is worth mentioning that the complexity of diffusion-dominated morphological development by mixing of a high viscous polymer and water in a concentrated system within a continuous process may eventually require new terminology in describing the chemistry and state of the mixture. However, O/W and W/O emulsion terminology was used in the current discussion to remain consistent with emulsification literature (i.e. lower viscous systems and batch emulsification processes).

2.3. Methodology

The trials began in each case by first reaching a steady screw speed and feed rate for the resin before liquids were added by the two pumps according to one of three different procedures described below:

- *Procedure 1.* Addition rate of the solution by Pump 1 increased incrementally until reaching its setpoint while water added via Pump 2 was immediately started at its setpoint flowrate.
- *Procedure 2:* Similar to Procedure 1 but Pump 2 was started only after the flowrate of Pump 1 had reached its setpoint.
- *Procedure 3:* Addition rate of water by Pump 2 increased incrementally until reaching its setpoint while Pump 1 started immediately to add the solution at its setpoint flowrate (the opposite case of Procedure 1).

To describe pump operations, a variable called transient time (TT) was introduced to indicate the rate at which the process reached setpoint conditions. For example, TT=0 min refers to the case when a pump immediately started at its setpoint, whereas TT=3 min meant three minutes elapsed for the pump in question to gradually reach its setpoint. The three procedures for an example of

TT=3 min are shown graphically in Figure 2. Three transient times of TT = 0, 3, and 6 min were evaluated in this study.

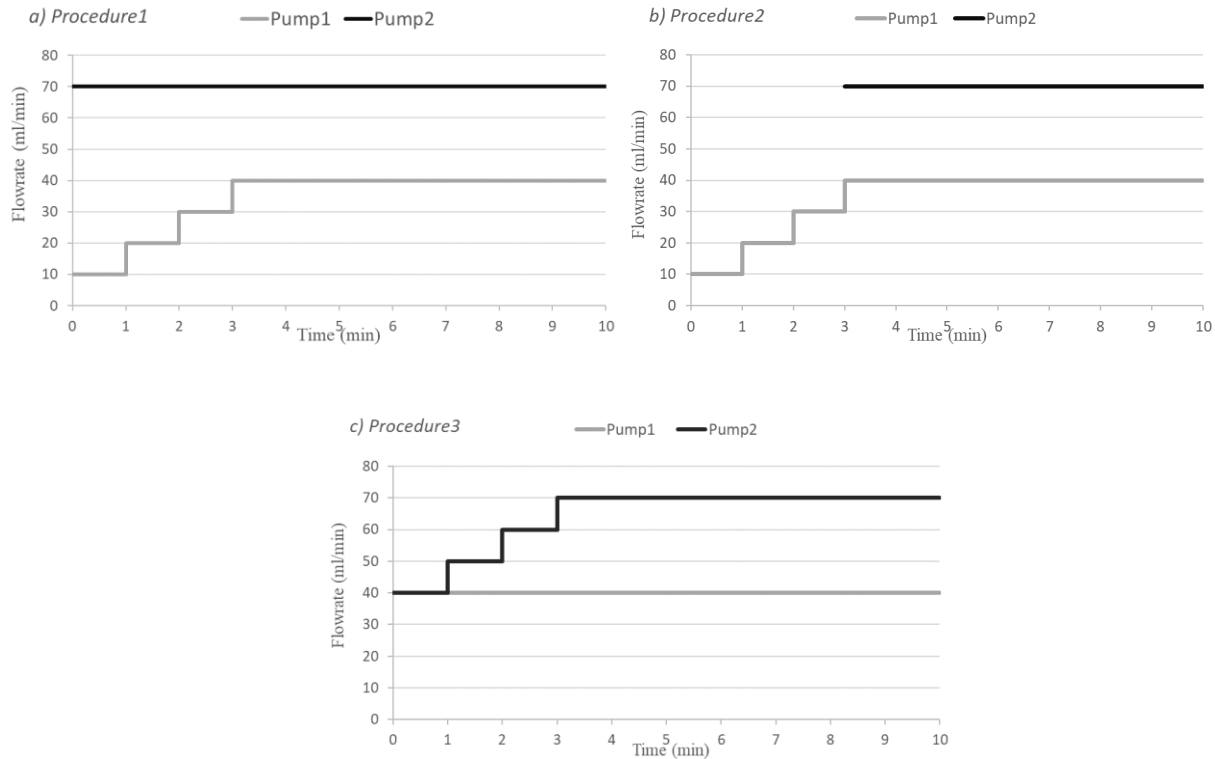


Figure 2. Flowrate charts for the three different starting procedures used for the study are shown using an example transient time of TT=3min

2.4. Residence time measurement

Mean residence time (MRT) was measured using the pseudo dirac pulse method for the three main SFEE zones (referring to Figure 1) in the extruder under conditions when both pumps were immediately started at setpoint. A pulse of 1 g graphite powder was introduced following the method published by Mu and Thompson [15] and its exiting concentration over time was determined using color intensity from a video recording of the trial. Video was collected during a trial at the site of Pump 1, Pump 2 and the end of the extruder; transparent barrel ports were used

at the two pump locations and a strobe light was used to illuminate the flow field. Trials for determining MRT were repeated three times.

2.5. Particle size analysis

Emulsion samples were collected from the process exit after 12 minutes from the start of an experiment, with the collected mass diluted (10 grams of sample with 300 ml of Milli-Q water) and then filtered using a sieve with the mesh opening of 106 μm to separate wet unemulsified plastic from any emulsified mass. Particle size distributions were measured using a Mastersizer 2000 (Malvern, UK), which was considered accurate for a size range of 0.02-2000 μm .

3. RESULTS AND DISCUSSION

Prior to our analysis of the process dynamics, some mention of SFEE's operations seem appropriate since batch emulsification is almost exclusively discussed in the literature. The continuous nature of the SFEE process differentiates itself from batch processes where water can be gradually added into the oil phase until the phase inversion point (PIP) is detected (usually based on ion conductivity) and further additions of water is knowingly diluting the emulsion [16]. In a continuous process like an extruder, where few addition points are possible over the moving system, the large amount of water introduced at the 2nd injection (Pump 2) will invariably be sufficient for inversion and subsequent dilution. The extruder operates well above PIP, since detecting this threshold by usual means (with an ion conductivity sensor) is problematic for SFEE; the conductivity sensor can not be placed into the flow field bounded within the rotating screws and samples extracted for testing that are close to the inversion threshold are likely to agglomerate if not diluted first. Therefore in the SFEE process, the resin-to-water (R/W) ratios described for the two zones (dispersion and inversion) were selected because they were found to result in complete emulsification of the polyester resin when both pumps were immediately operated at

their final setpoint conditions. This study of the transient phenomenon was never intended to find stable operating conditions since that was already understood, but rather, it was to improve our understanding about why it appeared so difficult to change the SFEE operating state (or even to scale to larger machines).

3.1. Effect of pump starting procedures on the particle size distribution

The trials started with Procedure 1 where the transient time of Pump 1 varied between 0, 3, and 6 min. The result showed with a transient time of $TT=0$ min (i.e. pump was immediately brought up to its setpoint condition), the final emulsion had a narrow monomodal particle size distribution where D_{10} , D_{50} , and D_{90} were all submicron values (70 nm, 147 nm, and 384 nm respectively); this case represented the baseline for the study with the process showing stable, completely emulsified output with particles of the desired size. When the transient time was increased to $TT=3$ min, D_{90} increased into the micron range (1.363 μm) though D_{10} and D_{50} did not significantly change. Increasing the transient time to $TT=6$ min, D_{90} further increased above 20 μm while D_{10} and D_{50} remained again unaffected, producing now a distinctly bimodal distribution for this condition. In all three cases, the polymer was completely emulsified in the process. The differences in particle size distribution between $TT=0$ min and $TT=6$ min for Procedure 1 is demonstrated in Figure 3. The dominant peak (comprised of particles between 30 nm to 700 nm) is attributed to phase inversion whereas the secondary peak (of particles between 1 μm and 100 μm) represents a potentially different generation mechanism and interestingly, both peaks are present for both transient times in the figure, though nearly negligible for the $TT=0$ min case. This secondary peak has been reported in the prior literature for SFEE when using ineffective

surfactants (such as exclusive use of non-ionics) for water incorporation into the polyester melt [11,14].

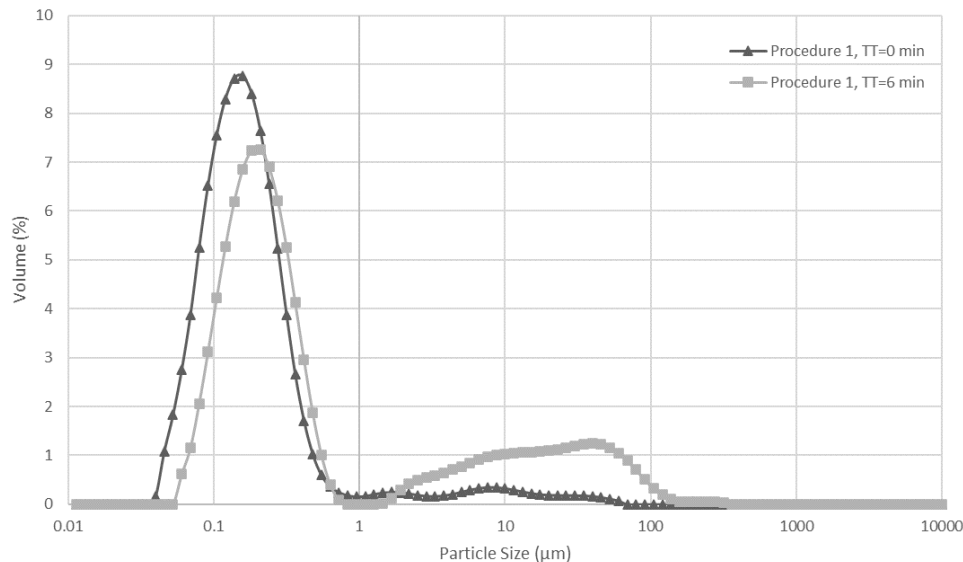


Figure 3. Particle size distributions corresponding to Procedure 1 comparing two transient times at start-up of SFEE (TT=0 min vs TT=6 min)

With Procedure 2, the results were similar to Procedure 1, indicating that any delay in starting up Pump 2 had no significant effect on the state of emulsification once steady state was reached. The process responded differently though for Procedure 3, with no change in the particle size distribution as the transient time was changed. Results of the three procedures and their effects on the emulsion particle size distribution at steady-state conditions are illustrated in Figure 4 using the metrics of D_{10} , D_{50} and D_{90} to convey changes. The resin was fully emulsified in all cases, regardless of the procedure or transient time used. The insensitivity of the process seen in the figure to Pump 2 start-up conditions indicated that the transient phenomenon being studied was localized to the dispersion zone and hence, it was surmised to be dependent on the dispersed state of water in the polymer melt because mixing is its primary function.

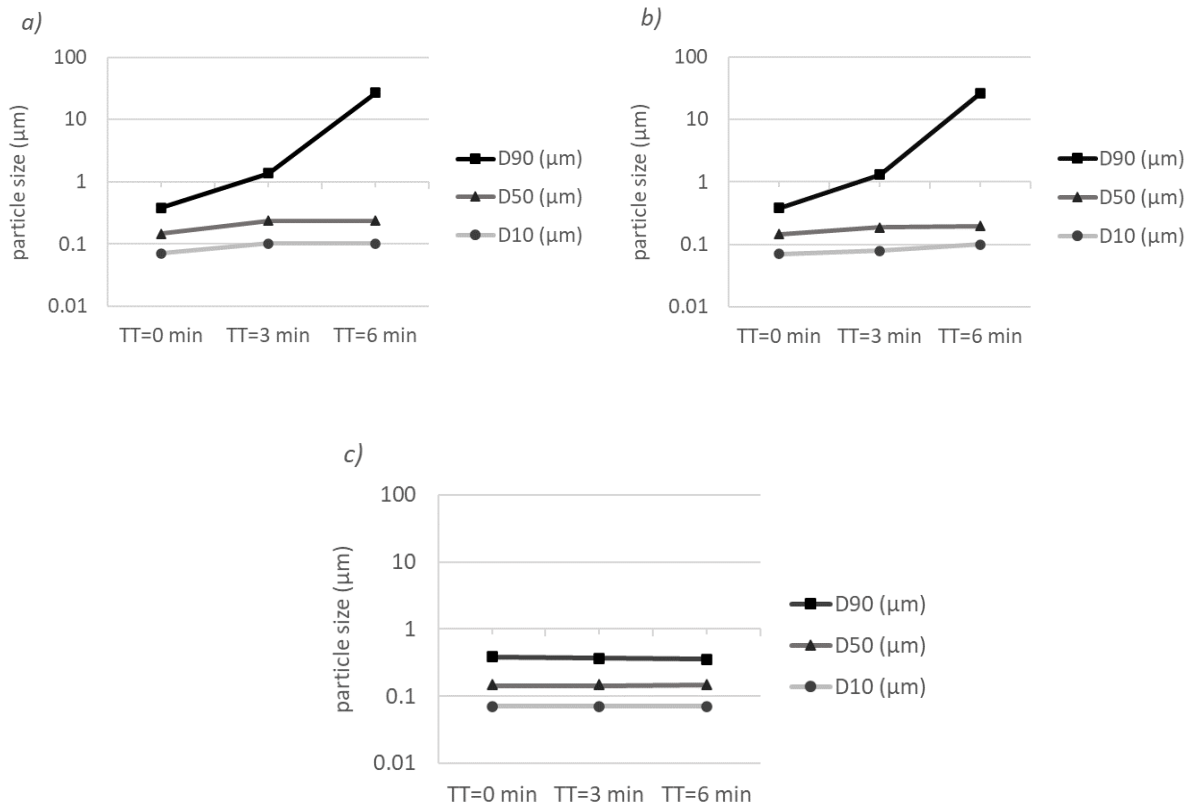


Figure 4. Particle distribution moments of D₁₀, D₅₀ and D₉₀ plotted versus three transient times for the start up procedures, a) Procedure 1, b) Procedure 2, c) Procedure 3

A more detailed investigation on the effect of transient time with D₉₀, specifically for Procedures 1 and 2, is presented in Figure 5. D₉₀ was seen to be the most sensitive metric of the size distribution for tracking the influence of transient phenomenon in SFEE on the quality of produced particles. As such, a threshold is highlighted in the figure to distinguish conditions considered to be producing particles exclusively by phase inversion (below the line) versus conditions where at least some particles were more likely created by mechanical/physical means (above the line). For transient times of TT=3 min or longer, a significant fraction of particles larger than 1 μm were being formed, which always corresponded to the particle size distribution having a more prominent bimodal shape.

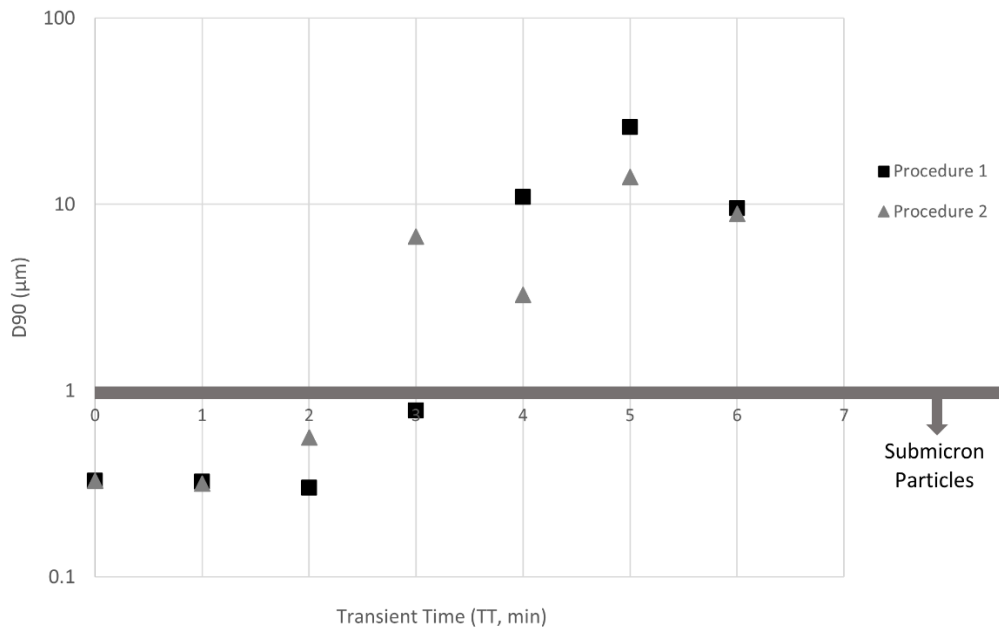


Figure 5. Average D90 versus transient time for Procedures 1 and 2 (at TT=0 min, Procedure 2 is equal to Procedure 1). Uncertainty based on three repeated samples was 8.91% RSD (Procedure 1) and 4.86% RSD (Procedure 2). Horizontal line included to highlight a threshold above which the process was considered to be operating in an unacceptable manner

As mentioned above, the larger micron-sized particles produced under Procedures 1 and 2 have been seen in the past, whenever the process operated without surfactant (i.e. reliant only on endgroup carboxylates generated with NaOH [6,10]). In the present case, increasing transient time meant the melted resin contained less surfactant, NaOH, and water for an increasingly prolonged period as the process started up. The lower NaOH would have also meant that fewer carboxylic acid end groups were converted to carboxylate [6] compared to the setpoint condition (TT=0), especially early in each startup period. With a lower surfactant concentration and fewer carboxylates for the morphologically developing W/O system, the greater interfacial energy early in the transition period meant dispersion of water into the resin was expectedly hindered and likely only to create a droplet morphology with increasing transient time. We recognize the need to create

a lamellar phase morphology for ideal performance in the inversion zone [10,17,18]. Figure 6 shows example SEM micrographs of SFEE samples collected from the dispersion zone in earlier studies, demonstrating the striated polymer structure which led to this understanding that a well-developed lamellae morphology is needed prior to phase inversion [17]; the porous, fibrillar nature seen in cross-sections of extruded polyester melt was always present for operating conditions that produced phase inversion. And so, the poor (large) particle sizes found with high transient times seem understandable, at least early during this period of start-up, but what is perplexing is that the system doesn't yield the same results as those corresponding to a short transition time once the end of the transient period is reached.

This presently reported transient phenomenon shares similarities with an earlier study using an inline rheometer to monitor the dispersion zone of the SFEE process, in which it was found that a slow decrease in the bulk system viscosity at startup corresponded to the process producing larger particles once at steady state whereas a more abrupt decline in viscosity resulted in the desired small particles expected from SFEE [6,10]. The study did not purposely create a transient time ($TT=0$ min) but nonetheless it appears that they were also observing the system becoming trapped within an undesirable W/O morphology just like in the present case.

The final particle size distribution and especially the dominant peak seen below one micron (referring to Figure 3) indicated that at some point in the transient period, for each tested TT, sufficient surfactant and NaOH was present for the majority of polymer to emulsify by phase inversion. With increased TT, a larger portion of the polymer flow seemed to be persistently fixed in a less-than-desirable morphological state, leading to more particles corresponding the peak above one micron and the increase in D_{90} seen in Figures 4 and 5; in other words, the flow field was considered as becoming more segregated into packets of polymer and water with uniquely

different lamellae development. It seems that the transient impact on bulk morphology is irreversible over time, unless as will be shown below, water addition is stopped completely to erase the cumulative prior state.

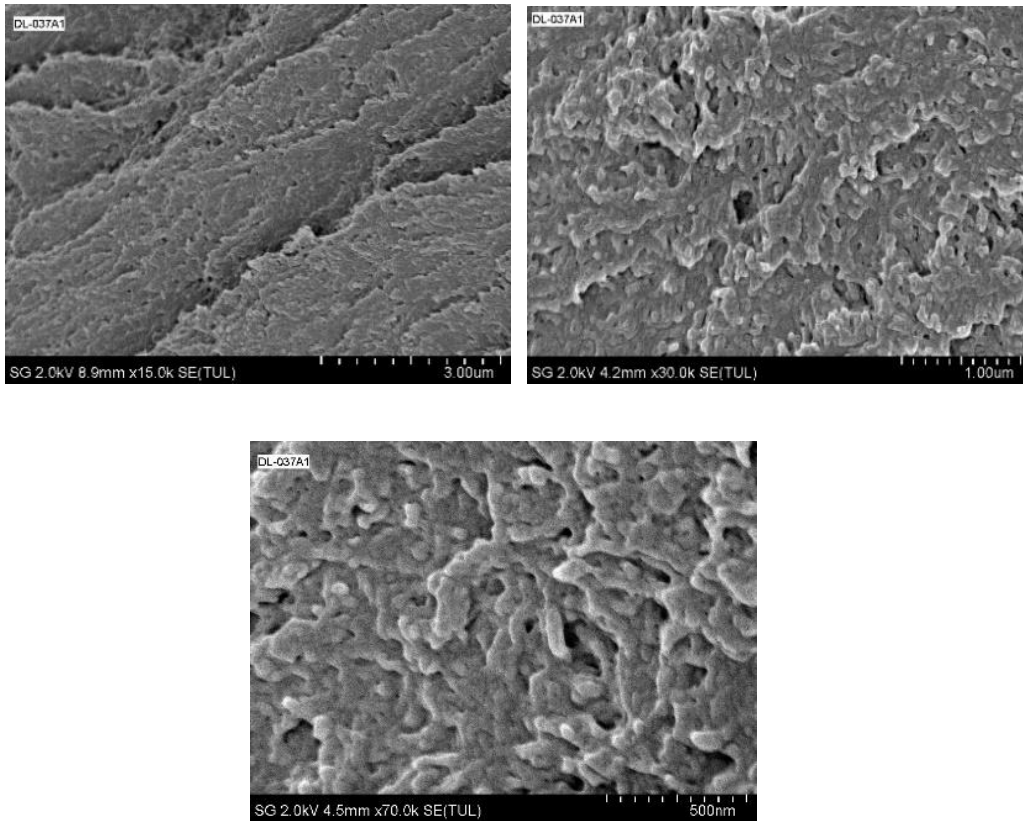


Figure 6. SEM micrographs of a co-continuous lamella morphology developed in the dispersion zone of the twin screw extruder at three resolutions (From right to left: 3µm, 1µm, 0.5 µm) [17]

Since the particle size distribution produced with SFEE appeared to have two peaks depending on how far the process operates away from optimal conditions, it was believed that there are different mechanisms present, each associated with one of those peaks since they appear consistently covering the same range of particle sizes whenever present. It makes sense that phase inversion only occurred in the segregated regions of flow where the lamellae were adequately thin due to sufficient surface-active functional groups present at the interface [6,11]; essentially each

segregated region corresponded to a different amount of water added relative to mass of polymer and based on the transient batch studies by others [1–4] it is expected that there is a different $f_{w,inv}$ for each region. The micron-sized particles are theorized to be associated with poorer water incorporation, where either thick polymer lamella or only disperse water droplets were present by the end of the dispersion zone. In this case, these less desirable W/O morphologies were only capable of producing large melt droplets in accordance with extensional dispersive mixing events (typical of twin screw extrusion) once isolated in the presence of excess water added at the beginning of the inversion zone [17,18]. For non-optimal process or material conditions, this behaviour is expectedly persistent. Unlike batch processes where the capacity to accommodate a longer needed residence time is always possible to complete mixing and developing the desired morphology, in a continuous process like SFEE, the state of mixing is highly constrained by the residence time of the extruder. Hence, an extruder's relatively short residence time was seen as a principal contributing factor to the transient behavior, by often not providing enough mixing time in the dispersion zone to fully reach the desired morphology (locally rather than uniformly achieving $f_{w,inv}$), even under seemingly steady-state conditions. Fortunately, the issues with this transient behavior do not appear influential beyond the dispersion zone, making the operation of Pump 2 to at least be much more robust.

3.2. Effect of starting procedures on process stability

All results presented in the previous sections were based on stable runs where the output appeared as a milky white emulsion (often with a bluish hue), albeit with occasionally larger-than-desired particles. However, not all repeats for a selected operation condition (Procedure and TT) were successful, with some experiments displaying instability and extremely poor quality output that included some portion of the exiting mass from the extruder that could be easily isolated using

a 1 mm mesh sieve; technically these mechanically ground particles (fragments) from the inversion/dilution zone correspond to a third possible characteristic peak in the particle size distribution for the process. Stable and unstable forms of SFEE extrudate are shown in Figure 7. This instability manifested as surging where the output from the extruder varied between the emulsified and unemulsified state. Analyzing the collected data of all experiments revealed that regardless of the applied procedure, when the transient time was high (especially greater than 3 min), the number of runs displaying instability increased as well; no instabilities were noted for TT= 0 min. Table 1 presents the number of successful and unsuccessful operations based on their transient times. Applying a Chi square test of independence (Minitab 18 software; Minitab LLC, USA) revealed that transient time and the stability of operations were correlated together (p-value of 0.040).

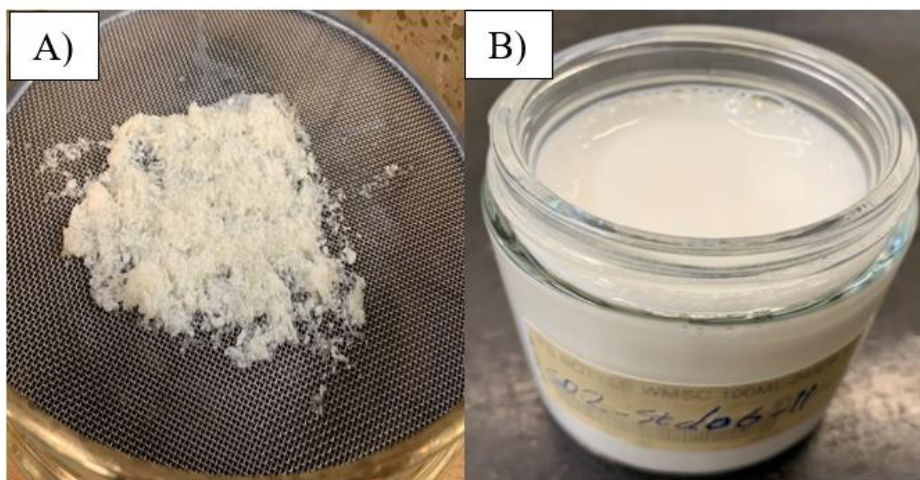


Figure 7. Examples of the output from the extruder indicative of an unstable and stable process. A) Unemulsified resin separated from water from unsuccessful emulsification collected on a 1 mm Mesh screen. B) Milky white emulsion from stable operations (will not accumulate on a screen)

Table 1. Number of successful and unsuccessful operations in various transient times (all procedures)

Operation results (final product)	Number of experiments	Number of experiments
	with $TT < 3$ min	with $TT \geq 3$ min
Successful operation (Emulsion)	19	22
Unstable operation (Wet plastic)	3	14
Total number of experiments	22	36

The surging behavior seen when large particles are formed during SFEE reinforces the segregated flow argument discussed in the previous section. The large particles (> 1 mm) are commonly referred to as ‘wet plastic’ where the polymer melt, far from exhibiting a thin lamella morphology (i.e the particles appear as dense polymer), appears to have been sheared or torn into particles that are thin and elongated in shape. These segregated regions of the flow field are associated with poor interfacial area development. In a sense, this study has noted three different mechanisms of particle formation, the desired phase inversion based on lamellae thinning initiated by the water added by the second pump, the classical droplet rupturing mechanism, and a mechanical fragmentation mechanism, with the water added at the second pump for the latter two being only used to solidifying the polymer melt. The latter two mechanisms are undesirable and the reason for the narrow processing window highlighted for this process.

3.3. Influence of residence time on the transient behavior

Considering the observations in the previous section describing the persistence of large particles initiated by unsatisfactory startup conditions, it was surmised that purging the undesired morphology in the dispersion zone should have some correspondence with the residence time of

the process. The residence time calculated from the tracer technique [19] corresponded to the polymer phase and was very difficult to monitor due to the small port openings in the barrel, and from the excess of water present at the end of the inversion zone that made detection difficult. The estimated mean residence times (MRT) for the melting, dispersion, and inversion zones, individually, were calculated to be 20 s, 145 s (2:25 min), and 75 s (1:15 min) respectively, measured at steady state (after 12 min of runtime) for $TT=0$ min. The error for the two barrel port measurements was ± 12 s, whereas the error at the end of the inversion zone was rounded up to ± 17 s. We only needed reasonable descriptors of fluid dwell time in each zone for the discussion below, and hence we assumed in this analysis that the MRT values were unaffected by TT ; however, the results below suggest this was not a bad assumption.

Using the residence time information above, trials followed in an attempt to purge the undesired portion of the segregated flow field, purposely created by starting up according to Procedure 1 and $TT=6$ min; this chosen state was considered since the particle size results were very different from the baseline (desired) state. Once the system was operating at the steady-state condition with this non-ideal morphology, the feeder and pumps were stopped while the screws remained at constant speed to allow the material present to leave the machine. After a specified period of time for purging the process, the process was re-started by resuming polyester feeding and now following Procedure 1 with $TT=0$ min where a monomodal distribution with all particles below $1\ \mu\text{m}$ would be expected. Similar to all trials before, samples were collected after the extruder had run at 12 minutes for the chosen TT condition. The effect of the purge time on D_{90} is illustrated in Figure 8, showing a collected sample immediately before the purge and then the final sample after purging and resuming by $TT=0$ min conditions.

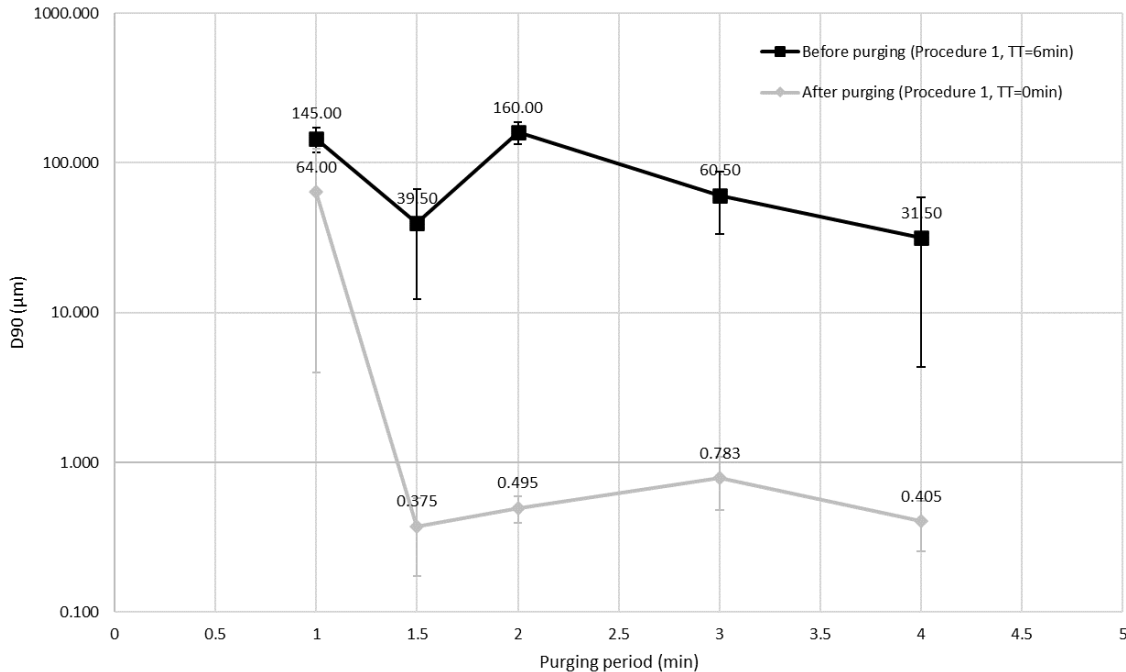


Figure 8. Average D90 for samples collected before purging (Procedure 1, TT= 6 min) and after purging (Procedure 1, TT= 0 min)

The results showed that 1 min was insufficient to purge the undesired morphology, with the system continuing to produce micron size particles once restarted. However, with 1.5 min or greater purge time, the system had cleared the interfering segregated fluid internally and the discharge now showed only emulsified polymer indicative of our earlier reference with the TT= 0 min start-up condition. For the purge periods of 1.5, 2, 3, and 4 min, the output after re-starting with Procedure 1, TT=0 min consisted of emulsion with all particles now being smaller than 1 μm ($D_{90} = 0.375 \mu\text{m}$, $0.495 \mu\text{m}$, $0.783 \mu\text{m}$, $0.405 \mu\text{m}$, respectively). While the results for purging time of 3 and 4 min appear logical as the time is sufficient enough to completely empty both melting and dispersion zones, exceeding their cumulative MRT (165 s) before a new developed morphology occurred in the system; it was surprising that 1.5 min, which only partial purged around 60% of the melting and dispersion zone, could be sufficient to erase the previous

undesirable morphology from re-establishing in the system. This result is believed to show the critical dependency of the dispersion zone on the start-up procedure; the 1.5 min purge time corresponded to a distance half-way between the two pumps (Figure 1). In previous studies on SFEE, it was shown that past this barrel position (part #5) in the machine both endgroup neutralization and any polymer chain degradation showed no significant change [6]. Examining the screw design (used in the earlier work and now), this location is a transition point with less vigorous distributive mixing upstream and intensive dispersive mixing for the remainder of the dispersion zone (up to Pump 2). Putting it all together, it appears that critical interfacial growth dependent on water and NaOH accessing the acid end-groups occurs in the first half of the dispersion zone and purging that section was necessary to erase the undesirable morphology. Interestingly, that prior study [6] found lower end-group conversion when surfactant was included with water and NaOH at Pump 1 and we now believe the interference by the surfactant only becomes significant at this half-way point in the zone. This implies that all critical chemical processes for establishing the lamellae morphology are established in the first 8 L/D of the dispersion zone, in the current extruder setup. If we are correctly interpreting present and previous findings, then the intensive dispersive mixing elements in the second half of the dispersion zone provide only the mechanical action to make thinner lamella morphology. Future studies should focus on expanding the length of the first half of the dispersion zone, and considering whether delaying the addition of the surfactant further into the dispersion zone would increase the robustness of the process and minimize transient sensitivities.

4. CONCLUSION

Transient effects of the start-up procedure for a continuous solvent-free extrusion emulsification process were investigated by considering the process stability and particle size

distribution of samples collected once steady state was achieved. The transient sensitivity corresponded to the residency of material in the dispersion zone. When a sub-optimal water/surfactant fraction was allowed to produce an undesired polymer-water (thick lamella) morphology, this morphology continued to persist until the critical first half of the dispersion zone was purged of existing mass. The current result revealed that the first half of the dispersion zone are more responsible for the interfacial growth and chemical processes regarding water/NaOH reaching the resin acid end-groups while the second half of this zone, which contains more vigorous dispersive mixing elements, plays a more mechanical role to thin the developed lamellar morphology. This was in agreement with previous findings on SFEE.

5. ACKNOWLEDGEMENTS

The authors wish to thank the Natural Sciences and Engineering Research Council (NSERC) and the Xerox Corporation for their funding of the study. Additionally, we wish to thank Xerox Corporation (Webster, NY) and the Xerox Research Centre of Canada (XRCC; Mississauga, ON) for supplying the resin and Calfax surfactants used in this study, technical advice, and analysis assistance.

6. REFERENCES

- [1] B.W. Brooks, H.N. Richmond, Dynamics of liquid-liquid phase inversion using non-ionic surfactants, *Colloids and Surfaces*. 58 (1991) 131–148. [https://doi.org/10.1016/0166-6622\(91\)80203-Z](https://doi.org/10.1016/0166-6622(91)80203-Z).
- [2] N. Zambrano, E. Tyrode, I. Mira, L. Márquez, M.P. Rodríguez, J.L. Salager, Emulsion catastrophic inversion from abnormal to normal morphology. 1. Effect of the water-to-oil ratio rate of change on the dynamic inversion frontier, *Ind. Eng. Chem. Res.* 42 (2003) 50–56. <https://doi.org/10.1021/ie0205344>.
- [3] B.W. Brooks, H.N. Richmond, Phase inversion in non-ionic surfactant-oil-water systems-II. Drop size studies in catastrophic inversion with turbulent mixing, *Chem. Eng. Sci.* 49 (1994) 1065–1075. [https://doi.org/10.1016/0009-2509\(94\)80012-X](https://doi.org/10.1016/0009-2509(94)80012-X).

- [4] F. Bouchama, G.A. Van Aken, A.J.E. Autin, G.J.M. Koper, On the mechanism of catastrophic phase inversion in emulsions, *Colloids Surfaces A Physicochem. Eng. Asp.* 231 (2003) 11–17. <https://doi.org/10.1016/j.colsurfa.2003.08.011>.
- [5] J. Galindo-Alvarez, V. Sadtler, L. Choplin, J.L. Salager, Viscous oil emulsification by catastrophic phase inversion: Influence of oil viscosity and process conditions, *Ind. Eng. Chem. Res.* 50 (2011) 5575–5583. <https://doi.org/10.1021/ie102224k>.
- [6] A. Goger, M.R. Thompson, J.L. Pawlak, M.A. Arnould, D.J.W. Lawton, Solvent-free polymer emulsification inside a twin-screw extruder, *AIChE J.* 64 (2018) 2113–2123. <https://doi.org/10.1002/aic.16066>.
- [7] A. Goger, M.R. Thompson, J.L. Pawlak, M.A. Arnould, D.J.W. Lawton, Effect of Viscosity on Solvent-Free Extrusion Emulsification: Varying System Temperature, *Ind. Eng. Chem. Res.* 57 (2018) 12071–12077. <https://doi.org/10.1021/acs.iecr.8b02649>.
- [8] A. Goger, M.R. Thompson, J.L. Pawlak, D.J.W. Lawton, In situ rheological measurement of an aqueous polyester dispersion during emulsification, *Ind. Eng. Chem. Res.* 54 (2015) 5820–5829. <https://doi.org/10.1021/acs.iecr.5b00765>.
- [9] A. Goger, M.R. Thompson, J.L. Pawlak, M.A. Arnould, A. Klymchyov, D.J.W. Lawton, Effect of Viscosity on Solvent-Free Extrusion Emulsification: Molecular Structure, *Ind. Eng. Chem. Res.* 56 (2017) 12538–12546. <https://doi.org/10.1021/acs.iecr.7b03370>.
- [10] A. Goger, M.R. Thompson, J.L. Pawlak, M.A. Arnould, A. Klymchyov, R. Sheppard, D.J.W. Lawton, Inline rheological behavior of dispersed water in a polyester matrix with a twin screw extruder, *Polym. Eng. Sci.* 58 (2018) 775–783. <https://doi.org/10.1002/pen.24613>.
- [11] T. Ivancic, M.R. Thompson, J.L. Pawlak, D.J.W. Lawton, Influence of anionic and non-ionic surfactants on nanoparticle synthesis by solvent-free extrusion emulsification, *Colloids Surfaces A Physicochem. Eng. Asp.* 587 (2020). <https://doi.org/10.1016/j.colsurfa.2019.124328>.
- [12] T. Ivancic, M.R. Thompson, J.L. Pawlak, D.J.W. Lawton, Influence of anionic and non-ionic surfactants on nanoparticle synthesis by solvent-free extrusion emulsification, *Colloids Surfaces A Physicochem. Eng. Asp.* 587 (2020). <https://doi.org/10.1016/j.colsurfa.2019.124328>.
- [13] C. Rauwendaal, Extruder Screw Design, in: *Polym. Extrus.*, 2014: pp. 509–652. <https://doi.org/10.3139/9781569905395.008>.
- [14] T. Ivancic, C. Lu, R. Sheppard, M.R. Thompson, J.L. Pawlak, C.M. Cheng, D.J.W. Lawton, Investigating the Synergistic Anionic/Nonionic Surfactant Interaction on Nanoparticle Synthesis with Solvent-Free Extrusion Emulsification, *Ind. Eng. Chem. Res.* 59 (2020) 9787–9796. <https://doi.org/10.1021/acs.iecr.0c00550>.
- [15] B. Mu, M.R. Thompson, Examining the mechanics of granulation with a hot melt binder in a twin-screw extruder, *Chem. Eng. Sci.* 81 (2012) 46–56. <https://doi.org/10.1016/j.ces.2012.06.057>.
- [16] A. Kumar, S. Li, C.M. Cheng, D. Lee, Recent Developments in Phase Inversion

Emulsification, *Ind. Eng. Chem. Res.* 54 (2015) 8375–8396.
<https://doi.org/10.1021/acs.iecr.5b01122>.

- [17] D. Lawton, M.A.Sc. Thesis – D. Lawton McMaster University – Chemical Engineering SOLVENT FREE EMULSIFICATION IN A TWIN-SCREW EXTRUDER i, McMaster Univ. – Chem. Eng. (2013). <https://macsphere.mcmaster.ca/handle/11375/15278>.
- [18] S. Lawton, David;Thompson, Michael; Faucher, Morphological development of latex particles in a solvent-free extrusion process, *Annu. Tech. Conf. - ANTEC, Conf. Proc. J.* 2 (2014) 1169–1174. <https://macsphere.mcmaster.ca/handle/11375/15278>.
- [19] B.K. Gogoi, K.L. Yam, Relationships between residence time and process variables in a corotating twin-screw extruder, *J. Food Eng.* 21 (1994) 177–196.
[https://doi.org/10.1016/0260-8774\(94\)90185-6](https://doi.org/10.1016/0260-8774(94)90185-6).

Chapter 3: Relationship of polyester properties with water content requirements for solvent-free extrusion emulsification

The formatting of this chapter has been set up as a journal manuscript. The work has not been submitted to any journal at the time of examination but is intended for publishing in the near future

ABSTRACT

The present study investigated the sensitivity of Solvent-Free Extrusion Emulsification to the polymer based on small variations in melt viscosity and surface energy that arise between batch lots of the same resin. The purpose of the work was to better understand how these polymer properties influenced the parameter-sensitive mechanism of continuous emulsification. The trials focused on the dispersion zone inside the extruder where an intermediary water-in-oil (W/O) emulsion develops prior to an induced phase inversion at its end. While melt viscosity did not appear as a sensitive parameter in forming the desired W/O morphology, a significant correlation was found between the maximum amount of water that could be injected into the dispersion zone prior to inversion and the surface energy contribution of the polyester end groups, as measured by the acid number (AN). The results showed that higher quantities of water could be dispersed into a resin of higher AN (i.e. solids content of 69%) whereas for a resin of lower AN, the process could only generate the desired W/O emulsion needed for phase inversion if the water content was reduced (i.e. solids content of 79%). This new finding for SFEE required the consideration of a dynamic inversion region associated with the emulsification mechanism that delays the inversion with resins of low AN at higher water content in the dispersion zone. On the other hand, although the extent of neutralization was independent of AN, the greater concentration of converted carboxylate end groups that occurred with high AN resins could grow a larger interfacial area with water needed to reach the phase inversion point within the limited mixing time of the extruder. This results in a wider stable operating window for the process based on the maximum amount of water that can be injected into the dispersion zone.

Keywords: phase inversion emulsification, twin-screw extruder, process stability, high viscosity, surface energy

1. INTRODUCTION

There are high demands for dispersions composed of nanoscale sized particles for their capacity to offer unique properties such as optical transparency, enhanced diffusive transport, and long-standing storage stability compared to microscale dispersions, making them more suitable for pharmaceutical and personal care applications [1]. While micron-sized dispersions can be obtained using high mechanical shear forces, submicron emulsions usually need a chemically-driven technique like phase inversion emulsification. Both approaches are well studied for low and medium viscosity oils (≤ 1 Pa-s) where mixing will not be the rate-limiting step with water, while more viscous polymers have normally required the use of a good solvent to lower their viscosity in the system to achieve the same outcome. These solvents increase environmental and health concerns though, which has fueled the demand for alternative, more benign methods to address the complexity of growing the interfacial area between water polymer phases [2]. Solvent-free extrusion emulsification (SFEE) is a new continuous technology for producing waterborne submicron polymer dispersions (100-500 nm) inside a twin-screw extruder (TSE), common equipment for the polymer industry, handling very high viscosity polymer melts (100-1000 Pa-s) without the use of any hazardous solvents [3]. Implementing SFEE on an industrial scale has been challenging due to the processing sensitivities displayed, which has made it difficult to translate learning to different formulations or different scales of manufacturing.

The main mechanism responsible for producing nano-sized particles in SFEE is catastrophic phase inversion, which is a spontaneous emulsification technique that is also a less expensive and a more energy-efficient alternative to conventional high-energy mechanical methods [4–6]. In the catastrophic phase inversion mechanism (CPI), the water-to-oil ratio (WOR) of the system is changed so that under a specific condition the emulsion inverts from the W/O

system to O/W (or vice versa for cases not studied in this work). The critical WOR at which the emulsion inverts is called the emulsion inversion point (EIP) or phase inversion point (PIP) [7,8]. Determining EIP for an emulsification system is not a straightforward task as it has been shown to be affected by variables such as formulation, stirring intensity, rate of water addition, and even the location of the impeller in batch systems [2,9,10]. For example, spontaneous inversion of a high viscosity water-in-oil (W/O) microemulsion to an O/W emulsion, as done in SFEE, can occur under specific conditions by a microemulsion phase coming into contact with a quiescent adjacent water phase [11]. However, in this referenced case, spontaneous inversion only occurred when the initial bulk water content was below 10% else water from the bulk fluxed into the oil phase to generate an undesirable, coarse heterogeneous emulsion system. In another work, Brooks et al. [12] discovered that the water content required for inversion decreased as the oil viscosity increased for low to moderate (0.0007 - 0.2 Pa-s). It seemed to Brooks that as the viscosity of the oil phase increased, the tendency of the oil phase to become the dispersed phase increased as well, requiring less water to invert. Considering the complexity associated with phase inversion, in reality, as the result of hysteresis the well defined EIP value is replaced by a region of uncertainty in the formulation-composition map where it is impossible to determine the exact location of the inversion point. This region is identified by a triangular shape or parabolic shaded regions called the phase inversion area (PIA) in Figure 1, and this behavior has become known as dynamic inversion in other works [8,13,14]. It should be noted the reason for this triangular geometry is that for example, in case of phase inversion of W/O to O/W emulsion, moving from the optimum formulation (i.e. Hydrophilic-Lipophilic Difference = 0) toward a more hydrophilic state can trigger early inversion of the W/O system because hydrophilic surfactant mixtures tend to be stable in O/W emulsion; this is also true for more lipophilic surfactant in O/W emulsions. However, it is

difficult to determine the exact shape and border for this uncertainty area, though it is typically shown with a triangular shape for simplicity.

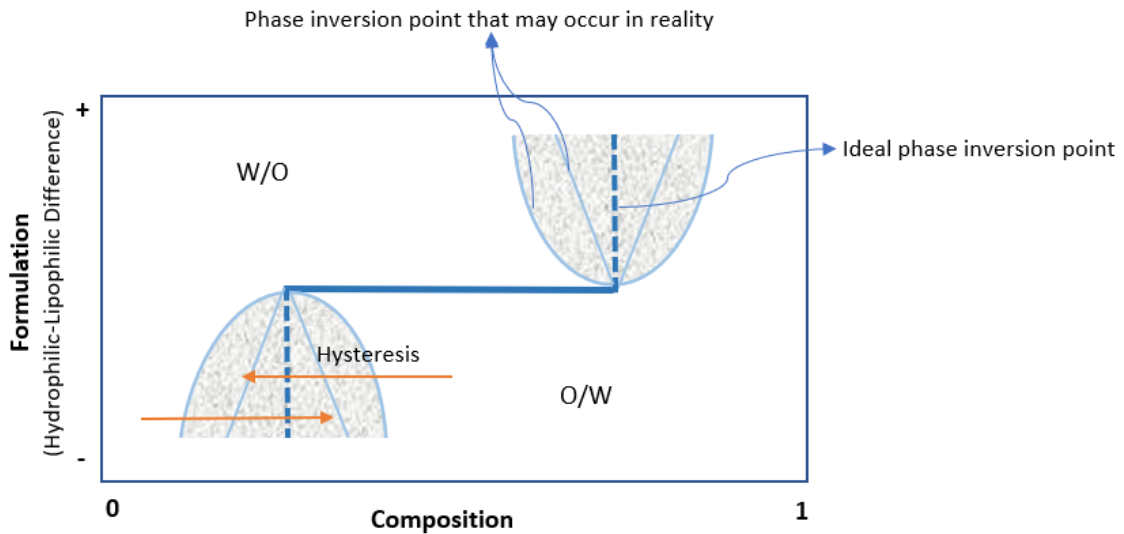


Figure 1. Schematic of dynamic emulsion inversion point in phase inversion emulsification systems

Many of the key elements of the SFEE mechanism have now been studied at the lab scale [3,15–20]. One noted example of process sensitivity that recently came to light during our work was lot-to-lot batch variation of the supplied polyester resin, which affected whether an emulsion could be obtained at the same water content. This observation gave rise to questions about the emulsification boundary and the dynamics of the critical WOR in its emulsification mechanism, and which of the properties varying in the resin had the most influence on both. In previous studies on SFEE, the effect of functional group and viscosity on morphology development and the final emulsion particle size was investigated [3,17,18], but those studies focused on a predefined WOR that was well within the emulsification boundary. It was never observed or tested how WOR changed with resin properties to obtain an emulsion. Therefore, to find out the relationship between water content and resin properties for successful emulsification in our residence time-limited process, different lot batches of the same resin were selected for the study. Variation in surface

energy, viscosity, and acidity were measured and their effects on the water requirement for a successful emulsification were investigated. The intent of this work was to update our understanding of the mechanism in solvent-free extrusion emulsification and improve its operational window.

2. MATERIALS AND METHODS

2.1. Material

Polyester resin and surfactant were provided by the Xerox Corporation (Webster, NY). Seven different batches of the same resin grade exhibiting normal production lot variation in their viscosity and acid number (AN) were collected from Xerox for the study. A summary of relevant properties for these different batches with respect to SFEE is found in Table 1. Alkyldiphenyl oxide disulfonate (Calfax DB-45) with a hydrophilic-lipophilic balance (HLB) of 16.7 was used as the anionic surfactant. Deionized Milli-Q water was used in all experiments, and sodium hydroxide (NaOH) was purchased from Caledon Laboratories Ltd.

2.2. Experimental Setup

Preparation of the aqueous polymer dispersions was carried out inside a 40 L/D, 27 mm Leistritz ZSE-HP co-rotating twin screw extruder (TSE) supplied by the Leistritz Advanced Technologies Corporation (Somerville, NJ) and configured with the same setup as previous work [3]. The barrel was configured for two injection points to add water, surfactant, and NaOH during the process. As shown in Figure 2, the first injection port was responsible for adding an aqueous mixture of surfactant and NaOH via pump P1 to make the W/O microemulsion whereas the second injection port was adding an excess of pure water via pump P2 to induce phase inversion. The figure mentions the critical mechanisms corresponding to the different zones of the extruder, as

described in earlier works [3,15–20]. The barrel temperature was kept constant at 95 °C whereas the extruder screw speed was fixed at 300 rpm for all trials.

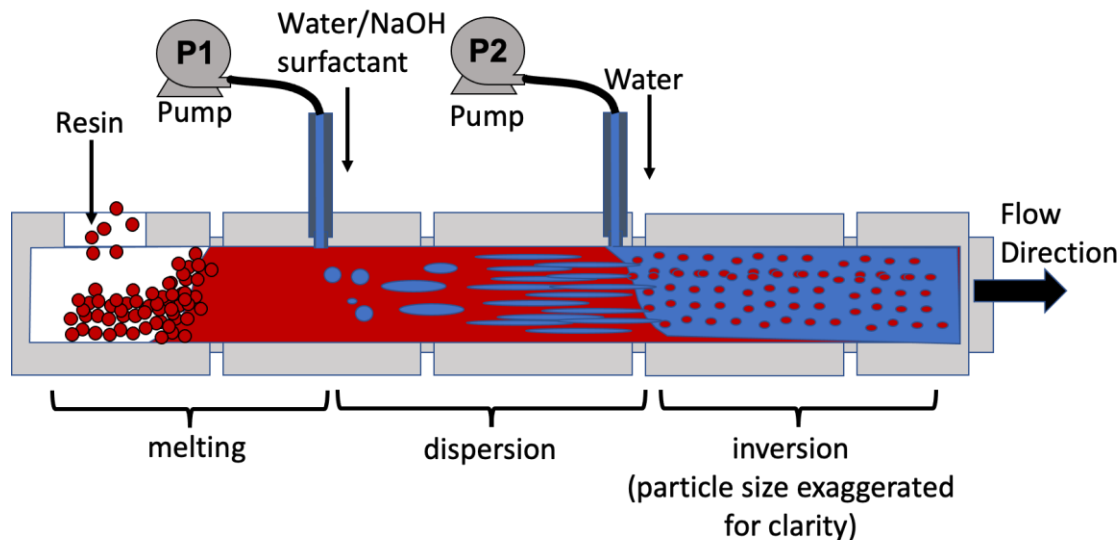


Figure 2. Conceptual progression of emulsification for the twin-screw extruder setup

2.3. Experimental trials

The primary study in this work varied the resin-to-water weight ratio (R/W_1) in the dispersion zone of the SFEE process, which was determined by the first pump (P1) in the extruder setup where the aqueous solution of surfactant and NaOH was introduced. NaOH was added for end group conversion to carboxylate to aid rapid water incorporation into the polymer matrix within the short residence time of the process (the residence time between pumps P1 and P2 has been measured to be only 118 s). The R/W_1 ratio was varied over the range of 2-5, beginning at 3.5 as noted by the flow chart in Figure 3, to define the lower and upper limits for each resin within which phase inversion occurred. The total resin-to-water ratio (R/W_T) is in reference to the final water content of the exiting product and is determined by the combined water added from both pumps P1 and P2. The final water content has never shown itself to be a sensitive parameter to emulsification, tending to be more of an economic constraint, and so it was fixed at $R/W_T = 1.3$.

Surfactant concentration was kept constant for all experiments at 4 wt.%, which has been previously established as a level offering a broad processing window at lower operational cost [19]. The NaOH content was adjusted for each resin (between 1% – 1.41%) to achieve a 100% theoretical neutralization ratio for each resin under investigation.

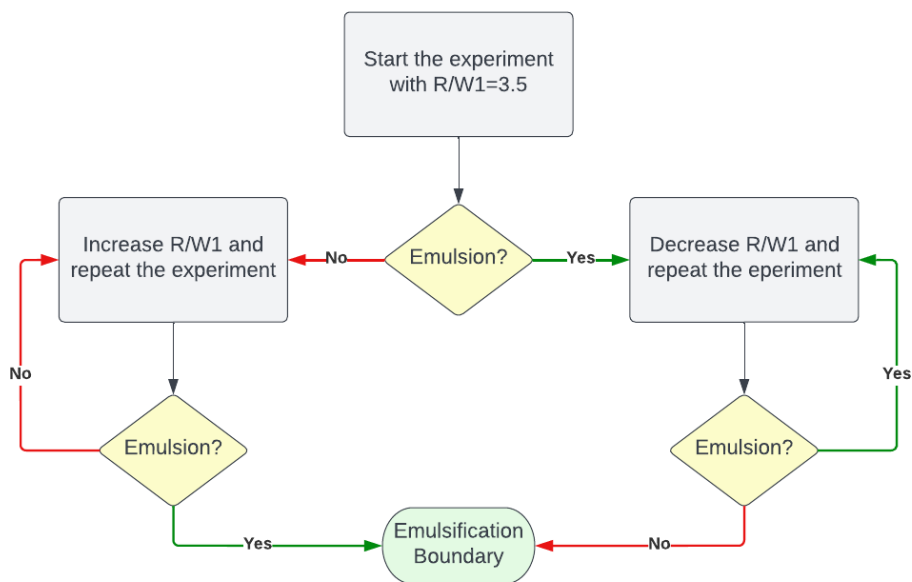


Figure 3. Flowchart for varying R/W_1 in the experiments to identify the emulsification boundary (i.e. lowest R/W above which the process was stable)

2.4. Acid number and neutralization ratio measurement

Extrudates were dried at 80°C overnight under vacuum for characterization. The acid number (AN) was determined using the standard method ASTM D974. By this method, 2 g sample was added to 100 ml methyl ethyl ketone (MEK) as the titration solvent along with 0.5 mL indicator solution (1 g p-naphtholbenzein in 100 mL MEK). The solution was titrated with 0.1 N standardized potassium hydroxide (KOH) solution in isopropanol (Sigma-Aldrich, certified standard). The neutralization ratio (NR) was calculated based on the ratio between AN of an extrudate sample and AN of the virgin polyester as stated in Eqn 1.

$$NR = \left(1 - \frac{AN_{extrudate}}{AN_{resin}}\right) * 100 \quad (1)$$

2.5. Molecular weight and degradation ratio measurement

All molecular weight measurements were conducted by the Analytical Team at Xerox Corporation (Webster, NY). Samples were prepared by dissolving approximately 5 mg extrudate samples/mL in spectral grade CHCl_3 spiked with 0.1% (v/v) toluene (HPLC grade) followed by filtration through a 0.2 mm syringe filter (Whatman PTFE) into 2 mL sample vials. The samples were injected using an autoinjector onto a Agilent 1260 LC System with refractive index detector equipped with 2 x 5 mm PL Mixed Bed C GPC columns (300 x 7.5 mm) and a guard column and eluted using 0.1% (v/v) triethylamine (99% purity). Polystyrene standards were used to calibration the instrument, for the determination of molecular weights. The degradation ratio (DR) was calculated based on the ratio between the number-average molecular weight (M_n) of an extrudate sample and the virgin polyester, as stated in Eqn 2.

$$\text{DR} = \left(1 - \frac{M_n \text{ extrudate}}{M_n \text{ resin}}\right) * 100 \quad (2)$$

2.6. Surface energy measurement

To determine the surface energy of each as-received resin, a sample was first molded using a Carver hot-press under 2 metric tonnes force at 100°C for 2 min to form specimens of 50 mm x 50 mm x 5 mm (thick). Measurements were done in a FTA200 contact angle analyzer (First Ten Angstroms, California, US). By the sessile drop method, the contact angle was measured for 1-bromonaphthalene (dispersive component $\delta^D=42.52 \text{ mJ/m}^2$, polar component $\delta^P=0.283 \text{ mJ/m}^2$) and glycerin ($\delta^D=35.541 \text{ mJ/m}^2$, $\delta^P=25.359 \text{ mJ/m}^2$). Each measurement was repeated five times at room temperature. Using the OWRK method, the total surface energy of each resin was calculated based on averaged contact angle values [21].

2.7. Rheology

To analyze rheological properties of the polyester feedstocks and dried extrudates, a Discovery Hybrid Rheometer (DHR) from TA Instrument (Delaware, US) was utilized. Initially, a strain sweep was used to evaluate the linear viscoelastic region at 100°C and a constant angular frequency of $\omega=10$ rad/s over a strain range of 0.01% to 100%. Then, a frequency sweep test was applied at 100°C and a strain amplitude of 0.05% (within the linear viscoelastic range) scanning angular frequencies between $\omega=0.1-100$ rad/s.

2.8. Particle size measurement

20 grams of extrudate was collected and diluted in 150 mL of water, this sample used for particle size measurements. The particle size distribution of emulsions sampled from the process was measured using a Malvern Mastersizer 2000 (Malvern, United Kingdom) with a detection range of 0.02-2000 μm . Testing was repeated three times for each sample. In this work, an ideal (or ‘good’) product displays a narrow monomodal size distribution with D_{90} less than 1 μm .

3. RESULTS AND DISCUSSION

Previous studies with the SFEE process found a resin-to-water ratio at the dispersion zone (R/W_1) of 3.5 (on a weight basis) provided a robust operating window, resulting in good emulsions while allowing other process variables such as surfactant concentration and NaOH content to be adjusted over a considerable range of conditions in order to study their effects on the dispersion particle size [3]. However, recently switching from an older batch of resin (surface energy 43.3 ± 0.7 mN/m; AN 17.7 ± 1.7 mg/g KOH [3]) to a new lot (Resin 1 in Table 1), it was found that emulsification at $R/W_1=3.5$ became quite sensitive to variations in those other process variables. Only by decreasing the water content ($R/W_1=5$) was it possible to return to a stable operating window and achieve emulsions with the new batch lot of resin. Reducing water content to re-

establish the emulsion was unexpected and it was felt that understanding this behavior would improve our conceptual mechanism of SFEE. Based on the high viscosity of the resin (~ 1750 Pa·s at 100 °C), it was considered that variation of the mixing dynamics was the most likely cause for the arising sensitivity. In light of the importance of water incorporation with the polymer melt and the associated relevance with interfacial growth in the SFEE mechanism [16], the selected characterizations of the different samples was focused on the interrelated factors of surface energy, viscosity, acid number and molecular weight.

3.1. Properties of the resins based on batch lots

Batch lots of the same grade of resin were collected over a span of several months from Xerox production, giving seven samples for consideration in this study, each with minor differences in their bulk molecular structure. Surface energy, acid number and M_n and M_w values are compiled in Table 1 while viscosity curves of these samples are presented in Figure 4.

Table 1. Total surface energy and acid number of polyester resins

Polyester Resin Batches	Surface Energy (mN/m)	AN (mg KOH/g resin)	M_n	M_w
Resin 1	40.6 ± 0.5	14.0 ± 0.4	4942	11599
Resin 2	39.8 ± 0.3	17.1 ± 0.4	4876	11848
Resin 3	40.2 ± 0.4	15.5 ± 0.5	5259	12510
Resin 4	40.2 ± 0.5	17.0 ± 0.4	5165	11544
Resin 5	41.3 ± 0.2	18.9 ± 0.3	5246	11888
Resin 6	39.4 ± 0.1	19.7 ± 0.5	5127	12233
Resin 7	40.7 ± 0.7	16.0 ± 0.3	5280	12019

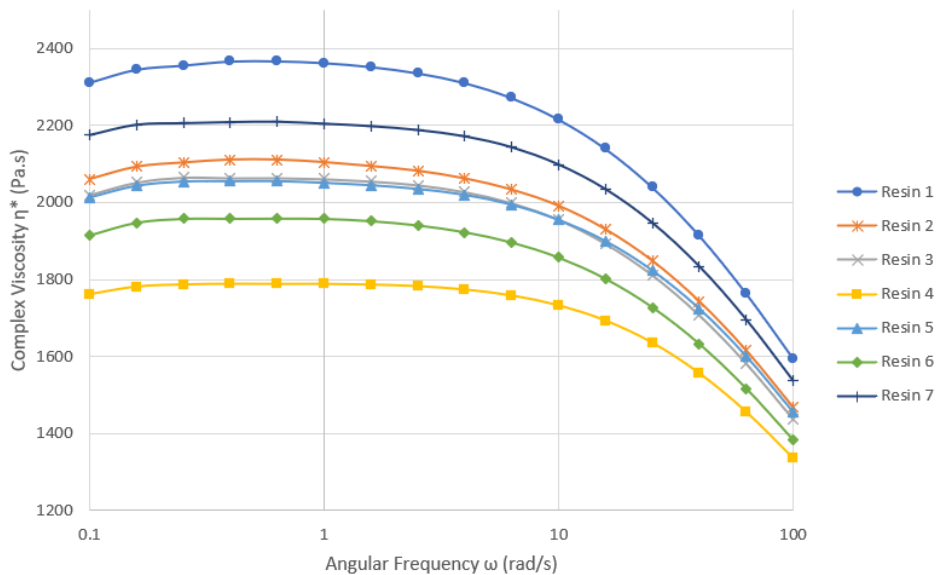


Figure 4. Complex shear viscosity curves at 100 °C for the different batch lots of the same grade of polyester (relative standard error of Resin 1: 9.2%, Resin 2: 8.5%, Resin 3: 8.6%, Resin 4: 3.5%, Resin 5: 7.6%, Resin 6: 8.1%, Resin 7: 7.8%)

The results for surface energy presented in Table 1 did not show any meaningful variation between the as-received resins. This was true for both polar and dispersive contributions to the total surface energy, and so only total surface energy was quoted in the table. This meant that none of the different lots had any greater advantage over the others for incorporating water with the polymer melt at the beginning of the process. Though surface energy was consistent among the group of samples, the acid number did notably vary, ranging from 14.0 to 19.7 mg KOH/g. Neutralization of these end groups alters the melt's surface energy value progressively throughout the dispersion zone of the process, depending on mixing, reaction time, and the surfactant. In fact, without neutralizing these end groups with sodium hydroxide, combining the polyester melt and water has never been sufficient to achieve phase inversion, even with surfactant present [15]. The number-average molecular weight values (used to calculate DR as molecular weight changed

through the process) did not correlate strongly with the acid number, indicative of some degree of branching across the fumaric acid double bonds during polyesterification. The viscosities of the different lots appeared generally to increase as AN decreased, as illustrated in Figure 5 using a shear rate of 50 s^{-1} as a typical value for extrusion to analyze the trend; Resin 4 was an outlier in this trend with a much lower viscosity than the other samples of similar AN.

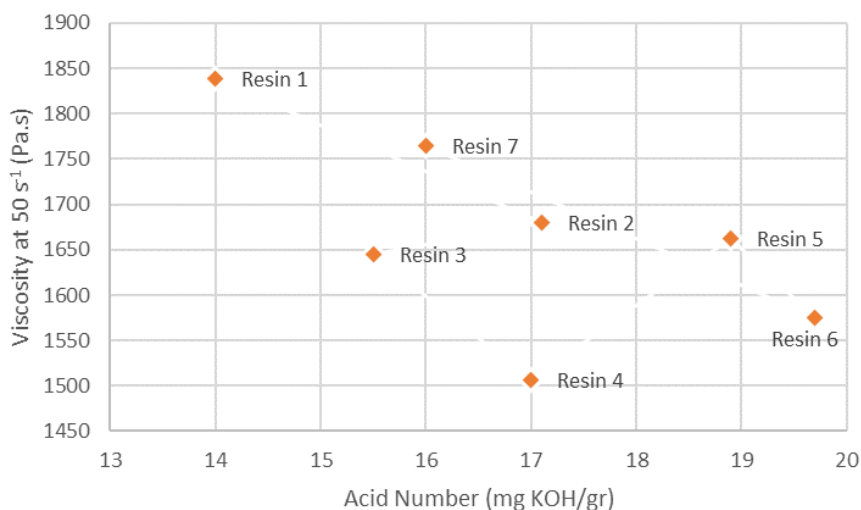


Figure 5. AN and viscosity (at a shear rate of 50 s^{-1}) for all resins

3.2. Assessment of the emulsification boundary

The results of the experimental trials for R/W_1 are shown in Figure 6 as an operational map of the emulsification region (area); the emulsification region defines conditions at which the material exits the extruder as a condensed milky fluid containing particles with D_{50} below $1 \mu\text{m}$. The boundary of this emulsification area was found to correspond to a progressively lower R/W_1 for batch lots where the original concentration of carboxylic acid end groups was higher; in a sense, one could consider the processing window is made broader for samples with a higher AN. For example, the batch lot having the lowest AN ($14 \text{ mg KOH/g resin}$), by SFEE it could only generate phase inversion if R/W_1 surpassed 4.5, which is a very high solids content (82%) for the dispersion

zone but admittedly meant there was less water that needed to be incorporated as well. Conversely, when the batch lot possessed the highest AN (19.7 mg KOH/g resin), R/W_1 only needed to exceed 2.5 (71% solids) to produce the desired phase inversion. This observed trend was statistically significant (significance level of 0.05) as the correlation between the boundary R/W_1 for emulsification and AN of the resin shows a p-value of 0.001. This strong relationship between water content and AN of the resin for the boundary appeared to be well-fitted by a simple linear regression (Eqn. 1; $R^2=0.88$) for the studied range ($14 \leq AN \leq 20$):

$$\text{Min } \{R/W_1\} = -0.37 * AN + 9.53 \quad (1)$$

The equation is interesting because it implies that there might be a R/W , albeit high in value, where the polyester with no AN can be dispersed, though likely with many other constraints that cannot be satisfied (like being in a similar range of viscosity and surface energy).

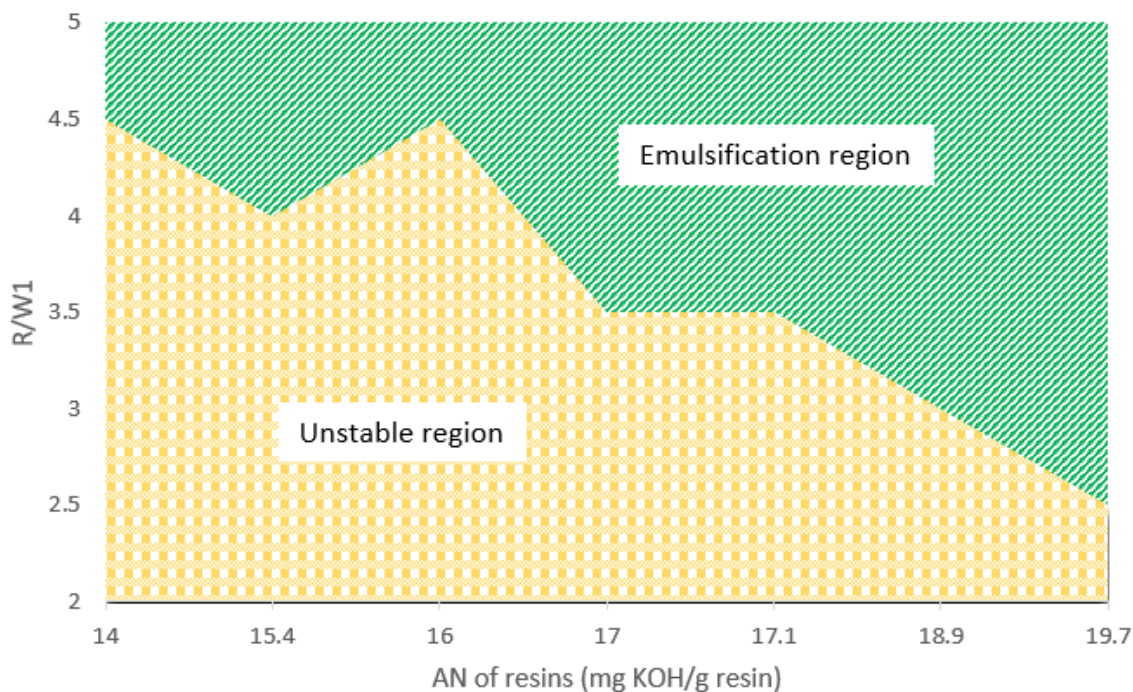


Figure 6. Emulsification boundary for R/W_1 for different batch lots of the polyester based on AN. All trials were conducted with a fixed NaOH concentration of 1% (w/w) on a resin basis

Resins with lower AN tended to have higher viscosity (referring to Figure 5) making it more difficult for NaOH molecules to diffuse to end group sites, meaning the apparent rate of neutralization should be governed by diffusion. Hence, it is logical to assume this emulsification boundary could be attributed, in part, to the viscosity of the resins or more specifically, to differences in diffusion rates. The statistical analysis presented in Table 2 revealed that the emulsification boundary varied significantly only with AN of the resin and not viscosity. It should be noted that this analysis is simplistic, focusing on the chemical state (and the reaction drivers) at the start of the process while ignoring for the moment interfering side-reactions like chain hydrolysis which will change AN and viscosity in a small manner across the dispersion zone [16]. To understand how the emulsification mechanism was involved in the varying boundary as well as appearing insensitive to other possible parameters in these experiments, a series of additional studies were conducted and analyzed below.

Table 2. Correlation between maximum water content in dispersion and resin properties (Significance level of 0.05)

Correlation type	Correlation coefficient	p-value
Min R/W1 and resin surface energy	+0.37	0.41
Min R/W1 and resin viscosity (at 50 s⁻¹)	+0.48	0.27
Min R/W1 and resin acid number	+0.93	0.001

3.3. Extent of neutralization and degradation

For the neutralization results presented in Figure 6, the NaOH content added was varied between 1% to 1.41% (w/w resin basis) for each batch lot of differing AN to achieve 100% theoretical neutralization of all end groups (compared to the fixed NaOH content used in

Section 3.2); all trials were conducted at $R/W_1=3.5$ because it is located in the middle of the emulsification boundary presented in Figure 6 and this helps to be consistent for the interpretation of the results. The experiment was set up in this manner to probe the significance of the lowered interfacial energy associated with the carboxylate (derived from the neutralization reaction) versus the initial concentration of NaOH added at the start of the dispersion zone (at pump P1). In this new trial, a resin of lower AN was being dispersed with water containing a lower NaOH concentration, which correspondingly meant there was a lower system basicity. In regards to system basicity, previous studies (in the range of 0.5-1.5% (w/w) NaOH) have found it to have only a minor influence on hydrolytic degradation, with a 10-12% decrease in number-average molecular weight (M_n) at most [3], and no notable effect on the surfactant's function [20]. Basicity was, therefore, minimized as a point of concern in these trials to focus on end group conversion. However, determination of NR is complicated by the fact that some hydrolytic degradation does occur, however little, and thus new carboxylic acid groups are generated across the dispersion zone (though predominately only in the first half of the zone) [15,16]. The results of both NR and NR corrected (based on measured M_n and the assumption of a monomodal distribution and one new acidic group per change in M_n), are shown in Figure 7.

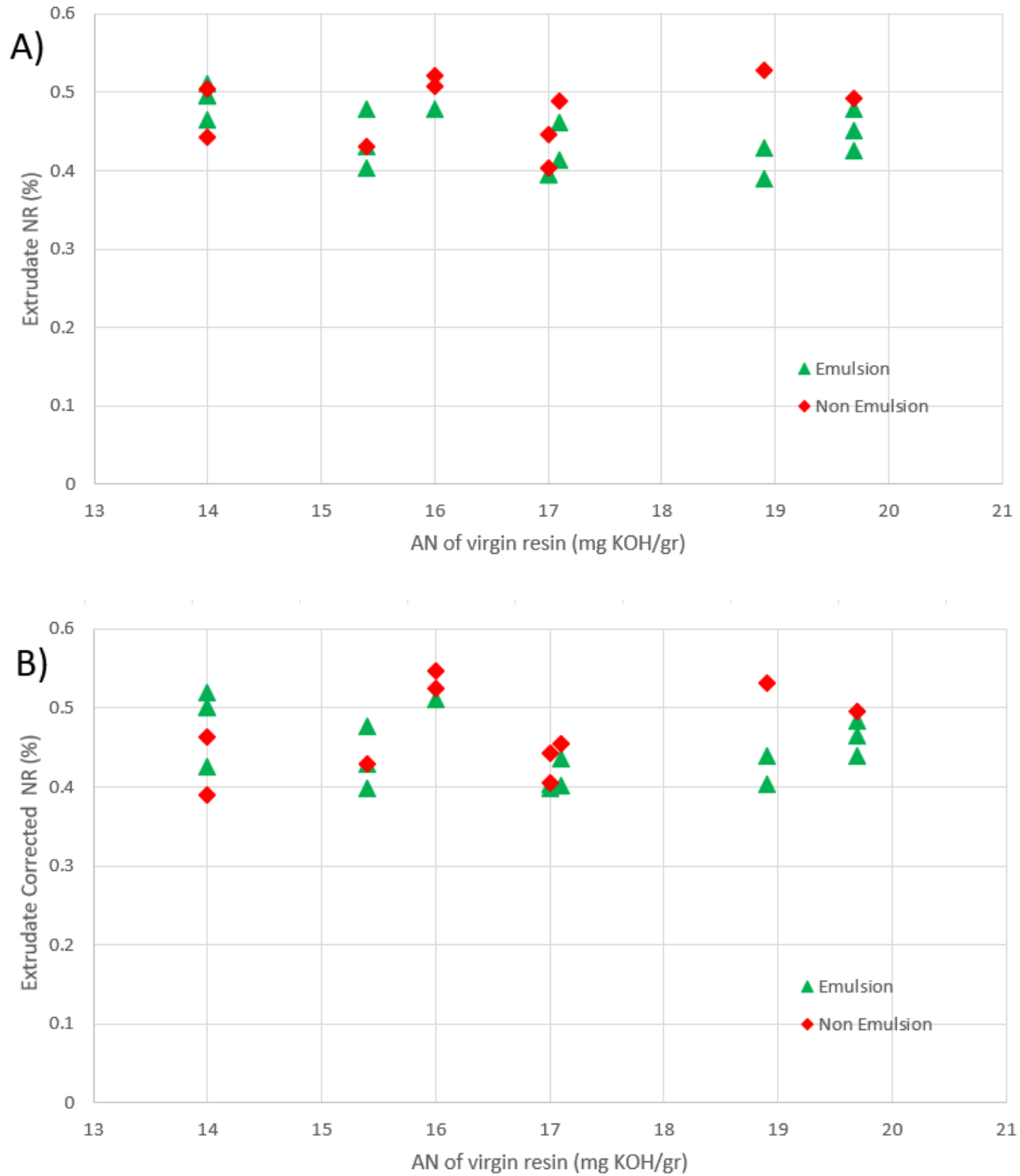


Figure 7. Extrudate neutralization ratio, NR vs AN of virgin resin for samples based on whether the extruded system emulsified or did not phase invert (non-emulsion). A) calculated NR, and B) NR corrected for hydrolysis

The NR values (corrected) reported in the figure varied between 0.4-0.55, which was consistent with previous studies [3] using a fixed 1% (w/w) NaOH solution (though in the absence of surfactant, that same work found NR values could possibly reach as high as 70%). The similarity between corrected and uncorrected NR was confirmation of the earlier reported findings that the resin is generally quite resistant to hydrolytic degradation in the presence of NaOH; in fact, the difference between NR and corrected NR was around 1%. The results show no trend for NR with respect to AN, which meant the concentration of carboxylates can be considered well represented by AN as we further analyze for correlations on emulsification performance.

Figure 7 included results based on whether the sample emulsified completely ('Emulsion') versus only partially ('Non-Emulsion'). To investigate the relationship between NR and the final product state (Emulsion vs Non-Emulsion), a one-way ANOVA analysis was carried out and the results revealed no statistically significant change in the neutralization ratio between emulsion and non-emulsion extrudates (p-value=0.094). This result showed that regardless of the final product state, the concentration of carboxylate groups generated were the same between the two cases and based solely upon the number of acid groups originally present. This meant that in the first half of the dispersion zone, where the neutralization reaction occurred, both cases (Emulsion vs non-Emulsion) possessed similar driving forces for water incorporation and interfacial growth.

3.4. Evaluating the influence of sodium hydroxide

Considering the apparent dependency of phase inversion area (PIA) on carboxylate concentration and R/W_1 , sodium hydroxide concentration was examined to see if more could be learned about the mechanism from the emulsification boundary. We sought to see how the dynamic PIA could be moved inside the extruder through a small set of trials, recognizing that the duality in the state of the product shown in Figure 7 pointed to the system operating where some portion

of the ‘triangular region’ overlapped with the Pump 2 location when $R/W_1=3.5$ (though for robustness it should ideally occur earlier). It was reasoned in these trials that increasing NaOH content did not change the PIA, whereas in a future study it will be shown to be affected by polymer flowrate, length of dispersion zone, and surfactant concentration.

Table 3 presents the neutralization ratio (NR) of three batch lots covering the full range of AN, comparing 100% theoretical neutralization (State 1, corresponding to the conditions in Figure 6 versus a fixed NaOH concentration (State 2, 1% weight with respect to the resin) at $R/W_1 = 3.5$; Resin 1 was considered the baseline condition in this case since 1% NaOH corresponded to 100% theoretical neutralization. For State 1, with no stoichiometric difference affecting the chemical driving forces for the end group reaction, as stated above NR varied consistently between 40-49% (corrected) with no apparent trend for NR corresponding to AN. With a fixed NaOH concentration for State 2, the maximum NR achievable (theoretically) declined slightly with higher AN, but the results seemed remarkably similar to State 1 for the same three resins. Although it might be ideal to reach a neutralization ratio of around 100% by converting all acidic end groups to carboxylate form, the results found that reaching a conversion ratio much above 50 % was not achievable because of diffusional limitation on the extent of reaction and the interference of the surfactant [3].

Table 3. Effect of varying NR on the process for different resins ($R/W_1=3.5$)

State 1: Original state (Resin 1 baseline)					
Resin	AN (mg KOH/g resin)	NaOH content (wt. %)	Theoretical NR	Result	Extrudate Actual NR
Resin 1	14	1.0%	100 %	Wet plastic	44.3 ± 0.9 %
Resin 2	17.1	1.2%	100 %	Emulsion	49.1 ± 1.5 %
Resin 6	19.7	1.4%	100 %	Emulsion	44.2 ± 0.8 %
State 2: New conditions with low NaOH content (Resin 1 baseline)					
Resin 1	14	1.0 %	100 %	Wet plastic	47.2 ± 1.7 %
Resin 2	17.1	1.0 %	82 %	Emulsion	43.4 ± 1.2 %
Resin 6	19.7	1.0 %	71 %	Emulsion	40.9 ± 2.3 %

For both states, only Resins 2 and 6 were emulsified successfully whereas Resin 1 produced only wet plastic; in fact, further tests with NaOH concentrations as high as 2% never saw Resin 1 produce an emulsion at $R/W_1=3.5$. The carboxylate concentrations were lower ($<1.2 \times 10^{-4}$ mol/g) for both states with Resin 1 compared to Resins 2 and 6 ($1.3-1.5 \times 10^{-4}$ mol/g). The NR values with State 2 were lower for Resins 2 and 6 compared to State 1, reflecting the decline in driving force for the acid groups to react with NaOH. The particle size distributions for the emulsified samples of Resins 2 and 6 for the two states are compared in Figure 8. Both size distributions for samples of Resin 6 (higher AN) were identical but shifted to a smaller size compared to the two matching distributions for Resin 2. Despite the lower carboxylate concentrations for Resins 2 and 6 for State 2 versus State 1, particle size seemed to be more dependent on AN.

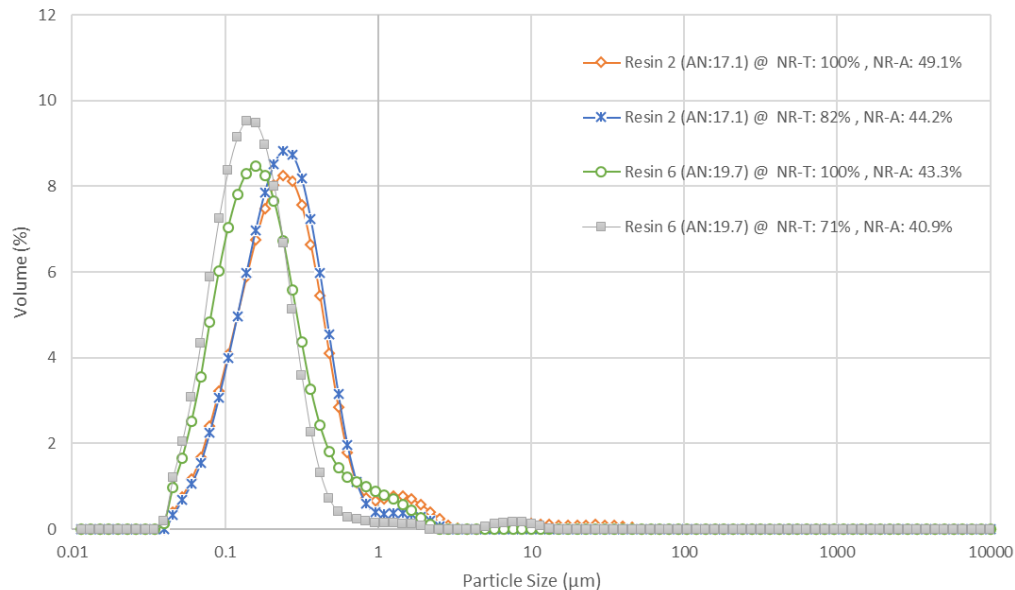


Figure 8. Particle size distribution of emulsion extrudates (NR-T and NR-A stand for the theoretical and actual NR respectively)

3.5. Dynamic phase inversion map

The results in Figure 6 showed that the maximum amount of water that can be used in the dispersion zone was directly related to the end group functionality of the resin, but Table 1 indicated that this variability in acid functionality produced no significant difference in surface energy for the polymer. Converting the acidic end groups to carboxylates increases their association with water molecules to aid in the solubilization of water into the oil phase. The importance of water solubilization in the oil phase, even in a very small amount, was observed in other studies [23,24]. The authors of that study discovered that in some systems, pre-solubilization of a small amount of water in the oil phase and then gradually adding more water to the mixture (oil with a small amount of added water) can significantly improve emulsification efficiency. In fact, they found out that solubilization is one of the necessary steps in generating double type emulsion (W/O/W) which allows for a more efficient emulsification mechanism to perform. With carboxylate group concentration directly related to the original acid group concentration (due to

the constant NR found), this suggests that with all other factors being equal, higher water solubilization should result with resins of higher AN and hence there is a higher probability that the polymer-water interface has appropriately grown, even with lower R/W_1 , such that the dynamic PIA (even partially) corresponds to the location of the second injection site (as noted in Figure 4). However, Figure 7 pointed out that the concentration of carboxylate groups was not the lone deciding factor in whether an emulsion or non-emulsion was produced by the end of the extruder. We believe that mixing (related to residence time of a packet of polymer/water fluid within the extruder) is a contributing factor in this mechanism for emulsification.

Typically, phase inversion emulsification in batch systems starts with a gradual increase of water into the oil phase was illustrated in Figure 1, for which the multiple emulsion system of O/W/O is located at a hypothetical starting point of $S_0(t_0, w_0)$ where the emulsion state is a function of time t_k , and water concentration w_k [7] (Figure 9D). On the other hand, in the twin screw extruder machine which is used for the SFEE process, the water concentration does not change in the dispersion zone but rather the mixed state of the polymer and water in the formulation-composition map changes as a function of the location and residence time of a packet of fluid in the extruder, ideally moving the composition state vertically (A to B) in Figure 9 from $S_0(t_0, w_0)$ to $S_1(t_1, w_0)$. The triangular gray area for phase inversion, which is related to the time- and location-dependent interfacial growth and morphology evolution within the dispersion zone is shifting from right to left in the figure. In this case, at the end of the dispersion zone, the state of the emulsion is ideally located within the potential phase inversion area, $S_2(t_2, w_0)$ in Figure 9C and right after starting the dilution zone, adding a larger amount of water inverts the emulsion causing the emulsion state to jump from $S_2(t_2, w_0)$ to the diluted O/W emulsion of $S'_2(t_2, w_2)$. Hence, the conventional approach in batch systems in determining of water content at which phase

inversion occurs (w_i) is not relevant, rather determining the location within the extruder at which the interfacial area growth has reached a state of emulsion positioned within the potential phase inversion area (PIA) is more relevant and meaningful for the SFEE. Since the position of the emulsion state on the formulation-composition map remains unchanged throughout the dispersion zone, if for any reason at the end of the dispersion zone the emulsion state is not located within the dynamic PIA, then the injection of more water at the 2nd injection port either does not trigger inversion (yielding an exiting mixture of liquid and resin called wet-plastic), or in better case, inverts some part of the developed lamella mixture depending on how close it was to the dynamic PIA (suggesting a very heterogeneous flow field where packets of fluid are in different states of mixedness). The location of the dynamic PIA in the extruder, relative to the formulation-composition map, is theoretically determined by the mixing time (residence time) allowing for interfacial growth between the polymer and incorporated water in said packet of fluid. This may explain the results in [Figure 7](#) where a resin of similar AN (and carboxylate concentration) could exit the extruder as either an emulsion or non-emulsion.

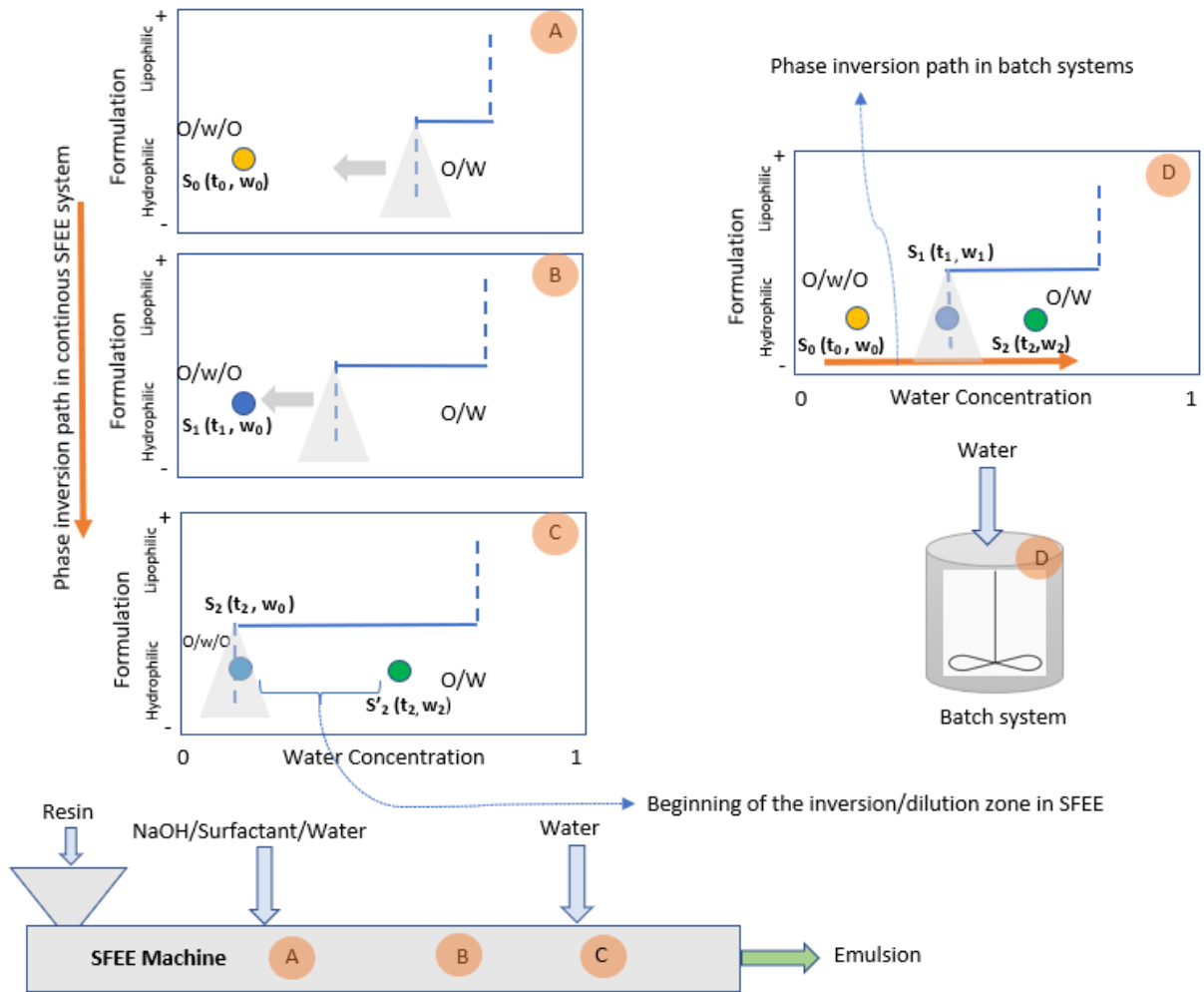


Figure 9. Formulation-Composition map for phase inversion mechanism in the SFEE vs Batch systems

Based on the discussion above about carboxylate groups and mixing, applying the theorized formulation-composition map, we can conceptually show that a resin of higher AN (more hydrophilic) versus lower AN (more lipophilic) is expected to reach the potential PIA earlier within the extruder (shorter residence time) for a constant water content based on the discussion about water incorporation above. And this effect on the state of emulsion should be made more severe by the fact that the lower AN resin has higher viscosity which makes diffusion of species more difficult and delays reaching the PIA. Hence, for the case of resin of low AN, the PIA will

not be reached within the limited space of the dispersion zone and emulsification only will occur if the dispersion zone is long enough that obtaining PIA is achieved before starting the dilution zone. This comparison between low and high AN resins and corresponding dynamic PIA is illustrated in Figure 10.

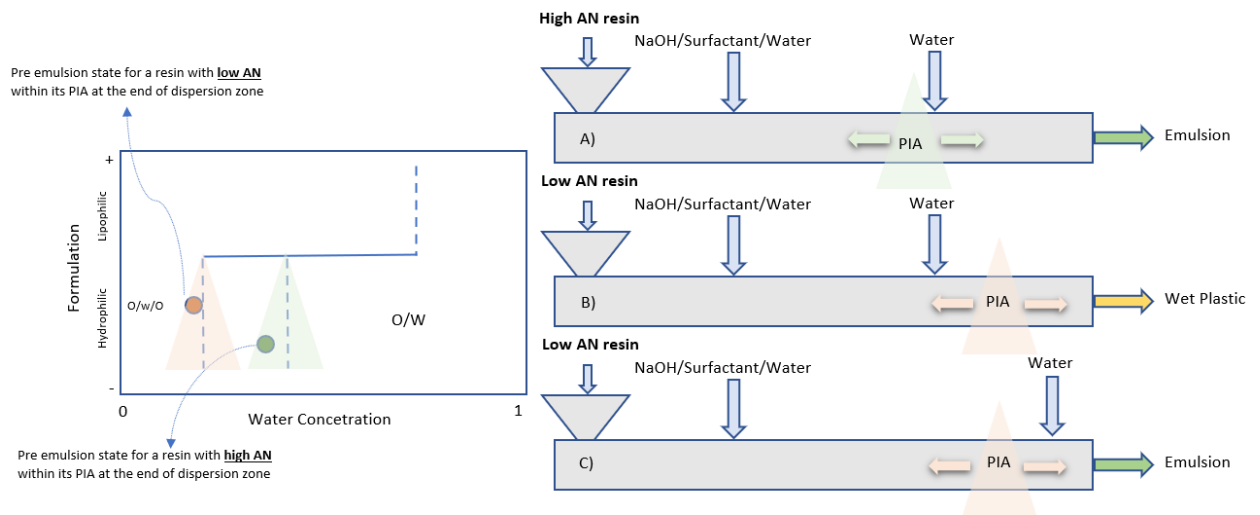


Figure 10. Illustration of dynamic PIA for low and high AN resin in formulation-composition map (at constant location that results in varied water content) and TSE machine (at constant water content that results in varied PIA location)

The dependency of the location of PIA within the extruder to the interfacial growth and the lack of results derived from the effect of increasing NaOH on NR can explain why increasing NaOH could not change the emulsification boundary with respect to the water. If a higher concentration of NaOH does not effectively increase the carboxylate concentration in the dispersion zone, it will not have an impact on the interfacial growth and therefore the location of PIA will not change. Therefore, this conceptual model helps to explain the emulsification boundary shown in Figure 6; That is, the location of the PIA is dependent on the degree of interfacial growth which in turn is dependent on the concentration of carboxylate groups and water content in the dispersion zone.

It is also worth mentioning that another effect of water content is related to the change in the viscosity of resin/water mixture prior to inversion (not the viscosity of the resin itself for which SFEE does not appear to be sensitive). The SFEE process operates as a concentrated (70-80% oil phase) emulsion system in the dispersion zone where the close-packed nature of the droplets in dispersion makes it distinguishable from dilute systems in terms of droplet breakup mechanism and hence the variables affecting the process. For example, while the viscosity of the oil phase plays an important role in the emulsification of the dilute systems, the effect becomes negligible above 70% of the oil phase, therefore in concentrated systems, the effective emulsion viscosity governs the emulsification mechanism [27,28]. In general, the increase in effective emulsion viscosity could significantly improve the transferring shear energy to the small droplets. This effective emulsion viscosity could be increased either by increasing oil phase content to reach the close-pack system [29] or by increasing the viscosity of the surfactant solution [26]. In the SFEE process, lowering water content in the dispersion zone not only creates a close-pack system similar to Dow's HIPE (high internal phase emulsion) process also known as BLUEWAVE technology [29] but also leads to a higher surfactant/water ratio in the solution which results in a higher surfactant solution viscosity, and therefore make emulsification more favorable in lower water content present in the dispersion zone.

5. CONCLUSION

Lot to lot variability of polyester resin was used to investigate the sensitivities of the SFEE process more deeply to better understand the mechanism involved. In this case, AN was shown to have a significant effect on the initial amount of water needed in the dispersion zone for phase inversion, resulting in an emulsification boundary dependent on the resin AN. In fact, a significant correlation was found between the acidic end groups of the resin and the maximum amount of

water content that could be used in the dispersion zone. Emulsification could be accomplished at higher water content in the dispersion zone with resins that possess higher AN, but for resins with lower AN, the process can only generate emulsion if the water content is decreased to a low enough level that ensures adequate mixing can be achieved. While the neutralization ratio remained relatively unchanged by changing water and NaOH contents for all batches, it is believed that this behavior is attributed to the importance of a small amount of water solubilization in the polymer phase in the dispersion zone. The more acidic end groups in resins of high AN can absorb more water in their structure widening the stable operating window for the SFEE based on the maximum amount of water that can be injected into the dispersion zone.

Finally, the result of the study suggests that water content in the dispersion zone can be used as a control variable while dealing with normal resin variation. In this case, for resins with lower AN, a reduction in the initial water content in the extruder can be used to ensure stable continuous emulsification and for resins with higher AN, a wider range of operation with respect to water injection would be expected.

5. ACKNOWLEDGEMENTS

The authors wish to thank the Natural Sciences and Engineering Research Council (NSERC) and the Xerox Corporation for their funding of the study. Additionally, we wish to thank Xerox Corporation (Webster, NY) and the Xerox Research Centre of Canada (XRCC; Mississauga, ON) for supplying the resin and Calfax surfactants used in this study, technical advice, and analysis assistance in measuring the molecular weight and acid number of resin samples.

6. REFERENCES

- [1] T.G. Mason, J.N. Wilking, K. Meleson, C.B. Chang, S.M. Graves, Nanoemulsions: Formation, structure, and physical properties, *J. Phys. Condens. Matter.* 18 (2006). <https://doi.org/10.1088/0953-8984/18/41/R01>.
- [2] A. Kumar, S. Li, C.M. Cheng, D. Lee, Recent Developments in Phase Inversion Emulsification, *Ind. Eng. Chem. Res.* 54 (2015) 8375–8396. <https://doi.org/10.1021/acs.iecr.5b01122>.
- [3] A. Goger, M.R. Thompson, J.L. Pawlak, M.A. Arnould, D.J.W. Lawton, Solvent-free polymer emulsification inside a twin-screw extruder, *AIChE J.* 64 (2018) 2113–2123. <https://doi.org/10.1002/aic.16066>.
- [4] C. Bilbao-Sáinz, R.J. Avena-Bustillos, D.F. Wood, T.G. Williams, T.H. McHugh, Nanoemulsions prepared by a low-energy emulsification method applied to edible films., *J. Agric. Food Chem.* 58 (2010) 11932–11938. <https://doi.org/10.1021/jf102341r>.
- [5] F. Ostertag, J. Weiss, D.J. McClements, Low-energy formation of edible nanoemulsions: Factors influencing droplet size produced by emulsion phase inversion, *J. Colloid Interface Sci.* 388 (2012) 95–102. <https://doi.org/10.1016/j.jcis.2012.07.089>.
- [6] M. Elgammal, R. Schneider, M. Gradzielski, Preparation of latex nanoparticles using nanoemulsions obtained by the phase inversion composition (PIC) method and their application in textile printing, *Colloids Surfaces A Physicochem. Eng. Asp.* 470 (2015) 70–79. <https://doi.org/10.1016/j.colsurfa.2015.01.064>.
- [7] M.A. Norato, C. Tsouris, L.L. Tavlarides, Phase inversion studies in liquid-liquid dispersions, *Can. J. Chem. Eng.* 76 (1998) 486–494. <https://doi.org/10.1002/CJCE.5450760319>.
- [8] A. Perazzo, V. Preziosi, S. Guido, Phase inversion emulsification: Current understanding and applications, *Adv. Colloid Interface Sci.* 222 (2015) 581–599. <https://doi.org/10.1016/j.cis.2015.01.001>.
- [9] B.W. Brooks, H.N. Richmond, Dynamics of liquid-liquid phase inversion using non-ionic surfactants, *Colloids and Surfaces.* 58 (1991) 131–148. [https://doi.org/10.1016/0166-6622\(91\)80203-Z](https://doi.org/10.1016/0166-6622(91)80203-Z).
- [10] Q. J.A., S. D.B., Phase inversion in the mixing of immiscible liquids, (1963) 15–18.
- [11] W.O. Microemulsion, R.W. Greiner, Spontaneous Formation of from Water-Continuous Emulsion a, (1990) 1793–1796.
- [12] B.W. Brooks, H.N. Richmond, Phase inversion in non-ionic surfactant-oil-water systems-III. The effect of the oil-phase viscosity on catastrophic inversion and the relationship between the drop sizes present before and after catastrophic inversion, *Chem. Eng. Sci.* 49 (1994) 1843–1853. [https://doi.org/10.1016/0009-2509\(94\)80069-3](https://doi.org/10.1016/0009-2509(94)80069-3).
- [13] C. Pierlot, J.F. Ontiveros, M. Royer, M. Catté, J.L. Salager, Emulsification of viscous alkyd resin by catastrophic phase inversion with nonionic surfactant, *Colloids Surfaces A*

- Physicochem. Eng. Asp. 536 (2018) 113–124.
<https://doi.org/10.1016/j.colsurfa.2017.07.030>.
- [14] N. Zambrano, E. Tyrode, I. Mira, L. Márquez, M.P. Rodríguez, J.L. Salager, Emulsion catastrophic inversion from abnormal to normal morphology. 1. Effect of the water-to-oil ratio rate of change on the dynamic inversion frontier, *Ind. Eng. Chem. Res.* 42 (2003) 50–56. <https://doi.org/10.1021/ie0205344>.
- [15] A. Goger, M.R. Thompson, J.L. Pawlak, D.J.W. Lawton, In situ rheological measurement of an aqueous polyester dispersion during emulsification, *Ind. Eng. Chem. Res.* 54 (2015) 5820–5829. <https://doi.org/10.1021/acs.iecr.5b00765>.
- [16] A. Goger, M.R. Thompson, J.L. Pawlak, M.A. Arnould, A. Klymchyov, R. Sheppard, D.J.W. Lawton, Inline rheological behavior of dispersed water in a polyester matrix with a twin screw extruder, *Polym. Eng. Sci.* 58 (2018) 775–783. <https://doi.org/10.1002/pen.24613>.
- [17] A. Goger, M.R. Thompson, J.L. Pawlak, M.A. Arnould, A. Klymchyov, D.J.W. Lawton, Effect of Viscosity on Solvent-Free Extrusion Emulsification: Molecular Structure, *Ind. Eng. Chem. Res.* 56 (2017) 12538–12546. <https://doi.org/10.1021/acs.iecr.7b03370>.
- [18] A. Goger, M.R. Thompson, J.L. Pawlak, M.A. Arnould, D.J.W. Lawton, Effect of Viscosity on Solvent-Free Extrusion Emulsification: Varying System Temperature, *Ind. Eng. Chem. Res.* 57 (2018) 12071–12077. <https://doi.org/10.1021/acs.iecr.8b02649>.
- [19] T. Ivancic, M.R. Thompson, J.L. Pawlak, D.J.W. Lawton, Influence of anionic and non-ionic surfactants on nanoparticle synthesis by solvent-free extrusion emulsification, *Colloids Surfaces A Physicochem. Eng. Asp.* 587 (2020). <https://doi.org/10.1016/j.colsurfa.2019.124328>.
- [20] T. Ivancic, C. Lu, R. Sheppard, M.R. Thompson, J.L. Pawlak, C.M. Cheng, D.J.W. Lawton, Investigating the Synergistic Anionic/Nonionic Surfactant Interaction on Nanoparticle Synthesis with Solvent-Free Extrusion Emulsification, *Ind. Eng. Chem. Res.* 59 (2020) 9787–9796. <https://doi.org/10.1021/acs.iecr.0c00550>.
- [21] D.K. Owens, R.C. Wendt, Estimation of the Surface Free Energy of Polymers, *J. Appl. Polym. Sci.* 13 (1969) 1741–1747.
- [22] J.L. Salager, A. Forgiarini, L. Márquez, A. Peña, A. Pizzino, M.P. Rodríguez, M. Rondón-González, Using emulsion inversion in industrial processes, *Adv. Colloid Interface Sci.* 108–109 (2004) 259–272. <https://doi.org/10.1016/j.cis.2003.10.008>.
- [23] T.J.L.I.N. Enchanted, Low-energy emulsification evaluation of emulsion quality, 29 (1978) 745–756.
- [24] T.J. Lin, H. Kurihara, H. Ohta, Prediction of Optimum O/W Emulsification Via Solubilization Measurements, *J. Soc. Cosmet. Chem. Japan.* 11 (1977) 32–42. https://doi.org/10.5107/sccj1976.11.2_32.
- [25] M. Pérez, N. Zambrano, M. Ramirez, E. Tyrode, J.-L. Salager, Surfactant-Oil-Water Systems Near the Affinity Inversion. XII. Emulsion Drop Size Versus Formulation and Composition, *J. Dispers. Sci. Technol.* 23 (2002) 55–63.

<https://doi.org/10.1080/01932690208984189>.

- [26] M.P. Aronson, The Role of Free Surfactant in Destabilizing Oil-in-Water Emulsions, *Langmuir*. 5 (1989) 494–501. <https://doi.org/10.1021/la00086a036>.
- [27] K.M.B. Jansen, W.G.M. Agterof, J. Mellema, Droplet breakup in concentrated emulsions, *J. Rheol. (N. Y. N. Y)*. 45 (2001) 227–236. <https://doi.org/10.1122/1.1333001>.
- [28] S. Tcholakova, I. Lesov, K. Golemanov, N.D. Denkov, S. Judat, R. Engel, T. Danner, Efficient emulsification of viscous oils at high drop volume fraction, *Langmuir*. 27 (2011) 14783–14796. <https://doi.org/10.1021/la203474b>.
- [29] R.D. Priestley, R.K. Prud'homme, *Polymer Colloids: Formation, Characterization and Application*, The Royal Society of Chemistry, 2020.

Chapter 4: Understanding the influence of mixing on a high viscous polymer emulsification process using a twin-screw extruder

The formatting of this chapter has been set up as a journal manuscript. The work has not been submitted to any journal at the time of examination but is intended for publishing in the near future

Abstract

Several factors affecting the operational window (polymer feed rate, screw speed, mixing length, and surfactant concentration) were investigated for their influence on phase inversion of a high viscosity (over 1000 Pa-s) polyester in a continuous process. The results showed that although increasing surfactant concentration could improve the robustness of emulsification, the most significant improvement was observed by designing a longer dispersion zone inside the extruder and lowering its feed rate, both which increased the residence time for mixing water into the polymer melt to create the initial W/O system. The effect of residence time was attributed to the total strain applied to grow the interfacial area in this sensitive mixing (dispersion) zone. However, it was residence time (more strongly impacted by feed rate) rather than shear rate (more strongly impacted by screw speed) that was discovered as the most influential on total strain. In fact, polymer feed rate showed the most promising impact on controlling the operational window, even though its favored lowering negatively impacts the economics of the process.

Keywords: phase inversion emulsification, twin-screw extruder, residence time, screw speed, high viscosity melt

1. INTRODUCTION

Typically, the preparation of an aqueous polymer dispersion is highly dependent on the oil phase viscosity and the means of lowering interfacial energy to achieve a desired final particle size, especially when sub-micron sizes are ideal. This is evident from the prior art, though there are few studies to reference for high viscosity systems. An aqueous dispersion of polyurethane (PU) anionomer was prepared in a batch process by slowly adding water under constant agitation (300 rpm) to obtain particles varying between 60-250 nm depending on the different neutralization agents utilized [1]. Mason et al. [2,3] showed that when the droplets are sufficiently packed together at near or above random close packing, an emulsion could exhibit viscoelastic properties showing elasticity at low shear strain and yielding behavior for larger deformations that resulted in a decrease in droplet radius. It was also shown that a higher surfactant concentration could increase the viscoelastic nature of the emulsion. Aqueous emulsification of several different high viscous polymer melts, including low density polyethylene with an average viscosity of 50 Pa-s, was achieved with a batch mixer by Akay et al. [4,5]. The obtained particle size was reported in the approximate range of 1-5 μm for varying content of the hydrophobic polymers. Preparation of aqueous dispersions of an epoxy resin with an approximate viscosity of 100 Pa-s via batch mixing was investigated by other researchers [6–8]. They showed that surfactant concentration and emulsification temperature played key roles in the phase inversion mechanism; a high surfactant concentration of 11 wt.% and the lowest possible system temperature of 73 °C could facilitate complete phase inversion, resulting in submicron-sized waterborne particles. We also mention the investigation by Xie et. al. [9] to emulsify polyisobutene in a styrene solution, though non-aqueous, because they discovered it was impossible to produce a stable emulsion using a transitional inversion path with different tested surfactants unless using a mixture of surfactants to pursue a catastrophic inversion route.

They found that the higher the HLB of their emulsifier mixture, the lower water fraction (f_w) that was required at the phase inversion point ($f_{w,inv}$). Despite this range of investigation of phase inversion emulsification of highly viscous systems in none of these examples above was a continuous system used, which notably prevents the gradual introduction of water into the polymer phase. In a new approach, a twin screw extruder (TSE) which is a conventional continuous mixing equipment for the polymer industry, was utilized for the emulsification of a polyester resin. This process is referred to as Solvent Free Extrusion Emulsification (SFEE). SFEE has been studied for several years [10–16], but the black-box nature of the continuous process creates challenges in fully understanding the phase inversion mechanism. Aside from the few locations to inject water into the extruder, there is a restrictively short residence time (3-4 minutes) making the process sensitive to various variables.

The purpose of this paper was to extend the operational window associated with these variables and gain an understanding of how these variables affect the emulsification boundary (minimum water content associated with producing an emulsion rather than some portion of wet plastic emerging from the machine). This was accomplished by applying a reverse problem-solving approach where a processing state was selected producing a non-emulsified wet plastic and by varying the variables of interest, the system was corrected to emulsify the resin. We then focused on understanding how the mechanism had been influenced by the variables to move the emulsification boundary. With this work, industrial and academic researchers will get a better understanding of how to implement a twin screw extruder to emulsify resins of interest.

2. MATERIALS AND METHODS

2.1. Material

A polyester synthesized from fumaric acid (FA) and dipropoxylated bisphenol A (pBPA) was provided by Xerox Corporation (Webster, NY). The polyester had a molecular weight of 14,215 g/mol and an acid number of 14 mg KOH/g. Alkyldiphenyloxide disulfonate (Calfax DB-45; Pilot Chemical Company) with a reported hydrophilic hydrophobic balance (HLB) of 17, was provided by Xerox Corporation (Webster, NY) as the surfactant. Deionized Milli-Q water was used for the experiments, and sodium hydroxide (NaOH) was purchased from Caledon Laboratories Ltd.

2.2. Experimental Setup

Preparation of the liquid-solid dispersions was carried out inside a 40 L/D, 27 mm Leistritz ZSE-HP co-rotating twin screw extruder (TSE) supplied by the American Leistritz Extruder Corporation (Somerville, NJ) shown in Figure 1. The machine is divided into three predefined zones, i) Melting zone (No. 2 in Figure 1), where the polyester is heated to be fully molten, ii) Dispersion zone (No. 3 in Figure 1), where NaOH, surfactant and a small fraction of water are added at the first liquid injection port (No. 5 in Figure 1) to create a striated lamellae morphology for the established water-in-oil (W/O) emulsion, and iii) Dilution zone (No. 4 in Figure 1), where a much larger amount of water is now added at the 2nd liquid injection port (No. 6 in Figure 1) to initiate phase inversion, changing the system from a W/O to O/W emulsion with a typical solids content of 50-70% before exiting at the die (No. 9 in Figure 1). The small fraction of water added at the 1st injection port is reported by its resin-to-water ratio (R/W_1), whereas the total amount of water in the system after the 2nd injection port is reported by its total resin-to-water ratio (R/W_T).

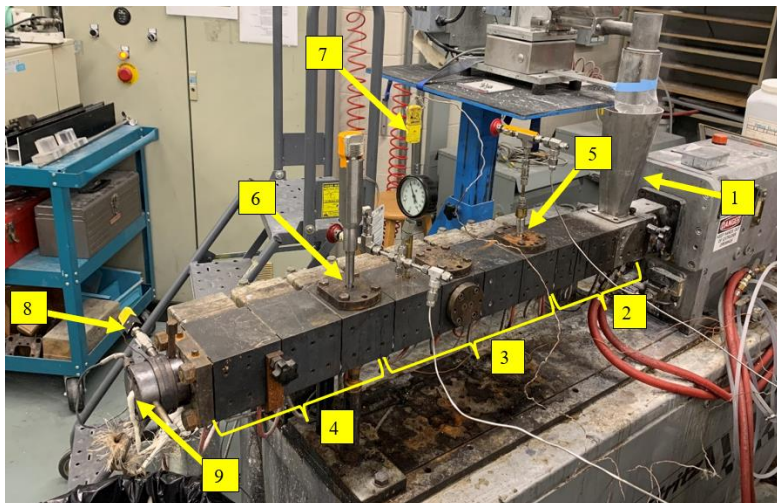


Figure 1. Twin Screw Extruder Setup used in the SFEE process- 1) Hopper for feeding resin in the TSE, 2) Melting zone, 3) Dispersion zone, 4) Dilution zone, 5) first liquid injection port 6) Second liquid injection port, 7) Thermocouple 1, 8) Thermocouple 2, 9) Submicron polymer dispersion extrudate

2.3. Emulsification trials

The emulsification boundary (expressed by R/W_1) is notably dependent on the Acid Number of the resin, as it was found from previous work that, for this resin, an acid number of 14 was unlikely to phase invert unless the R/W_1 ratio was set to at least 4.5 which lies above the chosen ‘base’ process conditions presented in Table 1, meaning the system was unlikely to phase invert; more robust emulsification conditions for this resin are found at R/W_1 of 5.0 as a matter of reference. This process condition was used as the base case and feed rate, screw speed, surfactant concentration and dispersion length were used as variables of interest for the study. A R/W_T of 1.3 has been established in all SFEE studies [12–15] to be above $f_{w,inv}$ for phase inversion of this polyester/surfactant system. The variables were changed based on the ranges presented in Table 2. The goal of the study was to widen the emulsification boundary (which will be defined in detail later in section 3.1) with respect to the resin to water ratio.

Table 1. Experimental conditions used as the base case

Process variables	Value
Resin to water ratio at 1 st injection port (R/W ₁)	3.5
Surfactant concentration	4% (w/w resin)
NaOH content	1% (w/w resin)
Total resin per water (R/W _T)	1.3
Feed rate	8 kg/hr
Screw speed	300 rpm
Barrel temperature	All zones @ 95 °C
Short dispersion length	16 L/D

Table 2. Variables of interest studied to widen the emulsification boundary

Variables	Range of investigation
Resin feed rate	2 – 8 kg/hr
Dispersion length	Short (16 L/D) vs Long (28 L/D)
Screw speed	150 – 600 rpm
Surfactant concentration	4 – 12% (w/w, resin basis)

2.4. Particle Size Measurement

Particle size distribution of emulsions sampled from the process was measured using a Malvern Mastersizer 2000 (Malvern, United Kingdom) with a detection range of 0.02-2000 μm . Three replications were made in water medium for each sample. The metrics and span of the distribution was used in analysis of the process. The metrics, D_{10} , D_{50} , and D_{90} represent the mean volume diameters for which 10, 50, and 90% of the particles are equal to or less than,

respectively. Span is a unitless value that represents the breadth of the particle size distribution and is defined by Eqn (1):

$$Span = \frac{D_{90} - D_{10}}{D_{50}} \quad (1)$$

A higher span indicates a wider distribution. In this work, an ideal (or ‘good’) product displays a narrow monomodal size distribution with D_{90} less than 1 μm .

2.5. Residence Time Distribution

To determine the residence time distribution (RTD) of the SFEE process, 1 g graphite powder was added into the extruder as a pseudo dirac pulse, similar to [17]. With the use of a digital camera, the color change of the extrudate was recorded. At a time interval of 10 seconds, a frame of the recorded video was captured for the analysis. Color intensity data were collected as a function of time. Adobe Photoshop CS4 software (Adobe Systems, San Jose, CA, USA) was applied for the color intensity analysis of individual frames. To simplify the analysis, all images in RGB mode were converted into Grayscale mode. An image was then measured for the percentage of black ink coverage in the fixed view of the end of the extruder (0% white-100% black); the extrudate without tracer was always white whereas the tracer impacted a dark black appearance when present. The color intensity was considered to have a linear relationship with the concentration of the graphite powder in an image. The procedure was repeated three times to determine measurement uncertainty.

2.6. Acid number and neutralization ratio measurement

Extrudates were dried at 80 °C over night under vacuum for characterization. The acid number (AN) was determined using the standard method ASTM D974. By this method, 2 g

sample was added to 100 ml methyl ethyl ketone (MEK) as the titration solvent along with 0.5 ml indicator solution (1g p-naphtholbenzein in 100 ml MEK). The solution was titrated with 0.1 N standardized potassium hydroxide (KOH) solution in isopropanol (Sigma-Aldrich, certified standard). The neutralization ratio (NR) was calculated based on the ratio between AN of an extrudate sample and AN of the virgin polyester as stated in Eqn 1.

$$NR = \left(1 - \frac{AN_{extrudate}}{AN_{resin}}\right) * 100 \quad (1)$$

3. RESULTS AND DISCUSSION

3.1. Effect on the emulsification boundary

As the purpose of the current work was to study the emulsification boundary, a method was required to display this threshold state. So, in addition to the trials that resulted in an emulsion (average particles with a D_{50} below 1 μm), the unsuccessful samples were also collected consisting of wet plastic and usually some milky white liquid. After filtering these latter samples through a wire mesh with a 106 μm opening to capture large lumps of unemulsified resin, the milky suspension was diluted and measured for particle size.

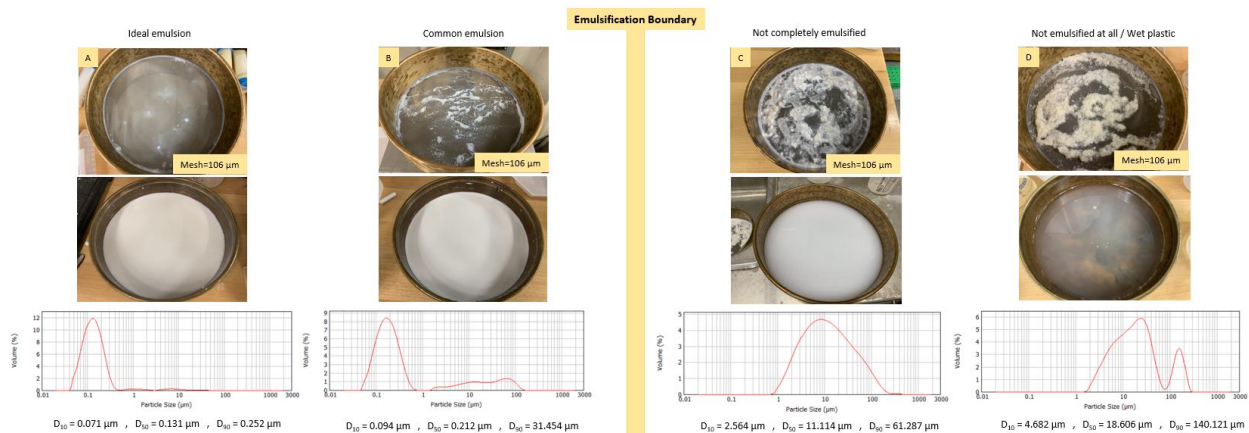


Figure 2. Possible outcomes of the SFEE process. A: Ideal/Perfect emulsion, B: Common emulsion, C: Not completely emulsified, D: Not emulsified at all/Wet plastic. (A & B classified as “Inside Emulsification” window and C&D classified as “Outside Emulsification” window)

Figure 2 presents all possible outcomes of the emulsification process inside the TSE. In an ideal or near ideal emulsification process (Figure 2. A), a little bit or no coarse particles remain on the selected sieve (106 μm opening) when the collected white milky emulsion possesses a narrow monomodal particle size distribution with all particles, D_{90} below 1 μm . However, in practice, most of the successful emulsification shows a behavior similar to (Figure 2. B) where some coarse particles (above 106 μm) are captured on the sieve and the remained milky emulsion presents a bimodal particle size distribution where the majority of particles are below 1 μm (major peak with D_{50} around 0.2-0.3 μm) and some particles are above 1 μm (short peak with $D_{90} > 1 \mu\text{m}$). When emulsification is not successful, in most cases, the resin is not emulsified at all and the extrudate exits the extruder as a heterogeneous mixture of resin and water called “wet plastic” which can be separated from each other using the sieve (Figure 2. D), and obviously, no submicron particles are obtained in this case. In some rare cases, the emulsification is incomplete which could cause some binary results (Figure 2. C) where unemulsified resin is retained on the sieve and the emulsified resin shows a higher particle size ($D_{50} > 1 \mu\text{m}$) than a normal emulsion (cases A&B). Based on these possible outcomes of the SFEE process, we define the emulsification boundary as a hypothetical boundary which separates cases A & B in Figure 2 where complete emulsification occurs and an emulsion with $D_{50} < 1 \mu\text{m}$ is obtained from incomplete and unsuccessful emulsifications corresponded to cases C & D. Therefore based on this defined boundary, we classify A & B as the cases which are “within the emulsification boundary” and C&D as “outside the emulsification boundary”. In general B and D are most common when the emulsification is either successful or unsuccessful, and in rare cases, A and C occurs.

The results of varying operating conditions to shift the emulsification boundary are summarized in Figure 3, Figure 4, and Figure 5.

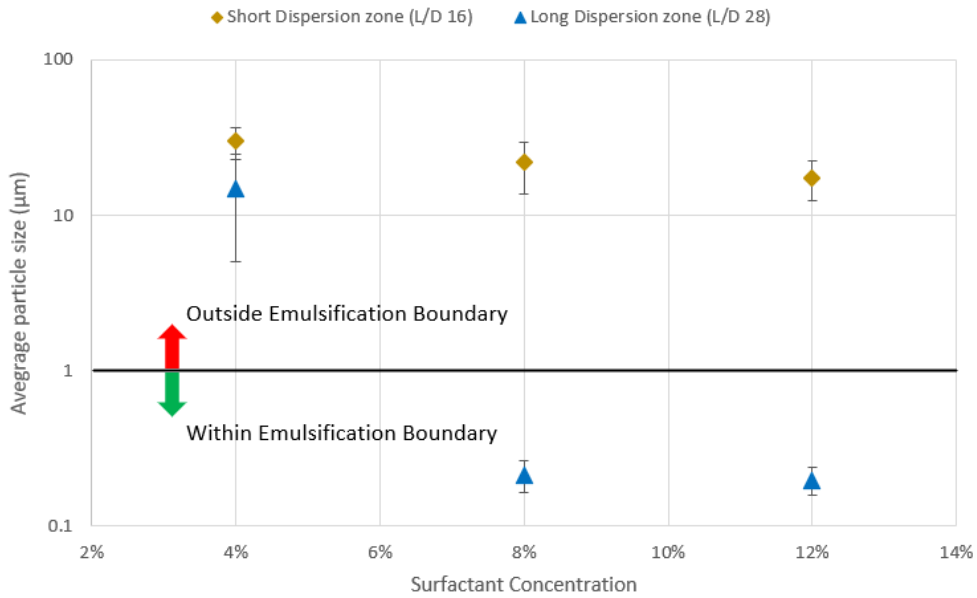


Figure 3. Effect of dispersion length and surfactant concentration on emulsification boundary (feed rate 8 kg/hr and screw speed 300 rpm)

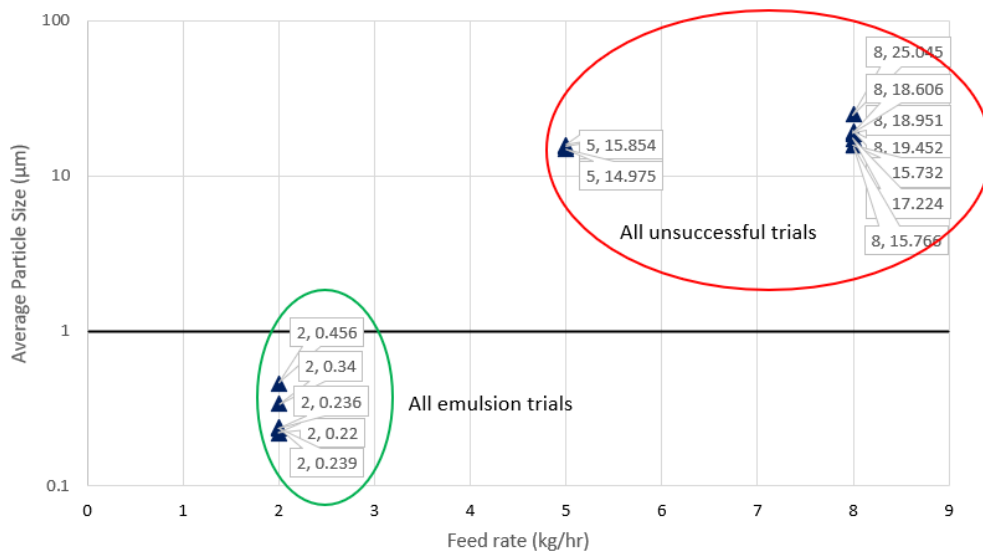


Figure 4. Effect of feed rate on the emulsification boundary at screw speed of 300 rpm for the short dispersion zone length and 4% (w/w) surfactant. Included balloons show the feed rate and D₅₀ value of each sample. No error bars shown for purposes of clarity

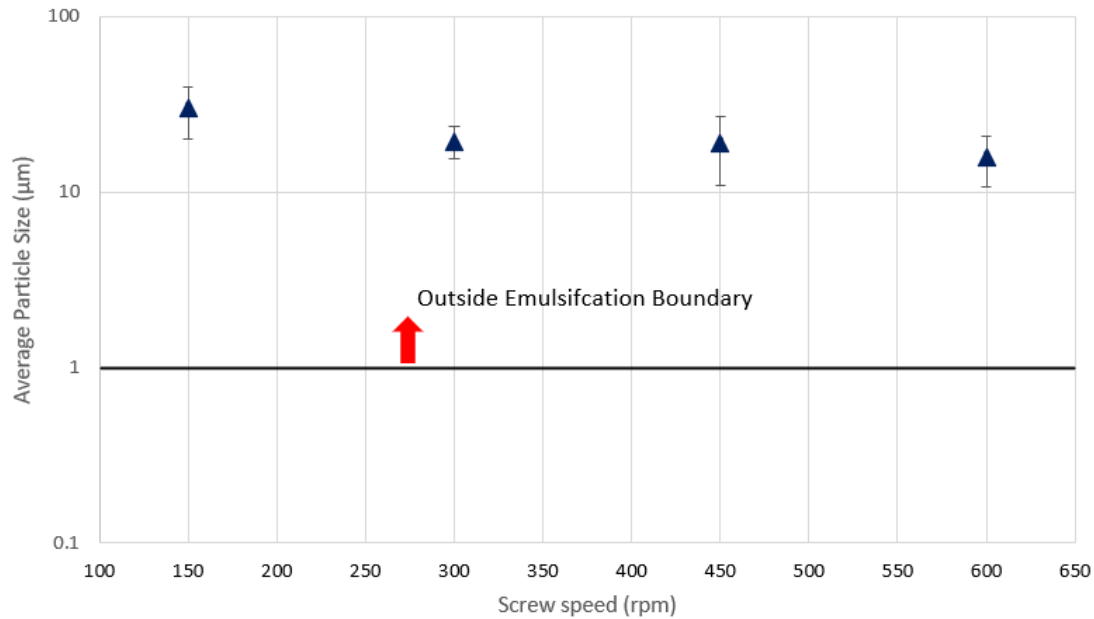


Figure 5. Effect of screw speed on the emulsification boundary at a feed rate of 8 kg/hr, 4% surfactant using the short dispersion zone length

Figure 3 shows the effect of increasing the dispersion zone length by 75% and increasing the surfactant concentration by as much as 300% (resin feed rate 8 kg/hr, screw speed 300 rpm) relative to the problematic base condition. With the short dispersion zone, increasing the surfactant from 4% to 12% (w/w) did not result in resin emulsification. However, there was a gradual decline in D_{50} with rising surfactant concentration, suggesting that some very high levels of surface active species could possibly produce an emulsion. Shifting to the long dispersion zone produced an emulsion but only at the higher surfactant concentrations of 8% and 12% (w/w). So, increasing the mixing length did not solely alter the emulsification boundary but a combination of both longer mixing and more surface active species did achieve the desired result.

The impact on emulsification with varied feed rates (screw speed of 300 rpm, short dispersion length, and 4% (w/w) surfactant) is presented in Figure 4. The results show that

higher feed rates of 5 and 8 kg/hr did not produce an emulsion but at 2 kg/hr, phase inversion occurred and a submicron emulsion was achievable. For comparison, decreasing the feed rate from 8 kg/hr to 2 kg/hr, increased the residence time in the zone by ~410 s whereas increasing the dispersion length from a L/D of 16 to 28 at 8 kg/hr increased the residence time by ~55 s (residence time analysis will be provided in the next section). A comparison between Figure 3 and Figure 4 shows that lowering feed flowrate is more effective than a longer dispersion zone as in the latter case the emulsification could happen only with an increase of surfactant content. However, the similarity in the results shown in Figure 3 and Figure 4 suggest that the ability of the process to provide emulsion with low AN resin might be attributed to an increase in mixing time and therefore improvement in time-dependent mechanisms occurring in the dispersion zone which will be discussed in detail in the next section.

Finally, investigation of different screw speeds at a constant flowrate of 8 kg/hr (Figure 5) showed that varying this parameter had no effect on the successfulness of emulsification and did not change the emulsification boundary. Some twin-screw extruders can go much higher in screw speed but the present machine was geared for high torque performance and hence could not go above the tested range. Changing screw speed will directly change shear rate applied to the polymer/water mixture in the dispersion zone but this has a notably weaker effect on residence time compared to feed rate [18,19]. Since kneading blocks make up almost 90% of the screw length and these sections can not be starved due to their nature of conveying, we have ignored the influence of screw speed on the degree of channel fill in this analysis.

With all examined variables seemingly showing residence time as an influential factor on the phase inversion mechanism, more direct studies followed to understand its impact.

3.2. Influence of residence time on continuous emulsification

In the previous section, it was shown that both lower feed and an extended dispersion zone shifted the emulsification boundary (though the latter variable needed an increase in surfactant concentration as well). Essentially, there are two phenomena occur in the dispersion zone that are important to the phase inversion mechanism and that could be affected by the feed rate and dispersion zone L/D. The first phenomenon was acid end group conversion to carboxylate species, which would give the polyester a higher affinity for water. The second phenomenon is the degree of water incorporation and dispersion into the highly viscous polymer melt (i.e. interfacial growth). These phenomena occur simultaneously but differ in rate of formation from start to end of the zone, and both will have some dependency upon time. Analyzing the residence time distribution (RTD) of the system based on both screw speed and resin feed rate highlights not only changes in time but also axial mixing characteristics, as illustrated in Figure 6 and Figure 7. As was mentioned above, in another trial (not shown in these figures) the mean residence time was only marginally increased when the dispersion zone L/D was substantially increased from 16 to 28 (8 kg/hr and 300 rpm).

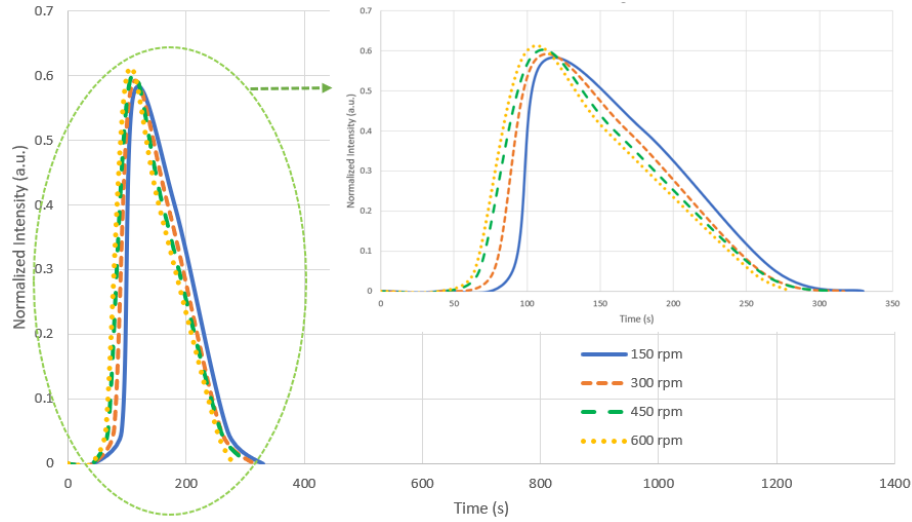


Figure 6. Residence time distributions at different screw speeds for a fixed feed rate of 8 kg/hr (short dispersion length, 4% (w/w) surfactant)

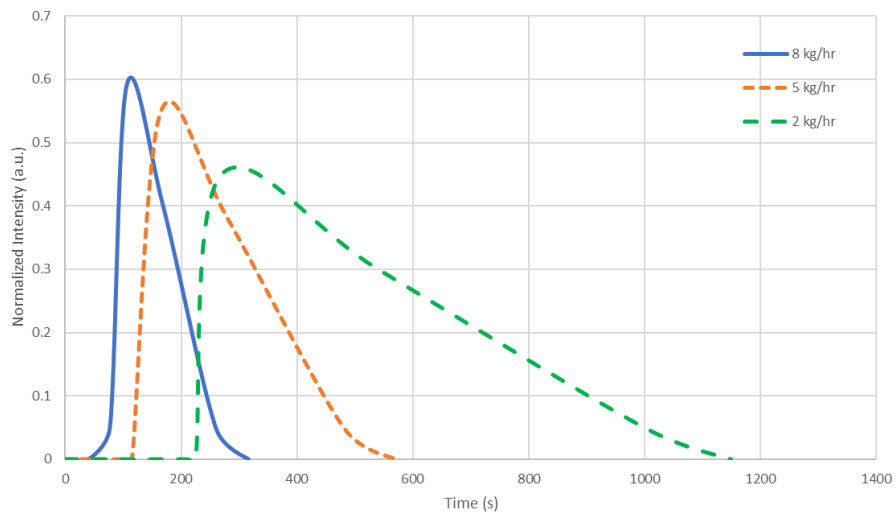


Figure 7. Residence time distribution at different feed rates for a constant screw speed of 300 rpm (short dispersion length, 4% (w/w) surfactant)

The results shown in Figure 6 revealed that increasing screw speed at the constant flow rate did result in a decrease of the residence time as shown in the graph and RTD moved toward the right of the plot. However, this effect was minor as the mean residence time decreased from

197 s to 180 s when the screw speed increased from 150 rpm to 600 rpm; uncertainty in the mean residence time was 5 s. On the contrary, changing the flow rate at the constant screw speed had a significant impact on RTD within the extruder as presented in Figure 7. A decrease in feed rate increased delay time, and widened the distribution; the significance of screw speed and feed rate on the distribution as well as the impact on delay time was consistent with earlier reported studies for twin-screw extruders [18,19]. The delay time is simply the minimum time for a plug of material to traverse the screw length without the effects of mixing. The delay time increased from 79 s at a feed rate of 8 kg/hr to 221 s at 2 kg/hr whereas the mean residence time tripled from 196 s to 605 s. Both space-time as well as extent of mixing are changed with feed rate. The widened RTD at low feed rate highlights a higher degree of distributive mixing in the extruder. As already mentioned above, due to the screw design used in SFEE, changes in residence time by screw speed and feed rate should be interpreted as occurring in fully-filled sections without variance in starvation. This means that shear rate and time can reasonably be directly interpreted as being applied to mix the two phases without the complication of how material moves under different states of channel starvation.

To apply the effect of residence time to the emulsification boundary, we considered its influence on end group conversion, measured by the neutralization ratio (NR) of the extrudate for the two different dispersion lengths (short vs long). The extent of neutralization was unchanged at 47.90 % \pm 1.45 (short) versus 47.32% \pm 0.89 (long) despite the gain of ~55 s. For reference, the measured mean residence time from the end of the melting zone to the start of the dilution zone is 139 s at the base conditions, indicating the extended time by lengthening the dispersion zone was significant. Despite the availability of acid groups for conversion, the extra residence time does not result in any apparent increase of end group conversion. It is suspected

that there is interference by the surfactant since higher NR has been reported when it is not present [12] but the cause is not relevant to the current analysis. The impact of residence time on emulsification was therefore, related to how mixing was affected as feed rate or dispersion length was changed. Therefore, an increase in residence time could favor time-dependent mechanisms such as incorporating water into the polymer phase, developing the water/polymer interface, and also by allowing more time for shearing, stretching, and breaking of droplets. This will be investigated in the next section.

3.3. Strain Distribution Function and Mixing Quality

The quality of laminar mixing in a mixing process is typically determined by the total strain imposed on the elements of a mixture, derived as the product of time and the rate of deformation (shear rate) [20]. In polymer processing equipment for both batch and continuous mixers, different segment (or packet) of fluid in the flow field experiences different strain levels and different residence times as well. Therefore, to quantify the various strain imposed on the fluid, strain distribution function (SDF) is defined, which is similar to the concept RTD discussed earlier but can not be experimentally determined. The strain function $f(\gamma)$ imposed at fluid at time t which is under the shear rate of $\dot{\gamma}$ is obtained by the Eqn (2) below:

$$f(\gamma) = t \cdot \dot{\gamma} \quad (2)$$

The average apparent shear rate in a twin screw extruder is estimated from Eqn (3) below:

$$\dot{\gamma}_{avg} = \frac{\pi D N}{\bar{h}} \quad (3)$$

where D is the screw bore diameter, N is the screw speed and \bar{h} is the average channel depth.

After the calculation of the strain distribution, the cumulative SDF, $F(\gamma)$ could be calculated by

the integration across the strain distribution function from the minimum strain γ_0 to γ by the Eqn (4) below [20]:

$$F(\gamma) = \int_{\gamma_0}^{\gamma} f(\gamma) d\gamma \quad (4)$$

The strain distribution functions for different flow rates and screw speeds are illustrated in Figure 8.

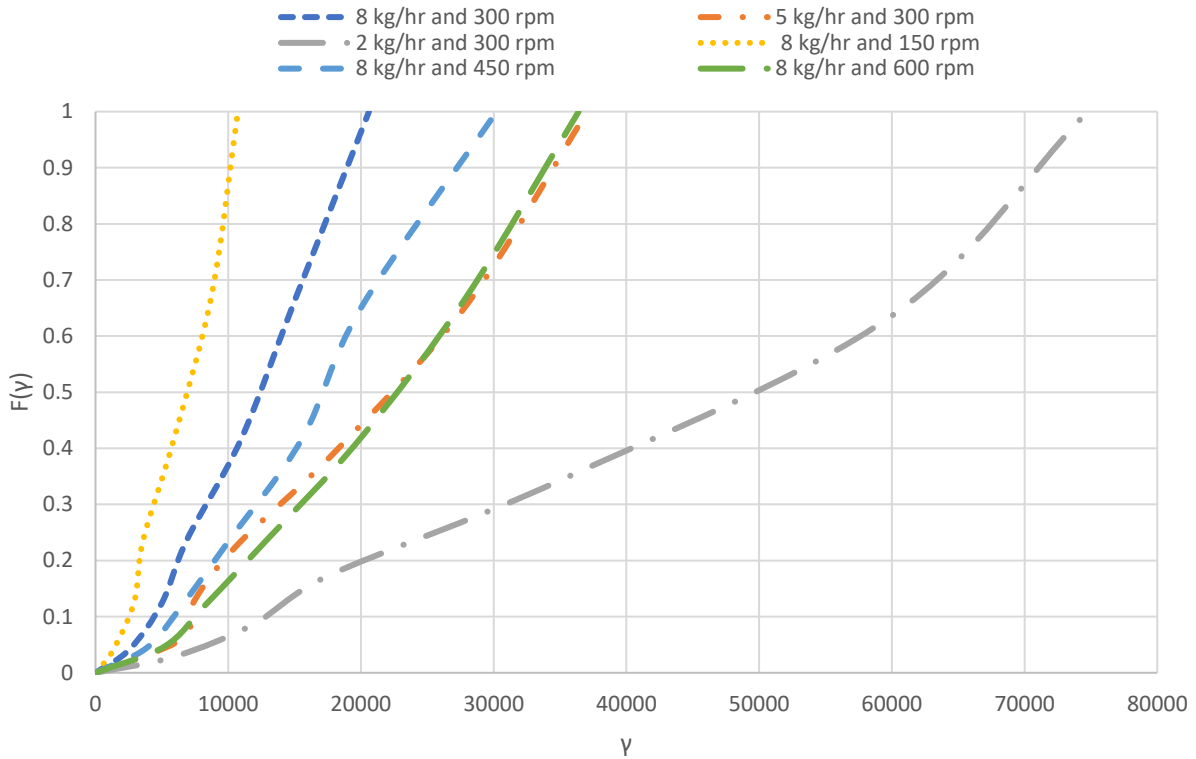


Figure 8. Strain Distribution Function for different flowrate and screw speeds inside the twin-screw extruder

Moving from left to right in the SDF plot infers that fluid segments experience more strain in the dispersion zone. It is believed that the amount of cumulative strain applied to the polymer/water mixture is directly associated with the interfacial growth between the two phases which impacts the readiness of the lamella-like morphology for phase inversion and successful

emulsification; thinner lamella have been equated with a higher fraction of the polymer undergoing phase inversion [11,12]. As shown in Figure 8, to the very left side of the plot, at 8 kg/hr and 150 rpm, a segment of the flow field will experience the lowest strain, and so interfacial growth was least likely to bring all areas of the mixture to $f_{w,inv}$ before it was exposed to the larger amount of water at the 2nd injection port. This corresponds with the unsuccessful emulsification shown in Figure 5 for this condition. On the other hand, at the very right case with 2 kg/hr and 300 rpm, the mixture experiences the highest strain level, which means, interfacial area growth is maximized for the conditions examined to reach or exceed $f_{w,inv}$ by the 2nd injection port.

One might assume that by keeping time at a constant level and changing the shear rate (varying screw speed) or vice versa, that the strain can be controlled in such a way that ensures phase inversion. This is true according to Eqn (2); however, it has some limitations or in other words, it works within a boundary, especially for screw speed changes. For example, a minimum screw speed (~150-300 rpm) is always required to provide enough shearing forces to affect the dimensionality of a fluid segment. On the other hand, when screw speed increases to a very high level, an increase in interfacial slip can act as an opposing force which can result in demixing [21]. Such slip has occurred in uncompatibilized polymer blends, giving larger microstructures (domains) at a higher rotation rate of 1000 rpm compared to 400 rpm.

The impact of the feed rate to extend the operational window for R/W_1 raises the question about its capability to also impact other variables' boundaries for emulsification. R/W_1 of 5 is chosen as a base case which is easier to create emulsion in any case. Figure 9 and Figure 10 present results showing how feed rate influences the lowest useful screw speed and surfactant concentration required for emulsification, respectively.

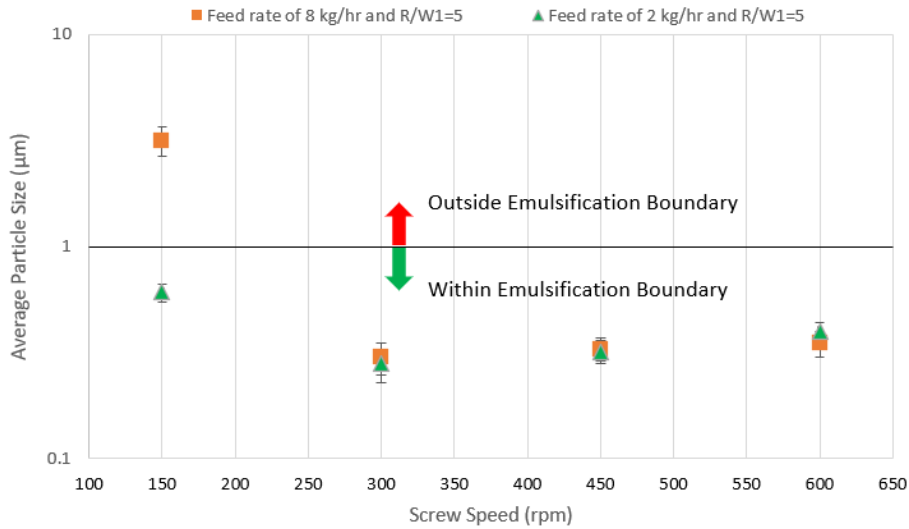


Figure 9. Effect of feed rate on different screw speed to find out minimum screw speed required for emulsification at $R/W_1=5$ and different feed rates (4% Surfactant and short dispersion length)

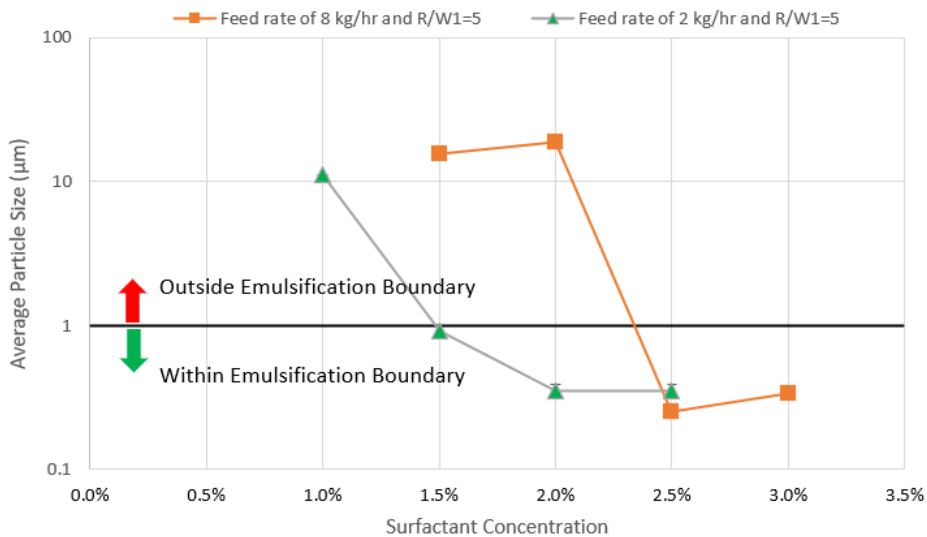


Figure 10. Effect of feed rate on the minimum surfactant concentration required for emulsification at $R/W_1=5.0$ (screw speed of 300 rpm). Lines included for purpose of clarity

The results in Figure 9 showed that at normal process conditions (8 kg/hr and $R/W_1=5$), a screw speed of 300 rpm can easily obtain an emulsion. This is considered an acceptable screw speed providing enough shear strain and mixing intensity to reduce the domain size and

sufficient disperse water within the polymer melt in the dispersion zone, and has been used frequently in previous SFEE studies [12–14,22]. However, at a lower screw speed of 150 rpm, the shear forces are not enough to create sufficient interfacial area between the two phases prior to the dilution point (2nd injection) and hence emulsification failed. However, by lowering the feed rate, emulsification was completed (though resulting in larger than ideal particles with D_{50} of 0.609 μm). The higher particle size could be attributed to a thicker lamella morphology developed as a result of the lower shear forces at the low screw speed, even though sufficient residence time and consequently, strain was applied for acceptable interfacial growth before dilution point to produce phase inversion. The effectiveness of a lower flowrate in extending the minimum required screw speed was also observed in the case of surfactant concentration in Figure 10. In this case, a higher mixing time at 2 kg/hr allowed growth of the interfacial area sufficient for phase inversion even with a much lower surface active species. A minimum of 1.5% (w/w) surfactant was acceptable at 2 kg/hr versus ~2.3% (w/w) at 8 kg/hr.

4. CONCLUSION

Improvement of the operational window in solvent-free extrusion emulsification was investigated. The effect of feed rate, screw speed, dispersion length, and surfactant concentration were studied for their individual influence on widening the emulsification boundary. The most significant improvement was observed by applying a longer dispersion length or lower feed rate because both significantly increase the residence time. The effect of residence time on the emulsification boundary was attributed to the total strain imposed on the polymer/water mixture which was related to interfacial growth in the dispersion zone. While both feed rate and screw speed could influence the total strain, the effect of feed rate was more significant because of the larger impact on residence time, versus screw speed's impact on the strain being limited to

mostly affecting shear rate and not residence time. Furthermore, in comparison to a high feed rate, operation at lower rates requires less surfactant and lower screw speed to create emulsion without sacrificing the emulsion quality, though a lower feed rate is not favorable from the industrial point of view.

REFERENCES

- [1] Y. Chen, Y. -L Chen, Aqueous dispersions of polyurethane anionomers: Effects of counteraction, *J. Appl. Polym. Sci.* 46 (1992) 435–443. <https://doi.org/10.1002/app.1992.070460308>.
- [2] T.G. Mason, J. Bibette, Emulsification in viscoelastic media, *Phys. Rev. Lett.* 77 (1996) 3481–3484. <https://doi.org/10.1103/PhysRevLett.77.3481>.
- [3] T.G. Mason, J. Bibette, Shear rupturing of droplets in complex fluids, *Langmuir.* 13 (1997) 4600–4613. <https://doi.org/10.1021/la9700580>.
- [4] G. Akay, Flow-induced phase inversion in the intensive processing of concentrated emulsions, *Chem. Eng. Sci.* 53 (1998) 203–223. [https://doi.org/10.1016/S0009-2509\(97\)00199-1](https://doi.org/10.1016/S0009-2509(97)00199-1).
- [5] G. Akay, L. Tong, Preparation of colloidal low-density polyethylene latexes by flow-induced phase inversion emulsification of polymer melt in water, *J. Colloid Interface Sci.* 239 (2001) 342–357. <https://doi.org/10.1006/jcis.2001.7615>.
- [6] Z.Z. Yang, Y.Z. Xu, D.L. Zhao, M. Xu, Preparation of waterborne dispersions of epoxy resin by the phase-inversion emulsification technique. 2. Theoretical consideration of the phase-inversion process, *Colloid Polym. Sci.* 278 (2000) 1103–1108. <https://doi.org/10.1007/s003960000376>.
- [7] Z.Z. Yang, Y.Z. Xu, D.L. Zhao, M. Xu, Preparation of waterborne dispersions of epoxy resin by the phase-inversion emulsification technique. 1. Experimental study on the phase-inversion process, *Colloid Polym. Sci.* 278 (2000) 1164–1171. <https://doi.org/10.1007/s003960000375>.
- [8] Z. Yang, D. Zhao, M. Xu, Y. Xu, Mechanistic investigation on the formation of epoxy resin multi-hollow spheres prepared by a phase inversion emulsification technique, *Macromol. Rapid Commun.* 21 (2000) 574–578. [https://doi.org/10.1002/1521-3927\(20000601\)21:9<574::AID-MARC574>3.0.CO;2-O](https://doi.org/10.1002/1521-3927(20000601)21:9<574::AID-MARC574>3.0.CO;2-O).
- [9] F. Xie, B.W. Brooks, Phase behaviour of a non-ionic surfactant-polymeric solution-water system during the phase inversion process, *Colloids Surfaces A Physicochem. Eng. Asp.* 252 (2005) 27–32. <https://doi.org/10.1016/j.colsurfa.2004.06.010>.
- [10] A. Goger, M.R. Thompson, J.L. Pawlak, D.J.W. Lawton, In situ rheological measurement of an aqueous polyester dispersion during emulsification, *Ind. Eng. Chem. Res.* 54 (2015) 5820–5829. <https://doi.org/10.1021/acs.iecr.5b00765>.

- [11] A. Goger, M.R. Thompson, J.L. Pawlak, M.A. Arnould, A. Klymachyov, R. Sheppard, D.J.W. Lawton, Inline rheological behavior of dispersed water in a polyester matrix with a twin screw extruder, *Polym. Eng. Sci.* 58 (2018) 775–783. <https://doi.org/10.1002/pen.24613>.
- [12] A. Goger, M.R. Thompson, J.L. Pawlak, M.A. Arnould, D.J.W. Lawton, Solvent-free polymer emulsification inside a twin-screw extruder, *AIChE J.* 64 (2018) 2113–2123. <https://doi.org/10.1002/aic.16066>.
- [13] A. Goger, M.R. Thompson, J.L. Pawlak, M.A. Arnould, D.J.W. Lawton, Effect of Viscosity on Solvent-Free Extrusion Emulsification: Varying System Temperature, *Ind. Eng. Chem. Res.* 57 (2018) 12071–12077. <https://doi.org/10.1021/acs.iecr.8b02649>.
- [14] A. Goger, M.R. Thompson, J.L. Pawlak, M.A. Arnould, A. Klymachyov, D.J.W. Lawton, Effect of Viscosity on Solvent-Free Extrusion Emulsification: Molecular Structure, *Ind. Eng. Chem. Res.* 56 (2017) 12538–12546. <https://doi.org/10.1021/acs.iecr.7b03370>.
- [15] T. Ivancic, M.R. Thompson, J.L. Pawlak, D.J.W. Lawton, Influence of anionic and non-ionic surfactants on nanoparticle synthesis by solvent-free extrusion emulsification, *Colloids Surfaces A Physicochem. Eng. Asp.* 587 (2020). <https://doi.org/10.1016/j.colsurfa.2019.124328>.
- [16] T. Ivancic, C. Lu, R. Sheppard, M.R. Thompson, J.L. Pawlak, C.M. Cheng, D.J.W. Lawton, Investigating the Synergistic Anionic/Nonionic Surfactant Interaction on Nanoparticle Synthesis with Solvent-Free Extrusion Emulsification, *Ind. Eng. Chem. Res.* 59 (2020) 9787–9796. <https://doi.org/10.1021/acs.iecr.0c00550>.
- [17] B. Mu, M.R. Thompson, Examining the mechanics of granulation with a hot melt binder in a twin-screw extruder, *Chem. Eng. Sci.* 81 (2012) 46–56. <https://doi.org/10.1016/j.ces.2012.06.057>.
- [18] M.D.W. Jun Gao, Gregory C. Walsh, David Bigio, Robert M. Briber, *AIChE Journal* - 2004 - Gao - Residence-time distribution model for twin-screw extruders.pdf, (n.d.).
- [19] B.V. A. POULESQUEN, *Polymer Engineering Sci* - 2004 - Poulesquen - A study of residence time distribution in co-rotating twin-screw extruders .pdf, (n.d.).
- [20] Z. Tadmor, *Principles of polymer processing*, 2nd ed., 2006.
- [21] H. Li, U. Sundararaj, Morphology development of polymer blends in extruder: The effects of compatibilization and rotation rate, *Macromol. Chem. Phys.* 210 (2009) 852–863. <https://doi.org/10.1002/macp.200800543>.
- [22] T. Ivancic, M.R. Thompson, J.L. Pawlak, D.J.W. Lawton, Influence of anionic and non-ionic surfactants on nanoparticle synthesis by solvent-free extrusion emulsification, *Colloids Surfaces A Physicochem. Eng. Asp.* 587 (2020). <https://doi.org/10.1016/j.colsurfa.2019.124328>.

Chapter 5. Conclusion and Significant Contribution

5.1. Key findings and contributions

Solvent-free extrusion emulsification (SFEE) is a recently developed process for producing submicron particles with high viscosity polymers inside a twin-screw extruder without the use of hazardous solvents. Its dependency on catastrophic phase inversion makes the process knowingly sensitive to a variety of formulation and operational variables, causing a narrow window of production. The purpose of this thesis was to investigate and improve the process stability as well as widening operational window. The key findings and contributions are summarized as follows:

1. The influence of rate of water phase addition on the output particle size distribution and process stability was investigated. The results showed the startup state was critical to achieving phase inversion. This transient sensitivity was related to thickened lamella being created by insufficient surface-active species for some of these transient startup cases. Once formed this morphology persisted as a segregated regime of the flow field inside the extruder long after start-up, making it impossible to return to a successful operating state unless the process was partially starved for a duration corresponding to residence time of melting zone and first half of dispersion zone. From these results, it was possible to recommend related to decreasing the transient time for the injected material in order to robustly achieve stable operations for producing polymer dispersions with a monomodal submicron particle size distribution.
2. SFEE sensitivity with first-stage water addition as it pertained to producing an intermediary W/O emulsion (as a necessary step before inverting to a O/W emulsion) was investigated through the batch lot-to-lot variability in the polyester resin. While viscosity and surface energy variations did not show any significant effect on the emulsification boundary, specifically the water fraction required in the dispersion zone for inversion, a significant correlation was found with the acid number (AN) of the resins. The results showed that resins

of higher AN could be more readily emulsified at higher water content, whereas for resins with lower AN, the process could only generate an emulsion if the water content was kept below a critical threshold. This new finding for SFEE was recognized as a dynamic inversion region associated with the emulsification mechanism that delays the inversion with resins of low AN at higher water content in the dispersion zone. On the other hand, although the extent of neutralization was independent of AN (a zeroth order reaction), the greater concentration of converted carboxylate end groups that occurred with high AN resins could grow a larger interfacial area with water (which was needed to reach the phase inversion point within the limited mixing time of the extruder). This results in a wider stable operating window for the process based on the maximum amount of water that can be injected into the dispersion zone.

3. Improvement of the operational window was investigated by studying the effect of feed rate, screw speed, dispersion length, and surfactant concentration for their individual influences on widening the emulsification region. The most significant improvement was observed by applying a longer dispersion length or lower feed rate because both significantly increased the residence time. The effect of residence time on the emulsification boundary was attributed to the total strain imposed on the polymer/water mixture, which was in turn related to interfacial growth in the dispersion zone. While both feed rate and screw speed could influence the total strain, the effect of feed rate was more significant because of its larger impact on residence time, whereas screw speed's stronger impact on the strain rate had a more limited effect (or contribution) to interfacial growth. The impact of a longer residence time was also shown to make emulsification possible with less surfactant and lower screw speeds without sacrificing the emulsion quality, though understandably a lower feed rate would not be a favorable approach to increasing residence time from an industrial point of view.

Instead of studying the variables within the operational window and investigating their effect on the particle size distribution, studies were carried out mostly on the emulsification boundary and it was shown that to understand the effect of variables on the process, not only their effect on the particle size should be studied but also their effect on operational boundaries must be considered. For example, while results of a previous study[1] showed that R/W_1 did not significantly influence mean particle size (D_{50}) for the studied range of conditions, the current studies have shown it has a noticeable impact on the operational boundary. Therefore an inversion methodology was developed to determine to widen the operational window by intentionally starting the process located in the unstable area and attempting emulsification to investigate the effect of variables on the operational boundaries.

Finally, while there are three sources of instability to consider for SFEE: Formulation, Kinetics, and Machine related instability, it has been shown that among machine-related instability causes, overwhelming internal melt seals (zones of pressurized melt) and the resulting backflow of liquid flow to the dispersion zone has little impact on the process for the current setup. This finding is important as it eliminates one of the key variables that was previously believed to be one of the main reasons for the process to become unstable suddenly in the middle of an otherwise stable trial. The major causes of instability in SFEE appear to be attributed to kinetics or time-dependent mechanisms, for which more work is needed.

5.2. Recommendations and Future Works

In addition to the key findings presented above, after four years of theoretical and practical research experience on the SFEE process, it is believed that the majority of the process instability

could be improved by the following recommendations and further studies, which could be helpful for a successful scaleup of the SFEE process:

1. In general, for catastrophic phase inversion-based emulsification techniques, the gradual addition of water to the oil phase triggers the inversion of the so-called W/O emulsion to O/W emulsion. While the stability of the final O/W emulsion is achieved by the presence of a surfactant, the presence of the surfactant in the oil phase before starting water addition is an important factor in the catastrophic phase inversion mechanism. So in general, it is believed that feeding the process with a premixed resin with a preferably low HLB surfactant (high HLB surfactant has a high tendency to quickly migrate to the water phase that may result in early inversion before sufficient interfacial growth which causes instability) before the first injection port could be helpful for the stability of the morphology developed in the dispersion zone and the process stability overall. To support the idea, in some unstable trials premixing the resin with 4 wt% SDBS surfactant (HLB=10) could emulsify the resin, while for the same condition even doubling the Calfax concentration at the 1st injection did not improve the stability. So, further study in this regard could be beneficial.
2. It is also believed from the findings that most instability issues for SFEE are attributed to an undesired fluid flow regime that starts developing soon after startup of the process. While, increasing residence time (mainly by lowering flowrate – or extending the length of the machine) is believed to mitigate the unpleasant impact of this flow regime as well as improve the quality of mixing, a computational fluid dynamics (CFD) study is highly

recommended for finding the exact source of instability that results in aqueous polymer phase separation within the extruder.

3. In the polymer compounding industry, some heuristics are used to establish feeding protocols. One of the heuristic rules is related to the mixing of the liquid with the polymer melt in which gear-like mixing, as shown in Figure 1, is strongly recommended for moderate-intensity mixing with the melt phase to prevent pooling as well as improve distributive mixing [2]. Therefore, the impact of adding gear mixers to the screw design as well as other screw design variations on the quality of mixing is recommended to be investigated.

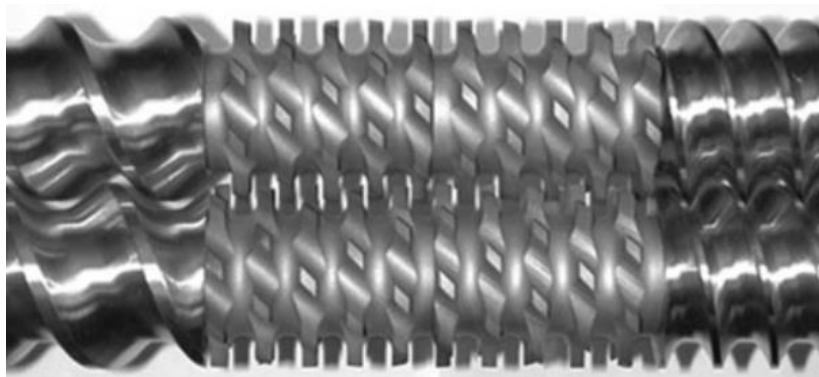


Figure 1. Gear Mixer used generally for liquid/polymer mixing [2]

5.3. References

- [1] A. Goger, M.R. Thompson, J.L. Pawlak, M.A. Arnould, D.J.W. Lawton, Solvent-free polymer emulsification inside a twin-screw extruder, *AICHE J.* 64 (2018) 2113–2123. <https://doi.org/10.1002/aic.16066>.
- [2] W.D. Seider, J.D. Seader, D.R. Lewin, S. Widagdo, *PRODUCT AND PROCESS DESIGN PRINCIPLES Synthesis, Analysis, and Evaluation*, 3rd ed., Wiley, 2009.